NTNU – Trondheim
Norwegian University of
Science and Technology

Optimized differentiation of THP-1 cells into macrophages for the study of TLR4 signaling and trafficking events

Håkon Schau Berg-Rolness

MSc in Biology
Submission date: May 2014
Supervisor: Atle M. Bones, IBI
Co-supervisor: Harald Husebye, IKM
Kristian Starheim, IKM

Norwegian University of Science and Technology
Department of Biology

Summary

Toll like receptors (TLRs) are a group of membrane bound pattern recognition receptors (PRRs). TLRs are able to detect a variety of pathogen associated molecular patterns (PAMPs) and start inflammation upon recognition of these. They are essential in the efficiency of the innate immunity as well as mobilizing an adaptive inflammatory response. TLR signaling has been studied intensively since their discovery, however, trafficking of the TLRs has not been given the same attention. In this study we hoped to develop a system that could be used to study the trafficking and signaling of TLR4, and potentially the other TLRs, in THP-1 cells that upon differentiation display a macrophage (Mφ)-like phenotype.

Rab GTPases have been described to be key regulators of intracellular trafficking. Rab GTPases have been reported in roles involving vesicular movement, vesicular integrity, and protein recycling. Their function in the intracellular trafficking events makes them the ideal targets when it comes to the study of trafficking and signaling of proteins involved in the innate immunity.

In this study we present data suggesting that Rab7a might be involved in regulating the coherence of the TLR4 inflammatory signaling pathways, especially the TRIF-dependent pathway leading to the induction of type I interferons. Our data on Rab11a showed that Rab11a depletion had a surprisingly weak effect on the TRIF-dependent pathway in the THP-1 model system contrary to what has been earlier reported in human monocytes. A possible explanation to this may be due to redundancy with Rab11b that seems to be up regulated during the rest period introduced after the PMA differentiation. The data from Rab4a knock down were inconclusive, but based on the observation made in these experiments we cannot exclude a role of Rab4a in the TLR4 inflammatory signaling pathways.

We believe that THP-1 cells, which are used in this study, can be used as a model system for Mφ signaling and trafficking. We have shown that optimization of the THP-1 differentiation has a substantial effect on LPS activated signaling and on the amount of Mφ markers such as CD11b and CD14 on the PM, however, the system appears to be somewhat unstable to obtain quantifiable data. We believe that these drawbacks can be negated with further optimization of the differentiation protocol

Acknowledgements

This master thesis was conducted at the Centre of Molecular Inflammation Research, Department of Cancer Research and Molecular medicine, St. Olavs Hospital, at the Norwegian University of Science and Technology (NTNU), in cooperation with the Institute of Biology, at the Faculty of Natural Sciences.

I would like to express my gratitude to my main supervisor Harald Husebye and co-supervisor Kristian K. Starheim for their guidance and support. I would also like to especially thank Astrid Skjesol and Mariia Yurchenko for all their contributions, both in the lab and in the writing process. I would also like to express my appreciation to the group that has welcomed me, as well as Terje Espevik for the opportunity to do the master thesis at his department.

Thank you

Takk

Takk sjøh

Дякую

E se

Grazie

Dank

To all the others, whom I've got the honor of making an acquaintance with, you have my thanks as well.

A small "apology" to Marria for making her share my troubles and strife in the work with the THP-1 cells.

Table of Contents

Summary I

Acknowledgements III

List of Figures IX

List of Tables X

Abbreviations XI

1 Introduction 1

1.1 The innate immunity system 1

1.2 Toll-like receptors 2

1.3 TLR4 inflammatory signaling 4

1.3.1 The MyD88-dependent pathway 7

1.3.2 The TRIF-dependent pathway 9

1.4 Small Rab GTPases in endosomal traffic 11

1.4.1 Endosomal trafficking 13

1.4.2 Rab4 and Rab5 13

1.4.3 Rab7 13

1.4.4 Rab11 14

2 Aim of study 15

3 Material and methods 17

3.1 Reagents, kits and solutions 17

3.2 THP-1 cells 18

3.2.1 Background 18

3.2.2 Maintenance of cell culture 19

3.2.3 LPS stimulation 19

3.3 Transient knock down using siRNA 20

3.3.1 siRNA transfection procedure 20
3.4 Flow Cytometry 21
3.4.1 Principle of method 21
3.4.2 Flow cytometry example procedure 21
3.4.3 Data collection and analysis 22
3.5 Quantitative-PCR analysis 23
3.5.1 Principle of method 23
3.5.2 Q-PCR example procedure 23
3.6 SDS-PAGE and western blotting 25
3.6.1 Principle of method 25
3.6.2 Western blotting procedure 25
4 Results 27
4.1 Optimizing the differentiation protocol of THP-1 cells 27
4.2 Further classification of PM located proteins 33
4.2.1 TLR4 33
4.2.2 CD11b 35
4.3 The effect of PMA concentrations and rest on LPS-induced IFN-β and TNF-α responses 37
4.3.1 IFN-β response in course of LPS stimulation 37
4.3.2 TNF-α response in course of K12 LPS stimulation 40
4.4 Dynamics of CD14 on the PM in different protocols 42
4.5 The effect of Rab4a depletion on LPS-induced TLR4 inflammatory signaling 44
4.1 The effect of Rab11a depletion on LPS-induced TLR4 inflammatory signaling 47
4.1.1 The effect of Rab11a depletion on LPS-induced cytokine expression 50

4.1.2 The effect of Rab11a depletion on proteins involved in regulation of LPS-induced TLR4 signaling 52

4.1 The effect of Rab7a depletion on LPS-induced TLR4 inflammatory signaling 55

4.1.1 The effect of Rab7a depletion on cytokine expression 58

4.1.2 The effect of Rab7a depletion on proteins involved in regulation of LPS-induced TLR4 signaling 60

5 Discussion 63

6 Final remarks and future aims 71

7 References 73

8 Appendix 83

List of Figures

FIGURE 1: TLR4 ACTIVATION TRIGGERS TWO DISTINCT PATHWAYS. 5
FIGURE 2: THE MYD88-DEPENDENT PATHWAY. 7
FIGURE 3: THE TRIF-DEPENDENT PATHWAY. 9
FIGURE 4: THE RAB GTPASES AND THEIR ROLE IN INTRACELLULAR VESICLE TRANSPORT. 11
FIGURE 5: THE CYCLING OF RAB GTPASES BETWEEN VESICLE MEMBRANE AND THE CYTOSOL. 12
FIGURE 6: THP-1 CELLS DIFFERENTIATED WITH 100 NG/ML PMA FOR 72 HRS. 28
FIGURE 7: THP-1 CELL DIFFERENTIATION PROTOCOL OPTIMIZATION (72 HRS PMA). 29
FIGURE 8: THP-1 CELL DIFFERENTIATION PROTOCOL (48 HRS PMA + 48 HRS PMA FREE). 30
FIGURE 9: THP-1 CELL DIFFERENTIATION PROTOCOL (48 HRS PMA + 72 HRS PMA FREE). 31
FIGURE 10: TLR4 PM LEVELS USING THE ALTERED DIFFERENTIATION PROTOCOL. 33
FIGURE 11: CD11B PM LEVELS USING THE ALTERED DIFFERENTIATION PROTOCOL. 35
FIGURE 12: LPS STIMULATED IFN-B EXPRESSION IN THP-1 CELLS DIFFERENTIATED WITH 48 HRS REST. 37
FIGURE 13: LPS STIMULATED IFN-B EXPRESSION IN THP-1 CELLS DIFFERENTIATED WITH 72 HRS REST. 38
FIGURE 14: LPS STIMULATED TNF-A EXPRESSION IN THP-1 CELLS DIFFERENTIATED WITH 48 HRS REST. 40
FIGURE 15: LPS STIMULATED TNF-A EXPRESSION IN THP-1 CELLS DIFFERENTIATED WITH 72 HRS REST. 41
FIGURE 16: THE PM DYNAMICS OF CD14 IN LPS STIMULATED THP-1 CELLS (48 HRS REST PMA-FREE MEDIUM). 42
FIGURE 17: THE PM DYNAMICS OF CD14 IN LPS STIMULATED THP-1 CELLS (72 HRS REST PMA-FREE MEDIUM). 43
FIGURE 18: WB CONFIRMATION OF RAB4A SILENCING (48 HRS PMA+ 48 HRS PM- FREE). 44
FIGURE 19: PM DYNAMICS OF CD14 IN RAB4A DEPLETED THP-1 CELLS (48 HRS PMA+ 48 HRS PMA-FREE). 45
FIGURE 20: WB CONFIRMATION OF RAB4A SILENCING (48 HRS PMA + 72 HRS PMA-FREE). 45
FIGURE 21: PM DYNAMICS OF CD14 IN RAB4A DEPLETED THP-1 CELLS (48 HRS PMA+ 72 HRS PMA FREE). 46
FIGURE 22: WB CONFIRMATION OF RAB11A SILENCING (48 HRS PMA + 48 HRS PMA-FREE). 47
FIGURE 23: PM DYNAMICS OF CD14 IN RAB11A DEPLETED THP-1 CELLS (48 HRS PMA+ 48 HRS PMA-FREE). 47
FIGURE 24: WB CONFIRMATION OF RAB11A SILENCING (48 HRS PMA + 72 HRS PMA-FREE). 48
FIGURE 25: PM DYNAMICS OF CD14 IN RAB11A DEPLETED THP-1 CELLS (48 HRS PMA+ 72 HRS PMA-FREE). 49
FIGURE 26: EXPRESSION OF IFN-B IN RAB11A DEPLETED CELLS. 50
FIGURE 27: EXPRESSION OF TNF-A IN RAB11A DEPLETED CELLS. 51
FIGURE 28: WB ANALYSIS OF KEY REGULATORS OF THE TLR4 SIGNALING PATHWAYS IN RAB7 DEPLETED CELLS. 52
FIGURE 29: WB ANALYSIS OF PROTEINS REGULATING TLR4 SIGNALING PATHWAYS IN RAB11A DEPLETED CELLS 53
FIGURE 30: WB CONFIRMATION OF RAB7A SILENCING (48 HRS PMA + 48 HRS PMA-FREE). 55
FIGURE 31: PM DYNAMICS OF CD14 IN RAB7A DEPLETED THP-1 CELLS (48 HRS PMA+ 48 HRS PMA-FREE). 56

FIGURE 32: WB CONFIRMATION OF RAB7A SILENCING (48 HRS PMA + 72 HRS PMA-FREE). 56
FIGURE 33: PM DYNAMICS OF CD14 IN RAB7A DEPLETED THP-1 CELLS (48 HRS PMA+ 72 HRS PMA-FREE). ... 57
FIGURE 34: EXPRESSION OF IFN-B IN RAB7A DEPLETED CELLS. 58
FIGURE 35: EXPRESSION OF TNF-A IN RAB7A DEPLETED CELLS. 59
FIGURE 36: WB ANALYSIS OF KEY REGULATORS OF THE TLR4 SIGNALING PATHWAYS IN RAB7 DEPLETED CELLS. 60
FIGURE 37: WB ANALYSIS OF PROTEINS REGULATING TLR4 SIGNALING PATHWAYS IN RAB7 DEPLETED CELLS. 61
FIGURE 38: LPS STIMULATED THP-1 CELLS BECOME APOPTOTIC (10X MAGNIFICATION). 83
FIGURE 39: LPS STIMULATED THP-1 CELLS BECOME APOPTOTIC (40X MAGNIFICATION). 84

List of Tables

TABLE 1: CHEMICALS AND REAGENTS 17
TABLE 2: KITS AND BUFFERS 17
TABLE 3: 2X LYSISBUFFER 18
TABLE 4: PREMADE LYSISBUFFER 18
TABLE 5: ANTIBODIES USED IN WB 85

|

Abbreviations

AP	Activated protein
ATCC	American type culture collection
BSA	Bovine serume albumin
CCL	Chemokine (C-C motif) ligand
CD	Cluster of differentiation
CLR	C-type Lectin receptor
CR3	Complement receptor 3
DC	Dendritic cell
DTT	Dithiothreitol
E. Coli	*Escherichia Coli*
ERC	Endosomal recycling compartment
FCS	Fetal calf serum
FIP	Rab11 family of interacting protein 2
FITC	Fluorescein isothiocyanate
FLC	Fluorescence channel
FSC	Forward scatter channel
GAP	GTPase activating proteins
GDF	GDI-displacement factor
GDI	GDP-dissociation inhibitor
GDP/GTP	Guanine di-/tri-phosphate
GEF	Guanine exchange factor
GPI-anchored	glycosylphosphatidylinositol-anchored
GTPases	guanosine triphospateses
HRP	Horse radish peroxidase
Hs	Homo Sapiens
IFN-β	Interferon-β
IκB	Nuclear factor of kappa light polypeptide gene enhancer in B-cells inhibitor
IKK	IκB kinase
IL	Interleukin
IRAK	IL-1 receptor-associated kinase
JNK	C-jun terminal kinase
KD	Knock down
LBP	LPS-binding protein
LRR	Leucine-rich-repeat
LPS	Lipopolysaccharide
Mφ	Macrophage
MAL	MyD88 adaptor like
MD2	Myeloid differentiation factor 2
MHC II	Major histocompatibility complex II
MyD88	Myeloid differentiation factor 88
NF-κB	nuclear factor kappa-light-chain-enhancer of activated B cells
NLR	Nod-like receptors
P-	Phosphorylated

PAMP	Pathogen associated molecular pattern
PBS	Dulbecco’s phosphate buffered saline
PE	Phycoerythrin
PIP	Phosphatidylinositol phosphate
PM	Plasma membrane
PMA	Phorbol 12-myristate 13-acetate
PRR	Pattern recognition receptors
Q-PCR	Real time quantitative polymerase chain reaction
Rab	Ras in brain
RIP	Receptor-interacting serine/threonine-protein
RLR	RIG-I-like receptors
RT	Room temperature
SDS-PAGE	SDS-Polyacrylamid gel electrophoresis
SSC	Side scatter channel
TAK1	Transforming growth factor-β-activated kinase 1
TANK	TRAF family member-associated NF-κB activator
TBK1	TANK-binding kinase 1
TGN	Trans golgi network
TIR	Toll-interleukin receptor
TIRAP	TIR-associated protein
TLR	Toll-like receptors
TNF	Tumor necrosis factor
TNFR1	TNF-receptor 1
TRAM	TRIF-related adaptor molecule
TRAF	TNF receptor associated factors
TRIF	TIR-domain-containing adapter-inducing interferon-β
UBC13	Ubiquitin-conjugating enzyme 13
VD3	Vitamin D3
WB	Western blotting
WT	Wild type

1 Introduction

1.1 The innate immunity system

The innate immunity system is the body's first line of defense, active from the day we are born. The ability of the innate immunity to respond to pathogenic invaders is essential for the health and survival of an organism. How the innate immunity responds to these threats, as well as its function as a primer forming a stronger and more specific adaptive immune response, have been subject to decades of intense research. How they work, and how the cells of the innate immune system detect and relay information about bacteria, viruses, parasites and fungi are yet to be fully comprehended.

Over the course of evolution, organisms have generated a number evolutionary conserved pattern recognition receptors (PRRs) in order to defend itself from invading pathogens. These germline encoded PRRs are expressed consistently during the life cycles of certain cells, and are independent of immunological memory, in contrast to that of B-cells. The PRRs recognize conserved pathogen associated molecular patterns (PAMPs) [1]. The PAMPs are highly evolutionary conserved molecular structures that are indispensable and specific for a group of pathogens, and different from the host molecules. In this way the innate immunity is able to distinguish between potentially dangerous invaders and self-molecules. As the evolutionary rate of change is exceedingly low for these PAMPs, so the PRRs of the innate immunity are able to target these with high specificity over several generations.

The first of the PRRs to be recognized was the Toll-like receptor (TLR) 4 [2]. To date there has been described thirteen known functional TLRs between humans and mice, however, only ten of these are expressed in humans[3]. Later other classes of PRRs have been identified such as the RIG-I-like receptors (RLR) [4], the Nod-like receptors (NLR) [5], and the C-type lectin Receptors (CLR) [6] and there are still suspected to be further classes of unknown PRRs. These PRRs are able to induce cellular responses towards a wide range of bacterial, viral, parasitic and fungal PAMPs, as well as cytokines and cellular stress. PAMPs can range from lipopolysaccharides (LPS), di- and tri-acyl lipopeptides, flagellin, or bacterial or viral DNA/RNA [7-10]. The detection of one of these pathogenic factors by a PRR will induce a cellular response that calls the innate immunity into action to fight of the infection, as well as priming a specific adaptive immunity inflammation if needed [11, 12].

Monocytes are cells of the innate immunity that carry an abundance of different PRRs. They are white blood cells that classified among the leukocytes and are extremely potent in reacting towards foreign threats. They are of special interest in the system of the innate immunity due to their extensive sum of responses when activated. Their ability to detect the presence of PAMPs via PRRs and consequently mount a specific inflammatory response towards these is crucial for the host's defense. Monocytes will in the case of an infection relocate to the site of infection, where they will be exposed to PAMPs from the invading microorganism. This will in turn cause them to differentiate into macrophages (Mφ) or dendritic cells (DCs), serving specialized functions in innate immunity. Mφs and DCs both play important roles as they phagocytose pathogenic microorganisms, release cytokines, and present antigens, necessary to induce an adaptive immune response[13, 14].

1.2 Toll-like receptors

TLRs are one of the classes of evolutionary conserved PRRs that have been one of the most intensely researched. TLRs are expressed on cells of the innate and adaptive immunity but also on cells such as fibroblasts and epithelial cells [15, 16]. They are a series of type I transmembrane receptors with a number of leucine-rich-repeat (LRR) motifs in their ligand binding domains [17].

TLRs recognize a wide variety of different PAMP's that are present in pathogens such as Gram-positive and Gram-negative bacteria, different types of viruses and fungi. Activation of a TLR by any such PAMP would prompt a specific cellular response in order for the cell and organism to defend itself. The various TLRs have evolved to be located at different sites or compartments in the cell. TLR1, TLR2, TLR4, TLR5 and TLR6 are all located at the plasma membrane (PM) and react towards PAMPs that can be found in the extracellular environment, such as LPS found on Gram negative bacteria or the flagellin protein [3, 7, 9]. TLR3, TLR7 TLR8 and TLR9 are expressed in intracellular vesicles in the endolysosomal pathway. Here they respond towards PAMPs such as bacterial or viral DNA/RNA that might be exposed in the endosomal compartments during infection [3]. This distinct compartmentalization is essential for the ability of TLRs to detect their specific PAMPs as well as their connection with the specialized signaling machinery associated with the TLRs [18]

The TLRs have the ability to form homo- and heterodimers such as TLR3-TLR3 [19] and TLR2-TLR6 [20], forming a horseshoe-shaped ectodomain that bind their ligands [3, 19]. The ability for some TLRs to associate with other TLRs in more than one way creates a broader

range of their pathogen detection abilities, increasing their capabilities to defend the host organism [20].

Activated TLRs are dependent on the recruitment of specific adaptor proteins initiate their inflammatory response. These adaptor molecules contain the toll-interleukin receptor (TIR) that binds the TIR-domain of the TLRs to initiate signaling. Members of the TIR-signaling adaptors are the Myeloid differentiation factor 88 (MyD88), TIR-associated protein (TIRAP) (also known as MyD88 adaptor like (MAL)), the TIR-domain-containing adapter-inducing interferon-β (TRIF), and the TRIF-related adaptor molecule (TRAM). Each of the TLRs are able to interact in a highly specific manner toward one of these adaptor molecules. This interaction is central to determine the signaling cascade created in response to pathogenic stimuli. However, MyD88 and TRIF are key regulators [21] and control two distinct signaling pathways upon TLR4 activation that are known as the MyD88-dependent pathway and the TRIF-dependent pathway, respectively [22]. TLR4 is to date the only TLR that is known to utilize all these adaptor molecules [23]. The recruitment of these adaptor molecules are the first link to the cytosolic signaling cascade that eventually leads to the recruitment of specific transcription factors, effectively inducing the expression of genes of essential inflammatory cytokines [18].

A series of regulating proteins are called into action to relay the inflammatory response upon activation of the TLRs. However, these inflammatory responses might be excessive and lead to life threatening conditions in the host organism. A disproportionally strong inflammatory response towards a pathogenic ligand can induce potentially fatal sepsis [24, 25]. Another potential risk is that unwanted chronic responses and autoimmune diseases arise due to a flawed genetic structure [26]. Achieving a greater understanding of how the inflammatory signaling through TLRs are both relayed and regulated is therefore vital to understanding how to treat bacterial and viral diseases, as well as chronic and autoimmune conditions.

1.3 TLR4 inflammatory signaling

TLR4, located on the PM and in the ERC [27], is the most well described of the TLRs. It induces inflammatory signaling upon recognition of LPS [28], a structural protein commonly found on Gram-negative bacteria, such as *Escherichia Coli (E. coli) [21]*. Upon contact with this PAMP in the extracellular environment, TLR4 is activated and initiates an intracellular signaling cascade by recruiting certain adaptor molecules.

TLR4 is able to induce two distinct pathways upon stimulation with quite different outcomes (Fig. 1). One being activated immediately from the PM known as the MyD88-dependent pathway and the other activated from the intracellular compartments known as early endosomes (EEs) known as the TRIF-dependent pathway [29].

Upon activation, TLR4 is dependent on several co-receptors such as Myeloid Differentiation Factor 2 (MD2) [30], Cluster of Differentiation 14 (CD14) [31], and LPS-binding protein (LBP) [32, 33] to initiate a full inflammatory response. CD14 is a glycosylphosphatidylinositol-anchored (GPI-anchored) protein and is considered to be one of the most essential factors in regulating the inflammatory response of TLR4. CD14 is necessary for the binding and translocation of LPS to the MD2-TLR4 complex [34], and an important regulator of the endocytosis of the LPS bound MD2-TLR4 complex [35] that is required to activate the TRIF-dependent pathway [11, 36].

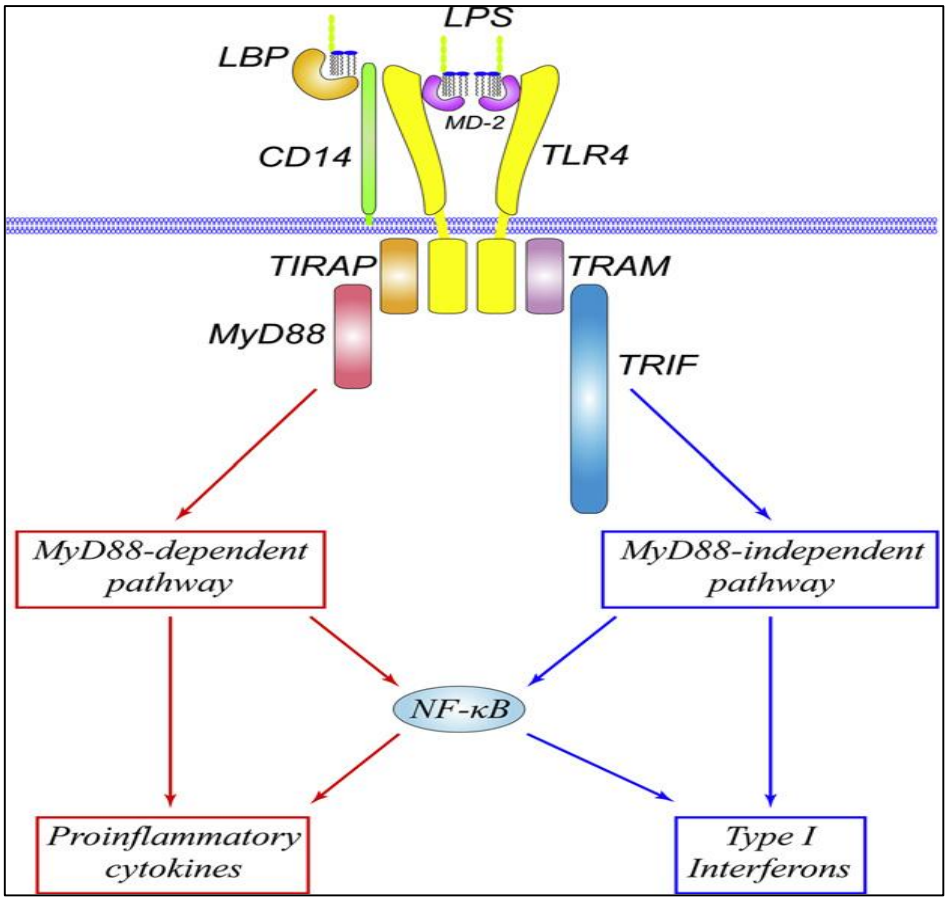

Figure 1: TLR4 activation triggers two distinct pathways.
LPS activated TLR4 at the PM. Activated TLR4 is able to recruit two sets of distinct adaptor molecules that triggers two distinct pathways. TIRAP and MyD88 trigger the MyD88-dependent pathway while TRAM-TRIF triggers the TRIF-dependent pathway (also known as the MyD88-independent pathway). TLR4 is the only known TLR that is able to utilize all of the four known TIR adaptor molecules. Illustration acquired from Lu, et al 2008 [22]

LBP is an acute-phase protein found circulating in the bloodstream. It is secreted from a variety of host tissues induced by Interleukin 6 (IL-6) and Interleukin 1 (IL-1) [33]that is found circulating in the bloodstream. At low concentrations it is able to effectively detect and bind LPS and subsequently interact with CD14 in order to effectively support an inflammatory response [32]. LBP also plays a role in the negative regulation of inflammation as high concentrations have been suggested to inhibit LPS-induced cell activation and thus preventing potentially lethal sepsis [37].

LBP promotes the transfer of LPS on to CD14 [32]. CD14 has not been linked to induce any form of cellular response on its own, but plays an essential part in the translocation of LPS along the PM to protein complexes serving this function [38]. It's most noted for its role in coherence with TLR4, where it is both necessary for the LPS transfer and sensitivity of the MD2-TLR4 complex [39], as well as a CD14/LPS-dependent endocytosis event required for the TRIF-dependent pathway of TLR4-stimulation [35, 40].

MD2 is a protein that physically interacts with TLR4 that is instrumental for TLR4 signaling [30]. CD14 interacts with MD2 in order to enhance its LPS binding properties although MD2 is capable of binding LPS in the absence of CD14 and LBP [41, 42]. Upon interaction with CD14 and LPS, MD2 forms a heterodimer with TLR4, and this interaction is crucial for TLR4 to steadily interact with LPS in order to increase TLR4s stimulatory abilities [43, 44]. The MD2-TLR4 complex subsequently dimerize on the PM, which allows the activated TLR4 to induce an intracellular inflammatory response. MD2 has also been reported to have a role in efficient recruitment of TLR4 to the PM as TLR4 was mostly restrained in an intracellular compartment in MD2 deficient mice [43].

1.3.1 The MyD88-dependent pathway

The initial pathway to be activated is the MyD88-dependent pathway (fig. 2). The MyD88-dependent pathway is activated directly from the PM when TLR4 is exposed to its ligand in the extracellular environment [31].

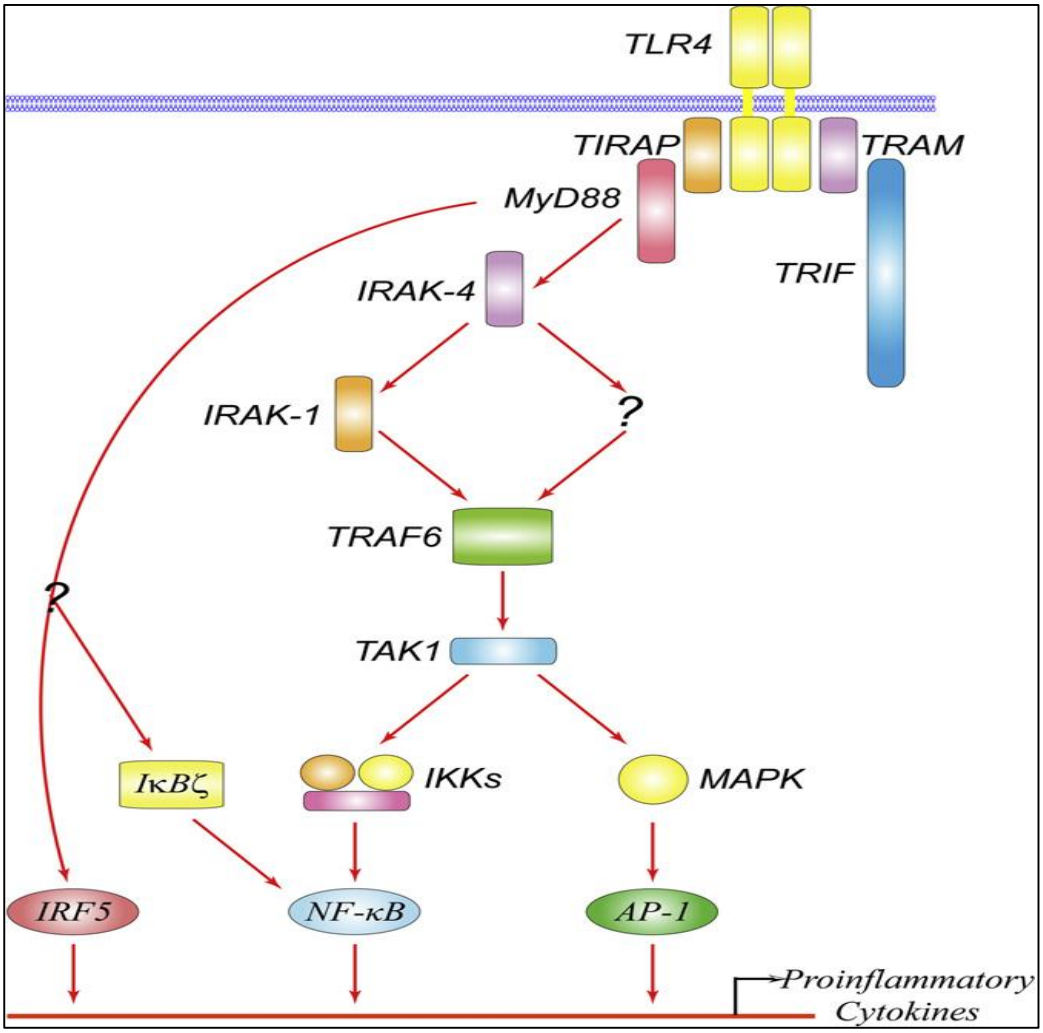

Figure 2: The MyD88-dependent pathway.
The recruitment of TIRAP and MyD88 to activated TLR4 on the PM results in the assembly a specific intracellular signaling cascade resulting in the production of proinflammatory cytokines. Proteins such as IRAK4, IRAK1 TRAF6, and TAK1 regulate the downstream activation of IKKs and MAPK. The activation of IKKs and MAPK result in the nuclear translocation of transcription factors such as NF-κB and AP1 that cause the transcription of proinflammatory cytokines such as TNF-α. Illustration acquired from Lu, et al 2008 [22]

The dimerization of the MD2-TLR4 complexes following LPS stimulation allows for the specific TIR-domain-containing proteins TIRAP and MyD88 to be recruited to the cytosolic TIR-domain of TLR4. The activated cytoplasmic TIR-domain of TLR4 readily interacts with the TIR-domain in the C-terminal portion of MyD88 [30, 45]. This interaction leads to the recruitment of TIRAP through their N-terminal death domains [30, 45]. TIRAP have in addition to its death domain a phosphatidylinositol 4,5-bisphosphate (PIP2) binding domain in its N-

terminal portion, which assist in its translocation to the plasma membrane, supporting its interaction with MyD88 [46-48].

When recruited the MyD88 and TIRAP complex in turn recruit the downward signaling protein IL-1 receptor-associated kinase 4 (IRAK4) through a homotypic interaction with both of their N-terminal death domains [49]. The role of IRAK4 in TLR signaling is thought to be to activate and degrade IRAK1 [50]. IRAK1 and IRAK2 establish a complex that mediates the signaling onward to TNF receptor associated factor 6 (TRAF6) [51] that in cooperation with ubiquitin-conjugating enzyme 13 (UBC13) activates Transforming growth factor-β-activated kinase 1 (TAK1) [52].

TAK1 is responsible for the activation of IκB kinase (**IKK**), c-jun terminal kinase (JNK), and mitogen-activated protein kinase (**MAPK**) [52, 53]. The mature forms of NF-κB are held in the cytoplasm by the physical interaction with IκBα that mask the nuclear translocation signal of NF-κB [54]. The activation of IKK result in amino specific phosphorylation of IκBα, consequently resulting in polyubqutination of IκBα and its degradation by the 26S proteasome. Now that the nuclear translocation signal of NF-κB is exposed it translocate to the nucleus and induce the production of proinflammatory cytokines [54]. MAPK regulates the activity of the transcription factor CREB [55, 56], while JNK activation result in in the nuclear translocation of Adaptor protein 1 (AP1) that both lead to their distinct induction of cytokines [57, 58].

MyD88 is also responsible in similar activation of all the other TLRs, with the exception of TLR3 [59], but are in many of these pathways not dependent on neither TIRAP nor IRAK4, though these and other effector proteins may play similar roles such as TIRAP in the activation of TLR2 [47]. MyD88 is then responsible for the recruitment of IL-1r-associated kinase 4 (IRAK4) and IRAK1. Activated IRAK-1 in complex with MyD88 and IRAK4 phosphorylates TRAF6 [60]. TRAF6 controls several downstream pathways which all regulate NF-κB dependent gene expression. MyD88 and its ability to interact with several of these adaptor molecules, makes it a potent seat for the initiation of signaling in many events.

1.3.2 The TRIF-dependent pathway

The TRIF-dependent pathway (also commonly called the MyD88-independent pathway) was discovered at a later time point when MyD88 deficient cells showed a delayed activation of NF-κB and MAPKs when stimulated with LPS (Fig. 3) [21]. The TRIF-dependent pathway is brought on by the internalization of TLR4 in a CD14-dependent manner [35]. This pathway can both boost the primary MyD88-dependent pathway response [51, 61], and induce the expression of type-1 interferons such IFN-β and IFN-α [62].

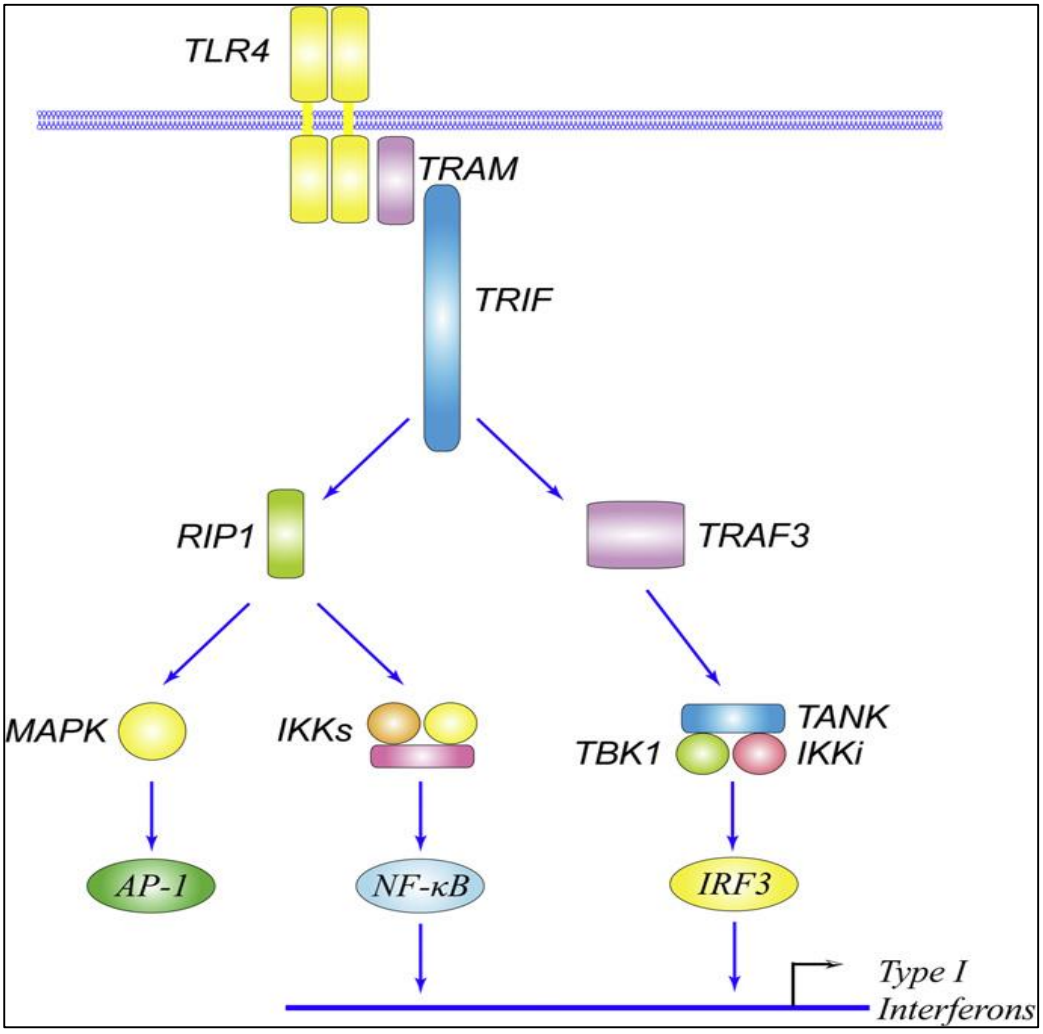

Figure 3: The TRIF-dependent pathway.
The TRIF-dependent pathway (also known as the MyD88-independent pathway) is activated from endosomes. TRAM and TRIF is recruited to activated TLR4 that has been internalized from the PM. TRIF is able to recruit proteins such as RIP1 and TRAF6 that result in the late activation of NF-κB, essentially boosting the MyD88-dependent pathways production of proinflammatory cytokines. TRIF is also able to recruit downstream effectors such as TRAF3, TANK, TBK1, and IKKι that regulate the activation of IRF3. IRF3 is a transcription factor that upon activation dimerizes and translocate to the nucleus to regulate the production of type I interferons whose expression is particular to the TRIF-dependent pathway *Illustration acquired and modified from Lu, et al 2008* [22].

Once located on EEs the cytoplasmic TIR-domain of TLR4 associates with TRAM [63, 64], which serves as an intermediate adaptor molecule for TRIF in much the same way as TIRAP in the TLR4 MyD88-dependent pathway [65]. TRAM is also found to be located on the cytosolic side of the PM as well, but have not been described to play any sort of function in TLR4 activated signaling from this location[66].

The TRAM/TRIF complex contributes to two signaling paths. TRIF actively recruits TRAF6 and Receptor-interacting serine/threonine-protein 1 (RIP1). Both proteins have been linked to the activation of late phase NF-κB, essentially contributing to the outcome of the MyD88-dependent pathway [67, 68]. TRIF binds to TRAF6 through its N-terminal region of TRIF [67], while RIP1 binds to the C-terminal part. TRAF6 and RIP1 undergo polyubiqunation and forms a complex with TAK1 leading to a substantial and prolonged NF-κB expression, as a complement to the MyD88-dependent pathway [61]. Rip1 has also been linked to regulating necroptosis and apoptosis through TNF-dependent activation of the TNF-receptor 1 (TNFR1) [69].

The alternate TRIF-dependent pathway starts with the TRAM/TRIF complex's recruitment of TRAF3 [70, 71]. TRAF3 interact with the N-terminal region of TRIF and undergo auto-ubiquitination [72] and the assembly of a complex consisting of TRAF family member-associated NF-κB activator (TANK) binding kinase 1 (TBK1) and nuclear factor of kappa light polypeptide gene enhancer in B-cells inhibitor (IκB) kinase- (IKK) –ι (also known as IKKε) [73]. The complex formed mediates downstream signaling as they regulate the dimerization and translocation of IRF3 to the nucleus [73, 74]. It is this translocation that results in the transcription of type I interferons such as IFN–β, IFN-α, and the Chemokine (C-C motif) ligand (CCL) 5 [75].

1.4 Small Rab GTPases in endosomal traffic

A unique group of the Ras superfamiliy of G-proteins are known as the Ras in brain proteins of small Guanosine Triphosphatases (Rab GTPases). They are essential regulators in intracellular vesicular trafficking (Fig. 4) [76]. They control endosomal maturation and transport of membrane enclosed vesicles all throughout the cell just to mention a few of their roles [76].

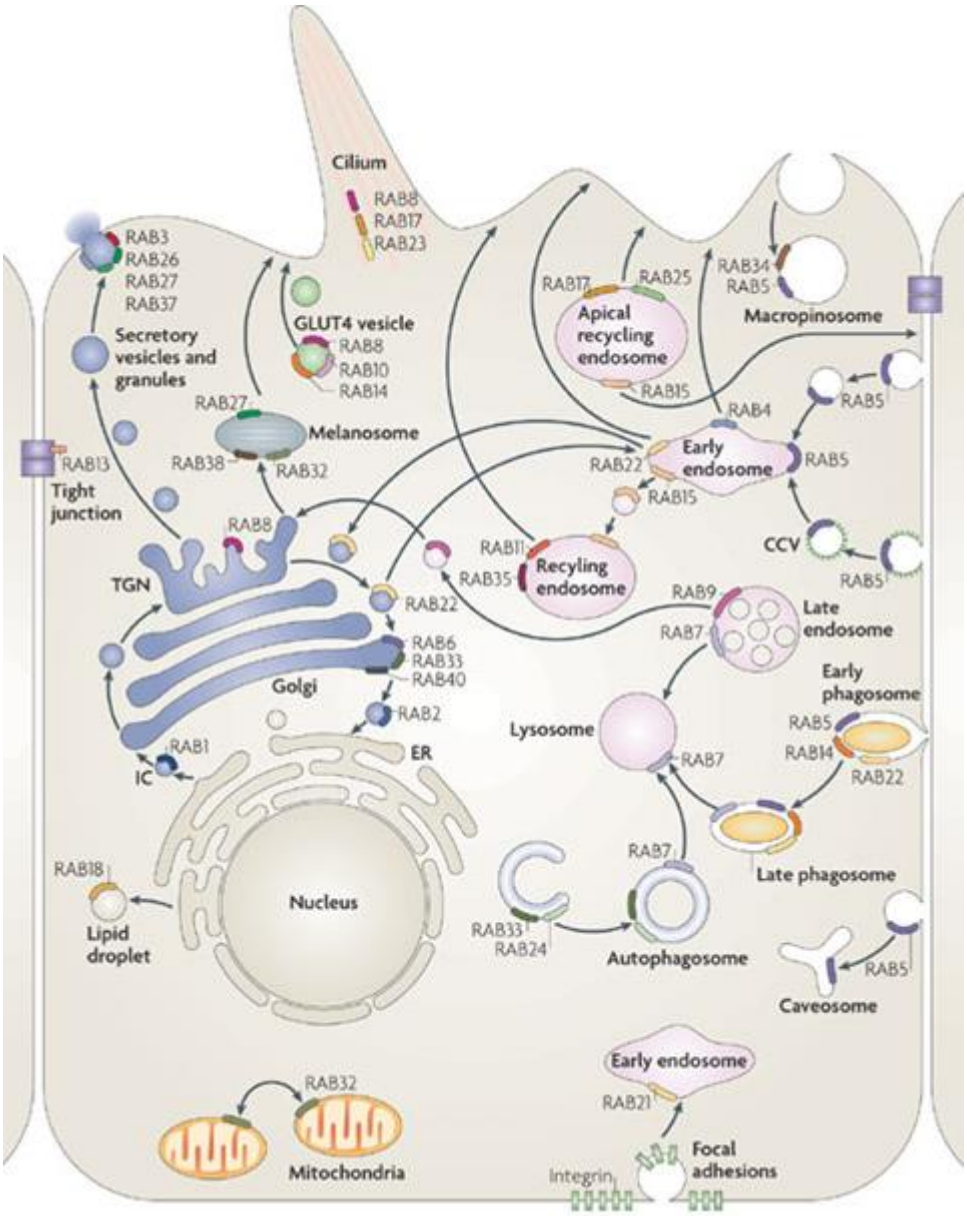

Figure 4: The Rab GTPases and their role in intracellular vesicle transport.
The Rab GTPases have been implemented in roles regulating most parts of the intracellular vesicle trafficking. They control vesicle movement, budding, membrane identity and recycling of endocytosed content. The vast number of Rab GTPases creates a highly specific intracellular network, allowing for highly specific vesicular interactions. *Illustration acquired from Stenmark, et al 2009* [76]

Their activity is regulated by the replacement of GDP to GTP, switching them from their inactive form to the active state (Fig. 5). In order for the Rabs to switch from their inactive to active state they rely on the attached GDP-dissociation inhibitor (GDI) to be released by the GDI-displacement factor (GDF). This reveals the Rabs prenyl groups that anchor the Rabs to the membrane [77, 78]. The GDFs are located on the cytosolic side of specific organelles in order to assure certain Rabs localization and specific function to that organelle. Once associated with the limiting membrane of an organelle a Guanine exchange factor (GEF) catalyzes the GDP/GTP exchange, that in turns activate the specific Rab to fulfill its function [79]. GTPase activating proteins (GAP) regulate this activity by hydrolyzing GTP back to GDP, inactivating and releasing the Rabs back to the cytosol. This ability to change between active and inactive states make Rab GTPases function as molecular switches turning signaling pathways and cellular processes on or off.

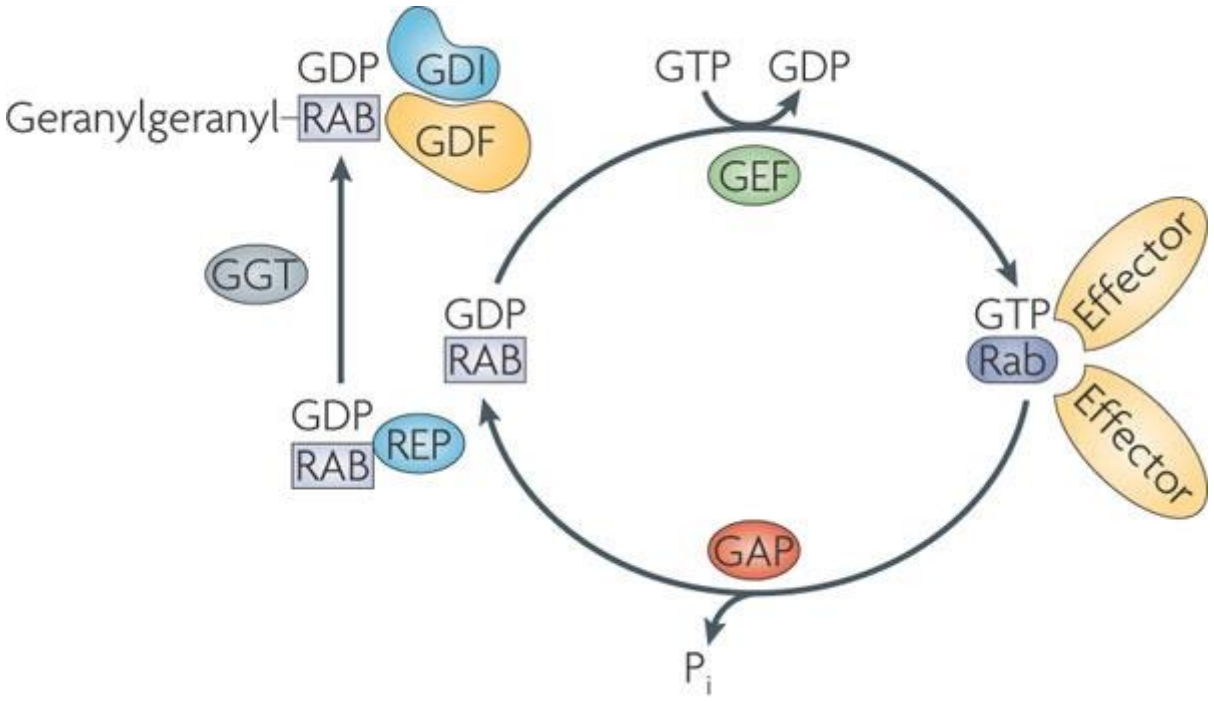

Figure 5: The cycling of Rab GTPases between vesicle membrane and the cytosol.
Rab GTPases cycle between their inactive GDP-bound form and their active GTP-bound form. In their inactive GDP-bound form they are found in the cytosol associated with GDI, stabilizing their GDP-bound form. GDI is detached through the means of GDF, allowing the activation of Rab GTPases through binding of GTP, assisted by the GEF. Activated Rab GTPases are able to associate with membrane and their specific effector proteins. Their activity is ended by GAPs that through hydrolytic actions cleave GTP to GDP, inactivating them and returning them to the cytosol. *Illustration acquired from Stenmark, et al 2009 [76]*

1.4.1 Endosomal trafficking

EEs continue to grow in size as they receive content from newly formed endocytic vesicles. Internalized content such as transmembrane proteins that are not recycled back to the PM are continuously internalized into intraluminal vesicles forming in the EEs. The interior of the EEs gradually increase in acidity, until a certain threshold is reached and it matures into a late endosome (LE) replacing their Rab5 positive membrane with a Rab7 positive membrane [80]. Rab7 is involved in several LE functions and regulates the formation of the endolysosome, the compartment that regulates the degradation of its vesicular contents [80]. The degraded material can either be reused in the cell, or it can in the event of foreign material be loaded onto Major histocompatibility complex II (MHC II) and exposed to the extracellular environment in order to alert cells of both innate and adaptive immunity of the current threat [81, 82].

1.4.2 Rab4 and Rab5

Rab4 and Rab5's roles are both connected to the EEs. Rab4 is involved in the rapid recycling of content back to the PM [83], whereas Rab5 is involved in several processes involving signaling, maturation and trafficking related to EEs [80, 84, 85].

The two isoforms Rab4a and Rab4b both function in EE to PM recycling [86]. They both have been described in certain roles related to immunity, recycling receptors such as MHC II by Rab4b [87], and recycling/regulation of CD4 by Rab4a [88]. That both of these isoforms can play other parts in immunity related signaling and trafficking is not unlikely.

1.4.3 Rab7

Rab7a is one of the key markers of LEs and has several functions including motility, trafficking, and endosome/phagosome maturation [89-92]. Rab7a has been shown to play a role in both motility of autophagosomes [91, 93] and the maturation of EEs/phagosomes [89] which is necessary for the degradation of active TLR4 [94]. It is not unlikely that Rab7a assert some direct control over immunity related events.

Rab7b was first described in 2004 and is located primarily on endolysosomes and in the TGN [95, 96]. It is mainly expressed in monocytes, monocyte derived DCs, and monocytic leukemia cells such as the THP-1 cells and it has been shown that it is also mainly expressed in cells expressing CD14 [95]. When stimulated with LPS the expression level of Rab7b was downregulated in DCs while it was up regulated in monocytes [95]. The expression is also up regulated in cells differentiated with PMA [95]. Rab7b was first linked to many of the same roles in trafficking such as Rab7a [94], however, it has now been recognized that its role is in

the trafficking of content from EEs to TGN [96]. Rab7b has been reported to be an important factor in the recycling of TLR4 through TGN and Golgi as cells silenced for Rab7b shows TLR4 restrained in EEs and LEs, likely resulting in a prolonged signaling of the TRIF-dependent pathway [94]. Overexpression of Rab7b resulted in the inhibition of the TRIF-dependent pathway as well as the MyD88-dependent pathway [94].

1.4.4 Rab11

Rab11 is another Rab that is associated with endosomes and play a function with the slow recycling pathway as cellular components that are tagged for recycling are transported to the peri-centriolar endosomal recycling compartment (ERC). From here the cellular components can be recycled back to the plasma membrane [97].

Rab11 exists in three isoforms. These are Rab11a and Rab11b which are generally expressed in all tissue, and Rab25 which expression is only found in epithelial cells [98, 99]. Rab11a are regulating the slow recycling of protein back to the plasma membrane and is mainly located in the endosomal recycling compartment **(ERC**) [97]. Rab11a is able to recruits Rab11 family of interacting protein 2 **(FIP2)**, which in turn recruits the actin motor Myosin Vb that regulates cargo containing vesicle movement along actin filaments [100, 101].

Rab11a has also been reported to be associated with phagosomes [102], and to be involved in the intracellular transport of pro-TNF from the Golgi complex to the phagocytic cup [103]. Rab11a is also involved in a regulatory role concerning the trafficking of TLR4 to phagosomes, linking Rab11a to a regulatory role in IFN-β production [27]. TLR4 vas first believed to have a large intracellular pool located in the Golgi apparatus [42, 104], however, Rab11a has been shown to colocalize with TLR4 in the ERC, which is located inside the Golgi ring [27, 105]. Rab11a was shown to control TLR4 trafficking in and out of this compartment and also the TLR4 translocation to the *E. coli* phagosome [27].

2 Aim of study

Rab4a and Rab11a are known to function in the recycling of internalized transmembrane receptors back to the PM in a rapid and slow recycling pathway, respectively. Rab7a participates in maturation of endosomes, and the delivery of transmembrane proteins for lysosomal degradation. We hypothesized that Rab4a and Rab7a are active participants in regulation of TLR4 signaling in general and the TLR4-TRIF signaling in particular, by governing the recycling and degradation of TLR4. We aimed to describe a role for Rab4 and Rab7 in TLR4 signaling, as earlier described for Rab11a, as well as investigating the role of Rab11a further in the THP-1 model system [27]. We will focus on the following aims:

Aim 1: Establish a working protocol for the differentiation of THP-1 cells, allowing the study of the signaling and trafficking pattern in a Mφ comparable model cell system.

Aim 2: Investigate changes in the PM expression levels of CD14 and TLR4 in differentiated THP-1 cells. CD14 might be a more viable choice as it is expressed in larger amount compared to TLR4 at the PM [106]. Using both flow analysis and real time quantitative polymerase chain reaction (Q-PCR) to achieve a preliminary understanding of signaling and trafficking on the basis of the developed protocol.

Aim 3: Use the developed THP-1 cell differentiation protocol to determine the effects of Rab4a, Rab7a, and Rab11a knockdowns on PM expression levels of CD14 and TLR4 using Flow cytometry analysis.

Aim 4: Correlate findings from Aim 1 & 2 with studies to determine how Rab4a, Rab7a and Rab11a knockdown affect the LPS-induced TLR4 signaling in optimally differentiated THP-1 cells.

3 Material and methods

3.1 Reagents, kits and solutions

Table 1: Chemicals and reagents

Distributor	Product	Usage
5 Prime	Isol-RNA lysis reagent	Q-PCR
AppliChem	DTT Molecular biology grade	WB
ATCC	RPMI 1640 High glucose	Cell cultivation
	THP-1 Cells	Cell cultivation
BD Pharmingen	CD11b/Mac-1 PE ICRF44	Flow Cytometry
	CD14 FITC M5E2	Flow Cytometry
	CD16 FITC 3G8	Flow Cytometry
Dako	Polyclonal Goat Anti-Rabbit Immunoglobulins (hrp)	WB
	Polyclonal Goat Anti-mouse Immunoglobulins (hrp)	WB
Gibco	Fetal Calf Serum (FCS)	Cell cultivation
	Ultrapure K12 LPS	WB, FLOW, Q-PCR
	OptiMEM	siRNA
	Tryphan Blue	Cell cultivation
Invitrogen	Lipofectamine RNAi max reagent	siRNA
Novex	4-12% bis-tris NuPage gradiant Gel	WB
	4x Sample Buffer	WB
	20x MOPS running buffer	WB
Roche	PhosphoStop	Lysisbuffer (WB)
	Protease inhibitor	Lysisbuffer (WB)
Sigma Aldrich	β-mercaptoethanol	Cell cultivation, WB
	Accutase	Flow Cytometry
	Bovine Serum Albumin	WB
	Dulbecco's phosphate buffered saline (PBS)	General Cell work
	Ganzumycin	Cell cultivation
	PMA	Cell cultivation
St. Olav Blood bank	A+ Serum	WB, FLOW, Q-PCR
Thermo Scientific	Maxima First Strand cDNA Synthesis Kits*	Q-PCR
Qiagen	Hs RAB4a 5 FlexiTube siRNA	Q-PCR
	Hs RAB7a 5 FlexiTube siRNA	Q-PCR
	Hs RAB11a 5 FlexiTube siRNA	Q-PCR
	Qiagen RNeasy mini kit*	Q-PCR

Table 2: Kits and buffers

Buffers	2x Lysisbuffer
	TBS-Tween (0.01% Tween)
	5% BSA
Thermo Scientific	Maxima First Strand cDNA Synthesis Kits
Qiagen	Qiagen RNeasy mini kit

Table 3: 2x Lysisbuffer

Components	Working solution
Glycerol	10%
NaF	50mM
Tris HCL	50mM
EDTA	1mM
EGTA	1mM
NaCl	157mM
Triton x-100	1%
Na_3Vo_4	1mM
Sodium Deoxycholate	0,5 %

Table 4: Premade lysisbuffer

Components	Chemicals and Reagents
2x lysisbuffer (Table 3)	5 ml
dH_20	~5 ml
Phosphostop	1 tablet
Protease Inhibitor	1 tablet
PMSF	100 µl
Benzonase	1 µl

3.2 THP-1 cells

3.2.1 Background

THP-1 cells were originally cultured from the peripheral blood of an infant boy suffering from acute monocytic leukemia, a disease that leads to the unimpeded growth of monocytes. THP-1 cells were first characterized in 1980 by S. Tsuchiya and was deemed to be a leukocytic cell line with a multitude for common markers equal to those of monocytes [107]. The THP-1 cells can be shortly described as singular cells with a large and round morphology. They have Fc- and C3b receptors, but immunoglobins are absent. They are able to induce inflammatory responses, such as the production of IL-1 and TNF-α. They can be differentiated into macrophage-distinct entities by either phorbol 12-myristate 13-acetate (PMA) or Vitamin D3 (VD3). It should be noted that PMA and VD3 results in differentiated THP-1 cells with distinct signaling and characteristics [108]. Cells differentiated with PMA become adherent and obtain more Mφ-like appearances, as VD3 differentiate cells do not. PMA differentiated cells display a higher rate of phagocytosis and expression of TNF-α. They also express higher levels of CD11b, but a lower amount of CD14, compared to VD3 differentiated THP-1 cells. [108]

3.2.2 Maintenance of cell culture

The THP-1 cells used originated from American Tissue Culture Center (ATCC). The cells were grown in ATCC modified RPMI 1640, containing L-glutamine and Hepes. In addition to this the medium was supplemented with 10 % FCS, β-merkaptoethanol, and Gansumycin in an environment of 5 % CO2 at 37° C. The cells were split after two or three days in order to keep the cells within optimal density (not exceeding 1,0 x 10^6 cells/ml) as they can undergo certain morphological changes if excessively stressed.

For experiments the cell suspension was transferred to a 50 ml Falcon tube and spun down for 8 min at 125 g, 20° C. The supernatant was discarded and the pellet dissolved in 5 ml of medium. For experiments involving siRNA transfection Ganzumycin was excluded from the medium, due to the toxicity of antibiotics when working with the specific transfection reagents.

A sample of 10 µl was mixed with 10 µl of Trypan blue and used to calculate the number of live cells using the Countess® Automated Cell Counter from Invitrogen and the total number of live cells was determined. Then the volume was increased by the addition of extra medium to obtain proper cell density for the experiment and PMA added to differentiate the cells. The suspension was then seeded in 6-well plates with 2 ml of suspension in each well. The preferable density of cells were 350 000- 400 000 cells per well. The seeded cells were transferred to incubators that maintained 5 % CO_2 at 37° C.

3.2.3 LPS stimulation

LPS stimulation was used when we were interested in studying the behavior of a target receptor or signaling cascade in the activated TLR4 pathways. We used the ultrapure K12 LPS, alternatively called rough LPS, for this task. K12 LPS is distinct by the fact that it lacks the O-side chain found on wild type (wt) LPS, which is commonly called smooth LPS. [109]. The ultra-pure form is required to reduce any cross activation of other TLRs such as TLR2. [110]

Prior to the LPS stimulation the medium was removed and replaced with 1 ml of fresh medium. The K12 LPS by vortexing and sonication for 30 seconds each. Then K12 LPS was dissolved in a 1:1000 ratio in A+ serum and heated to 37° C. 100 µl of the K12 LPS mix (100 ng/ml) was added to the wells at specific time points

3.3 Transient knock down using siRNA

Small interfering RNA, commonly called siRNA, is a method of targeting and greatly reducing the expression of a certain mRNA. Double stranded RNA (dsRNA) oligos that is complementary towards the mRNA of interest is transfected into the cell using a specific set of reagents, ensuring the optimal conditions for both cell vitality and transfection success. Once the dsRNA oligos has been transfected into the cell it is subsequently targeted by dicer enzymes, reducing the dsRNA into short on average ~22 basepair long siRNA strands. These ~22 long siRNA strands are guided by the dicer complex and assisting the siRNA to form an RNA interacting silencing complex (RISC) that possesses catalytic cleavage activity towards the transfected siRNA. The siRNA is untwined in the RISC complex and generates a single stranded RNA strand that are able to locate and associate to complementary mRNA strands situated in the cytosol. This triggers the sequence specific degradation of the mRNA in question and results in the abolished expression of the target protein [111].

3.3.1 siRNA transfection procedure

Cells were seeded as described above, 24 hrs pre-transfection with siRNA. During siRNA transfection it is important to reduce the possibility of RNase contamination that could offset the results. In order to reduce this risk of contamination filter tips and separately packed eppendorf tubes were used, as well as increased caution overall. In order to make the transfection mix, two separate mixtures were prepared. The first mix contained 490µl OptiMEM and 10µl Lipofectamine RNAi max reagent was subsequently set aside to rest for 5 min. The second mixture contained 496µl of OptiMEM and 4µl of the target siRNA (specific targets can be found in the table in section 3.1.1). The mixtures were combined to create one final 1ml transfection mix, and subsequently set aside to incubate for 18-20 min at room temperature (RT). Upon transfection 475 µl of the medium was discarded from the wells, and 485 µl of the transfection mix added to the cells. This ensured a final solution of approximately 16nM of siRNA in each well. The cells were returned to the incubator for 24 hrs, before the total medium in the wells were substituted with 2 ml of fresh medium without PMA, siRNA and antibiotics. The cells were then incubated for either 48 hrs or 72 hrs depending on the experiment.

3.4 Flow Cytometry

3.4.1 Principle of method

Flow cytometry is the monitoring of physical and/or chemical characteristics of cells or particles when passed through a ray of light at a certain wavelength (commonly a laser beam) in a laminar flow of fluids. When passing the detector highly precise measurement of both physical and fluorescent characteristics within a cell population can be monitored. The basic properties measured by a flow cytometer are cell size, detected in the forward scatter channel (FSC), granularity, measured in the side scatter channel (SSC) and fluorescence detected at specific wavelengths [112].

The cell size detected in the FSC gives you a rough overview of the cell size and allows you to separate between living and dead cells. The granularity, which is measured in the SSC, tells you something about the composition of the cells. As many cells have very unique sizes and cytoplasmic contents (i.e. basophils, dendritic cells etc…), the SSC in combination with FSC can be used to separate distinguished cells from each other when located in the same suspension [112].

If the cells have been labelled with a fluorochrome towards a cell surface or intracellular protein, fluorescent signal can be detected in one of the flow cytometers fluorescence channels (FLCs). The specificity of these channels are adjusted by filters, separating light with different wavelength, either by exclusion of wavelengths higher or lower than the filter specifics, or by reflecting light with different wavelengths through different paths. It is essential to select both the optimal laser for excitation of the fluorochrome, as well the proper filters as to detect the emission light [112].

3.4.2 Flow cytometry example procedure

The cells were seeded as described in *Material and Methods 3.2.2*, and LPS stimulated accordingly to in *Material and Methods 3.2.3*

After LPS stimulation it is important to reduce the amount of cellular activity. Cellular processes initiated by LPS will continue to work and it is important to reduce these processes to a bare minimum in order to create reproducible results. If the cells are to be labeled with antibodies, then after detaching the cells, it's imperative to keep the cells on ice in order to reduce any excess of cellular processes that can affect the results. Keeping the cells on ice when lysing the cells is also ideal in order to reduce the actions of phosphatases and proteases that might cleave proteins that are significant for the result.

At the end of the LPS stimulation, the medium was removed and the wells washed with 1 ml of PBS. 500 µl of undiluted Accutase was added in order to detach the cells, and treated 10-15 min at 37^{o} C. Accutase was used due to its ability to detach cells without cleaving surface proteins [113]. This is important as we were investigating surface protein levels. The cells were transferred into specifically designed flow tubes and centrifuged at 1500 g at 4^{o} C for 5 min to harvest the cells. The supernatant was discarded and the tubes were shaken in order to detach the cells. One sample served as a negative control and remained unstained while another control sample was added 10 µl of an associated isotype control. Experimental samples were added 10 µl of a fluorochrome conjugated antibody towards the target protein and it is important that the isotype control is added in the same concentration as this. The cells were put on ice for 30 min in the dark before washing with PBS to remove excess antibody. The samples were then spun down at 1500 g at 4^{o} C for 5 minutes, and the supernatant discarded. The cells were resuspended in 300 µl of PBS and analyzed by Flow cytometry.

3.4.3 Data collection and analysis

The samples were analyzed using the BD LSR II flow cytometer. The LSR II hold four individual lasers at wavelengths 405 nm, 488 nm, 565 nm and 633 nm. This collection of lasers can detect a broad range of fluorescent labels, and with the combination of precise optical solutions it gives the user flexibility to maximize the results. The information from the LSR II is interpreted using the BD FACS DIVA software, allowing easy manipulation of voltage, fluorescent targets, gating and data collection. The collected data from the experiments were interpreted using specialized software named FlowJO. Using FlowJo one can analyze different subgroups by gating, compensate for spectral overlap if more than one fluorochrome has been used, obtain a wide range of different statistics, and create layouts of the different samples.

3.5 Quantitative-PCR analysis

3.5.1 Principle of method

Real time quantitative polymerase chain reaction (Q-PCR) is the improved extension of the PCR method. The improvement lies within the ability to detect the levels of nucleic acid after each thermal cycle using fluorescent dyes or probes [114].

The first of the three fundamental principles within PCR is the denaturing of double stranded DNA by applying high temperatures, usually just slightly below 100^{o} C. The reaction is then cooled down so that target specific primers are allowed to anneal to the denatured single stranded DNA. Once the primers are annealed the temperature is increased in order for the Taq DNA polymerase to elongate the strand. This process is repeated for a set number of cycles, resulting in an exponential growth of the PCR-product until the reagents are depleted and the reaction levels out [114].

Q-PCR is achieved by addition of a fluorescent dye or probe which amount can be detected after every thermal cycle. One such probe is the TaqMan probe. The TaqMan probe is built up in three parts, a probe sequence, fluorescent marker, and a quencher. The probe sequence that specifically binds to the single stranded target DNA in the sample is enhanced with a fluorochrome at the 5'-end, and an additional quencher in the 3'-end. As long as the fluorochrome and quencher are in proximity the energy that would have excited the fluorochrome is transferred to the quencher. Only when the exonuclease activity of the Taq polymerase cleave the probe the fluorescent marker is released from the tight proximity of the quencher and emits wavelength specific light that can be detected by the thermal cycler [114].

The Applied biosystems "Step one Plus thermal cycler" provides a quantitative detection of the target nucleic acid using real time analysis. It also provides a qualitative analysis of the product based on the melt curve analysis. Samples are analyzed in technical duplicates and the system software provides a distinction of valid and invalid results based on the variation of standard deviation. A variation of < 0.3 in standard deviation between Ct-values signify a valid result.

3.5.2 Q-PCR example procedure

Cells were seeded as described in *Materials and Methods 3.2.3* and LPS stimulated as described in *Materials and Methods 3.4.3*. Upon harvesting the wells were washed with 1 ml of PBS, and added 375 µl of Isol to lyze the cells. The cell lysate was collected after a couple of minutes in the Isol solution and stored overnight at -80^{o} C.

The RNA was extracted with phenol chloroform before isolated using the Qiagen RNeasy mini kit according to manufacturer's protocol. The final RNA concentration was measured by using Nanodrop.

The RNA was then used to synthesize complementary DNA (cDNA). An equal amount of RNA was added to 14 µl of RNase free water. The volume was finalized to 20 µl by addition of 4 µl of 5x reaction mix and 2 µl Maxima enzyme mix. In one of the samples, the Maxima enzyme mix was replaced with 2 µl of water to serve as a reverse transcriptase control to assess the purity of final product. The cDNA reaction was synthesized using a program set to 10 min at 25^{o} C, 30 min at 50^{o} C, and finally 5 min at 85^{o} C to cancel the reaction.

The cDNA product was diluted in a 1:100 ratio and used in the final Q-PCR reaction. A mix containing 10 µl of Fast mix, 1 µl of a specific TaqMan probe, and 4 µl of H_2O was added to the wells in the Q-PCR plate, before 5 µl of the cDNA was added. The Q-PCR plate was sealed and centrifuged before transferred to the thermal cycler for measurement of specific mRNA levels.

3.6 SDS-PAGE and western blotting

3.6.1 Principle of method

SDS-Polyacrylamid gel electrophoresis (SDS-PAGE) combined with western blotting (WB) is a well-established method for separating and analyzing proteins from cell samples. The cell lysate is treated with a sample buffer containing SDS, giving all proteins a negative charge so they can be separated linearly accordingly to the protein size during electrophoresis. The samples are then added to the wells of a polyacrylamide gel for separation. The SDS-PAGE gels can vary in density in order to increase the separation of the proteins at certain sizes [115, 116].

Once the gel has been run, it can be transferred to a nitrocellulose blot using either wet, semi-dry, or dry transfer. Dry transfers are time efficient compared to wet transfers, however, they all have advantageous compared to each other [115, 117]. Proteins are transferred from the gel to the blot by the means of an electrical field that is applied to the gel. Once the proteins has been transferred to the blot it's placed in a blocking solution.

The blocking buffer can be solutions such as bovine serum albumin (BSA) and skimmed dry milk, and its purpose is to block nonspecific bindings on the blot. After the blocking is complete, a primary antibody specific to the target protein is applied, and incubated with the blot. The incubation period may vary depending on the quality of the antibody. A HRP-conjugated secondary antibody targeting the isotype of the primary antibody is then added. The blot is then washed and a chemical substrate added that reacts with the secondary antibody. The reaction of the chemical substrate with the secondary antibody creates a chemi-luminescent signal that can be detected using specialized hardware [118].

3.6.2 Western blotting procedure

Cells were seeded as described in *Materials and Methods 3.2.3* and LPS stimulated as described in *Materials and Methods 3.2.3*. The cells were washed with 1 ml PBS, and lysed in the well, with the addition of 170 µl of premade lysisbuffer (Table 3 and 4) on ice for 15 min. In order to enhance lysis the cells were shaken every 5 min. The lysate was transferred to eppendorf tubes and centrifuged at 13000 g at 4^{o} C for 15 minutes. The supernatant was transferred to new eppendorf tubes and mixed with 3.6 x loading buffer (containing 100mM DTT, a protein reducing agent that also protects cysteine residues from oxidation) in a 1:3 loading buffer/lysate ratio. The lysate was denatured in a heating block at 70^{o} C for 10 min.

The denatured lysate was loaded into a 4-12% bis-tris NuPage gradient gel that was assembled according to manufacturer's instructions. MOPS-buffer was used as running buffer. The gel was run for 10 min at 100 V in order for the samples to be evenly loaded into the gel, and subsequently for 1.5 H at 155 V. For WB an iBlot® gel transfer device from Invitrogen was used to dry transfer proteins from the polyacrylamide gel to a nitrocellulose membrane. The blot was then transferred to a 5 % BSA blocking solution for 1 hr. After blocking, the membrane was incubated with a primary antibody in 2 % BSA. The incubation period of the primary antibody depends on the quality of the antibody and amount of the protein of interest transferred to the nitrocellulose membrane. Whereas housekeeping genes need 1 hr of incubation, other antibodies might need to incubate over night or longer in order to obtain detectable levels.

After the incubation of the primary antibody, the blot was washed 3 x 5 min with TBS-Tween, before a secondary antibody was added, incubated for 1 hr. The blot was washed 3 x 5 min with TBS-tween. Super signal substrate was added to the blot and it was successively developed using LI-COR Odyssey Fc according to manufacturer's instructions.

4 Results

4.1 Optimizing the differentiation protocol of THP-1 cells

THP-1 cells are derived of an acute monocytic leukemia cell line, obtained from the peripheral blood of a 1-year old child [107]. As THP-1 cells are of monocyte origin, signaling in THP-1 cells share similarities with primary monocytes and Mϕs, thus they potentially provide a good model system for studying the cell biology of innate immune signaling. Specifically we wanted to establish the THP-1 cell line as a human model system to study TLR4-mediated signaling. THP-1 cells endogenously express proteins regulating the TLR4 signaling pathways. They are easily grown and maintained, can easily be differentiated to express Mφ morphology using either PMA or VD3 [108], and can be used for both siRNA and transfection experiments. These properties could make THP-1 cells a valuable tool in exploring TLR4 signaling.

TRIF activation is dependent on the internalization of LPS and activation of TLR4 on endosomes. This internalization has been shown to be tightly regulated by CD14 [35, 66]. Hence one of our main interests was the surface expression of CD14 and TLR4 and the effect LPS-stimulation would have onto this. We wanted to study the dynamics of TLR4 on the PM, however, TLR4 proved hard to visualize using flow cytometry. We chose to address this problem by investigating the CD14 levels on the PM relative to that of TLR4 [106]. CD14 is tightly linked to TLR4's activity when stimulated by LPS. CD14 regulates the transfer of LPS to TLR4 [30] and controls the internalization of TLR4 [119], and it is likely that their dynamics on the PM are co-dependent.

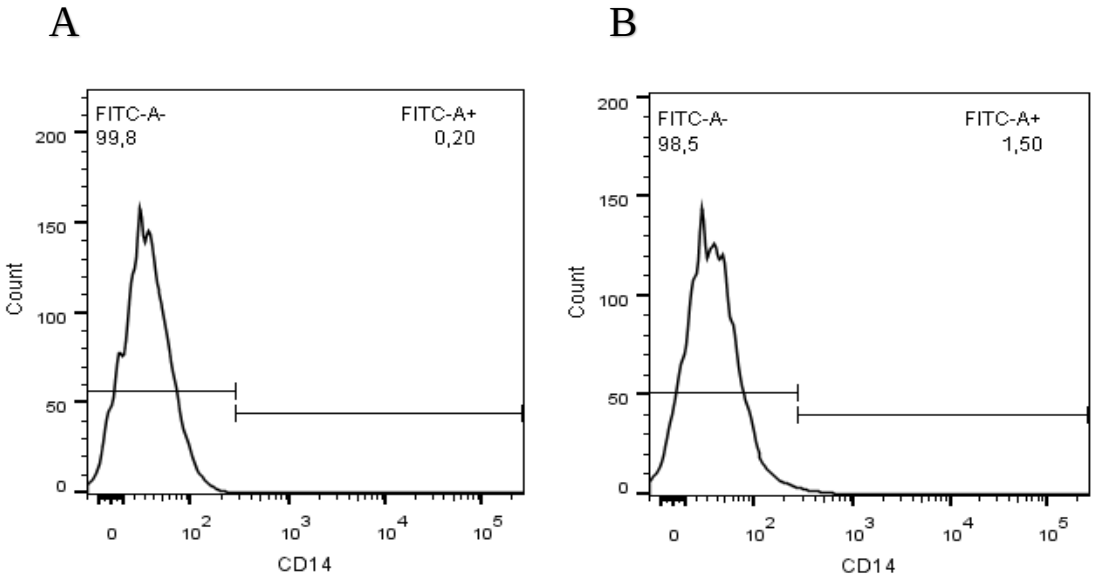

Figure 6: THP-1 cells differentiated with 100 ng/ml PMA for 72 hrs.
THP 1- cells differentiated with 100 ng/ml PMA for 72 hrs. The cells were labeled with a CD14 FITC-conjugated antibodies and analyzed by flow cytometry. A) THP-1 cells labeled with isotype control B) THP-1 cells labeled with CD14 FITC. Data was interpreted using FlowJo. Cell count = 5000

In our first experiments we used 100 ng/ml PMA for 72 hrs to differentiate THP-1 cells into Mφ-like structures. As displayed in Figure 6 and Figure 7c the use of this protocol resulted in a very limited population of CD14 positive cells. As CD14 is readily detectable in primary cells [120], including earlier observations that CD14 was expressed at mRNA and proteins levels in THP-1 cells [121], we found it strange that CD14 displayed such limited PM levels. We speculated that this problem could be addressed by optimizing the differentiation protocol.

It was reported that total protein levels of CD14 could be increased using lower concentrations of PMA [121]. Using a PMA concentration as low as 10 ng/ml PMA were beneficial for both CD14 expression, as well as reducing unwanted background expression of cytokines [121]. Other works suggests that replacing the medium of THP-1 cells 48 hrs after PMA differentiation to PMA-free medium was beneficial in promoting a more Mφ like phenotype [122].

Combining these two observations we set up an experiment using six different conditions in order to investigate if any of these would yield a higher percentage of THP-1 cells expressing CD14 on the PM.

First we were interested to see if reducing the concentration of PMA from 100 ng/ml to 10 ng/ml PMA, with 72 hrs incubation period would have any significant effect upon CD14 expression. Analysis was performed by flow cytometry.

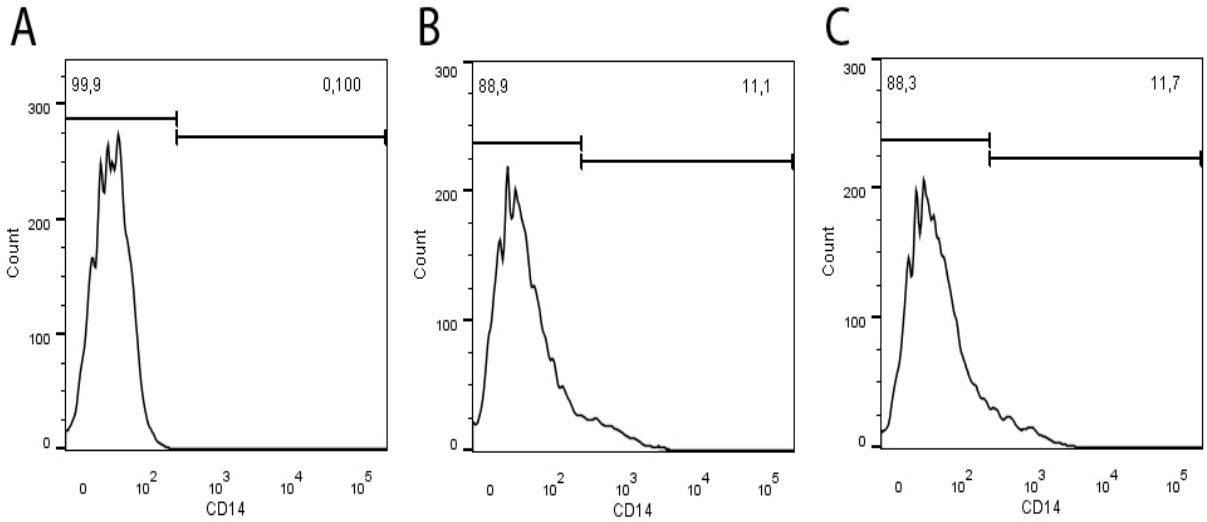

Figure 7: THP-1 cell differentiation protocol optimization (72 hrs PMA).
THP-1 cells differentiated with different PMA concentrations and incubated for 72 hrs. The cells were labeled with a CD14 FITC-conjugated antibody and analyzed by flow cytometry. A) Isotype control B) THP-1 cells treated with 10 ng/ml PMA. C) THP-1 cells treated with 100 ng/ml PMA. These results are representative data of 4 experiments and presented as percentage of positive cells. This was chosen over median + standard deviation, in correspondence with engineers and external advice. This is due to the variations in the results and the bimodal populations observed in later results. Count = 10000

We observed that there was no essential variation in the expression of CD14 on the PM between the two conditions. Both 100 ng/ml PMA (Fig. 7c) and 10 ng/ml PMA (Fig. 7b) resulted in basically the same minor amount (11.1 % and 11.7 % respectively) of CD14 on the PM. This result signifies that changing the PMA concentration alone was not enough to provoke a change in the expression of CD14 on the PM in THP-1 cells after 72 hrs of incubation time, and that further optimization of the protocol was necessary.

For the next experiment we introduced a resting period of 48 hrs, which meant that the cells would rest in PMA-free medium after the initial 48 hrs of incubation in either 10 ng/ml PMA or 100 ng/ml PMA [122]. This changes was based on other studies and we theorized that including this resting period, combined with the lower concentration of PMA would confer some changes into the PM CD14 expression levels.

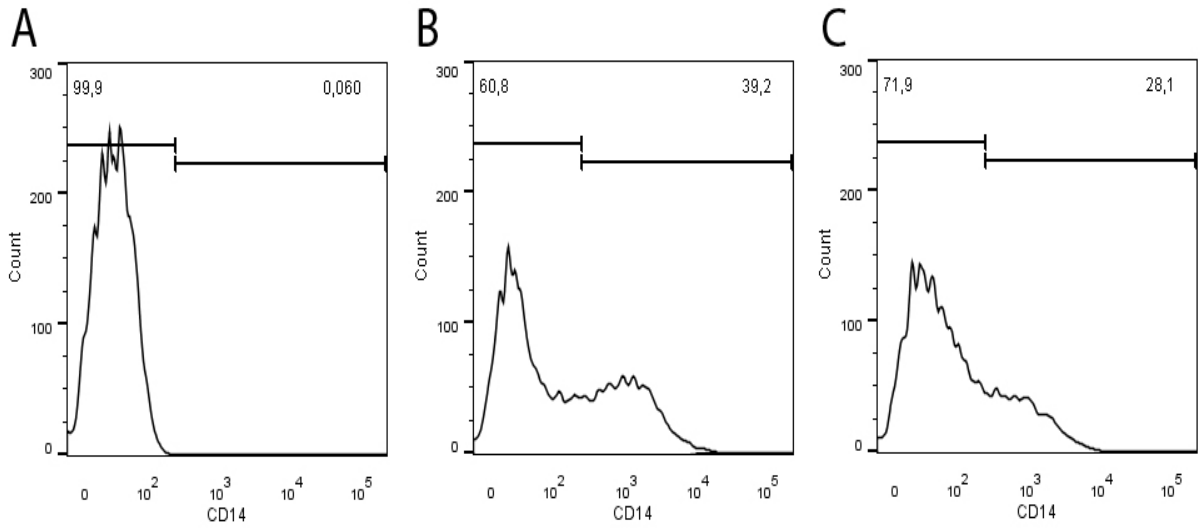

Figure 8: THP-1 cell differentiation protocol (48 hrs PMA + 48 hrs PMA free).
THP-1 cells were differentiated with different concentrations of PMA for 48 hrs and rested for 48 hrs in PMA-free medium. The cells were labeled with a CD14 FITC-conjugated antibody and analyzed by flow cytometry. A) Isotype control B) THP-1 cells treated with 10 ng/ml PMA. C) THP-1 cells treated with 100 ng/ml PMA. These results are representative data of 4 experiments. Count = 10000

The 48 hrs rest period without PMA in the culture media had a substantial effect on the CD14 levels on the PM. In cells treated with 100 ng/ml PMA we could observe an increase of CD14 positive cells to slightly less than 30 % of the cell population (Fig. 8c). For the cells treated with 10 ng/ml PMA we observed an increase of CD14 positive cells closer to 40 % (Fig. 8b), a significantly greater number than what was observed on the cells treated with 100 ng/ml PMA. We also observed that the population of CD14 positive cells treated with 10 ng/ml seemed to be a more homogeneous population, separated from the CD14 negative cells (Fig 8b), whereas the cells treated with 100 ng/ml PMA displayed a more heterogeneous population (Fig 8c).

Next we increased the resting period to 72 hrs, with the same set up for PMA concentrations. This was due to the observation by *Daigneault et al* that there were no significant changes to the morphology of the THP-1 cells after 72 hrs of rest in PMA-free medium [122]. Even though we had a desirable effect after only 48 hrs of rest, we wanted to make sure that the PM-composition was stable.

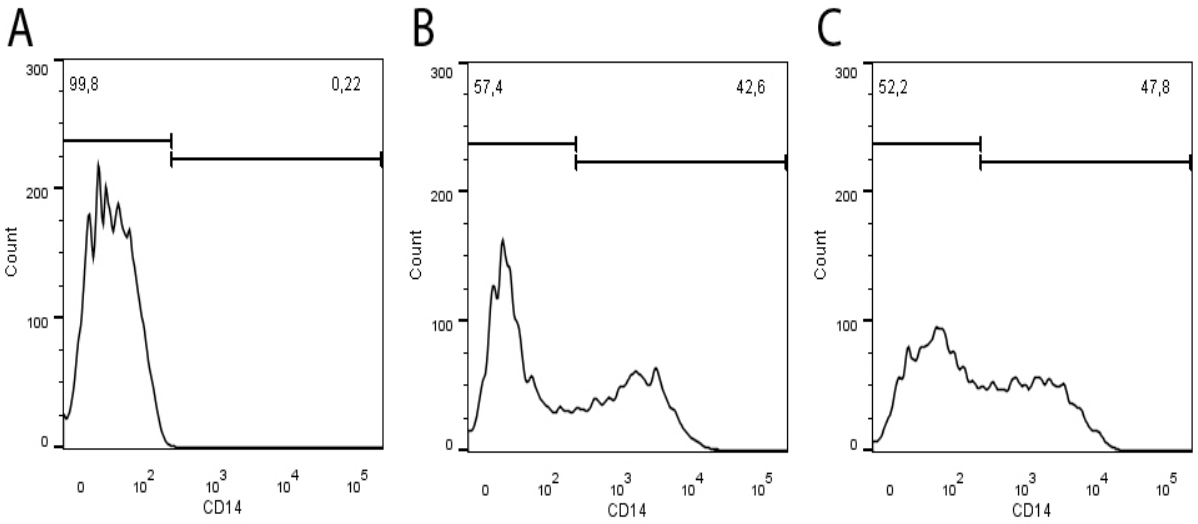

Figure 9: THP-1 cell differentiation protocol (48 hrs PMA + 72 hrs PMA free).
THP-1 cells were differentiated with different concentrations of PMA for 48 hrs and rested for 72 hrs in PMA-free medium. The cells were labeled with a CD14 FITC-conjugated antibody and analyzed by flow cytometry. A) Isotype control B) THP-1 cells treated with 10 ng/ml PMA. C) THP-1 cells treated with 100 ng/ml PMA. These results are representative data of 4 experiments. Count = 10000

The cells treated with 10 ng/ml PMA displayed much the same phenotype both for 48 hrs and 72 hrs rest (Fig. 8b and 9b). This could indicate that the most major changes toward the differentiation to Mφs have been achieved after 48 hrs rest when the PMA concentration is reduced to 10 ng/ml.

For cells treated with 100 ng/ml PMA the increased rest period of 72 hrs prompted a significant change in the amount of CD14 expressed on the PM from ~30% to ~45% compared to the results for the similar concentration, but 48 hrs of rest (Fig 8c and 9c).

Even so, there still was a difference in the manner of which these cells differentiate depending on the concentration of PMA. Whereas the cells treated with 100 ng/ml PMA now displayed an even higher portion of cells expressing CD14 on the PM compared to 10 ng/ml PMA (Fig. 9), the latter display a much more homogenous population of CD14 positive cells, separate from the CD14 negative cells in the sample (Fig. 9b). This observation strengthens our theory that cells differentiated with 10 ng/ml PMA appear to be more fully differentiated.

From these data we concluded that reducing the PMA concentration from 100 ng/ml to 10 ng/ml had a clear effect upon the PM levels of CD14. We also demonstrated that a resting period in PMA-free medium, after the initial 48 hrs of incubation with PMA, resulted in a higher CD14 positive population suggesting that this protocol was necessary for obtaining optimal differentiation of THP-1 cells.

4.2 Further classification of PM located proteins

4.2.1 TLR4

We had previously tried assessing the amount of TLR4 on the PM, but not found any striking expression. Due to the great alteration in the expression of CD14 on the PM, induced by both reduced PMA concentration and the inclusion of a rest period, we investigated the effects of these on the PM levels of TLR4. We used both 10 ng/ml and 100 ng/ml to differentiate the THP-1 cells and rested the cells for 48 hrs, 72 hrs, and 96 hrs in PMA-free medium in order to see if any of these conditions had any improved effect on the PM levels of TLR4.

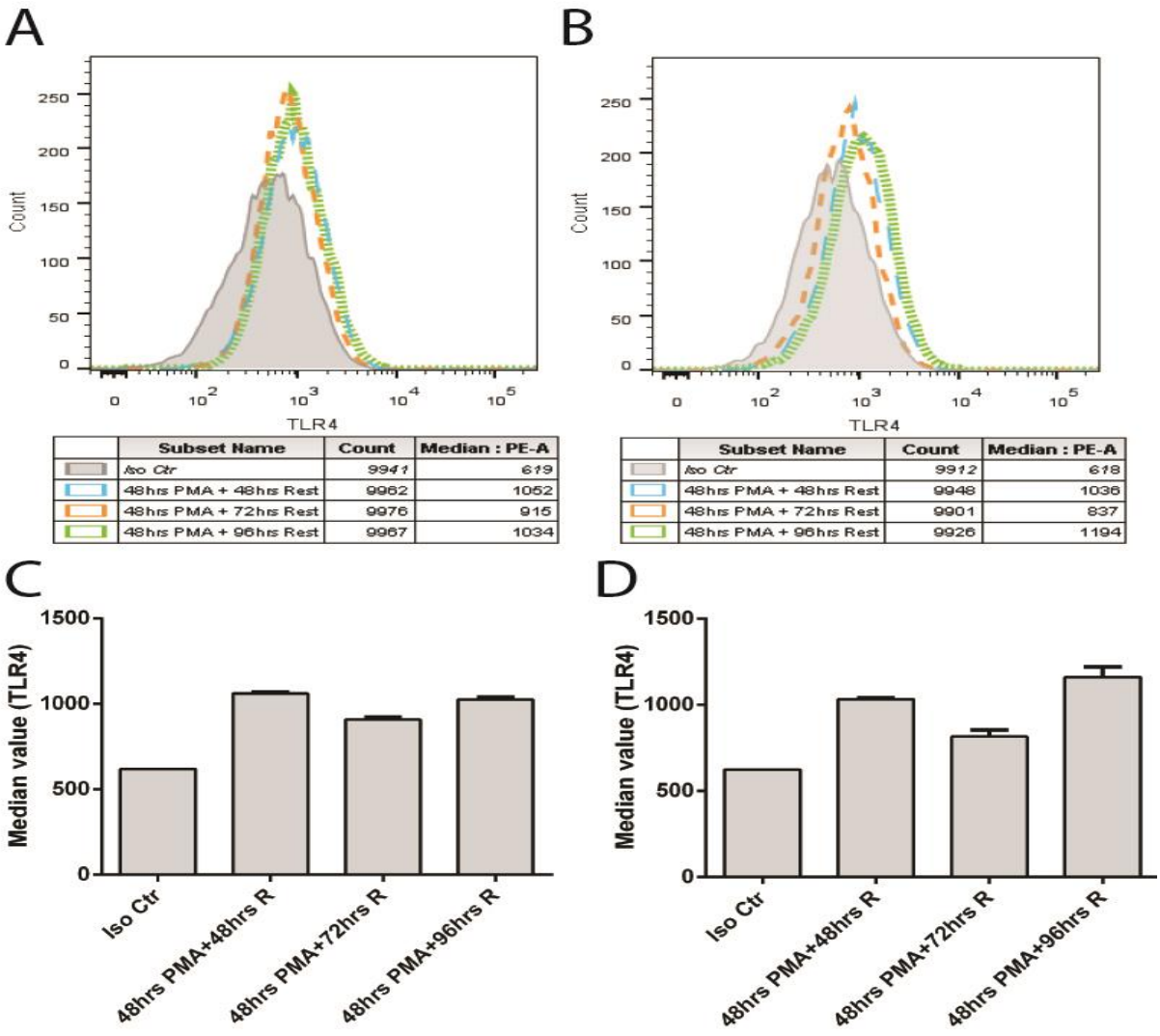

Figure 10: TLR4 PM levels using the altered differentiation protocol.
THP-1 cells were differentiated using A) and C) 10 ng/ml PMA, B) and D) 100 ng/ml PMA. The cells were incubated in the PMA-medium for 48 hrs before the medium was replaced with PMA-free medium. The THP-1 cells were rested for 48 hrs, 72 hrs, and 96 hrs. The THP-1 cells were labeled with TLR4-HTA125-PE conjugated antibodies and analyzed with flow cytometry. The data in A). and B) are representative of two parallel experiments. The data in C) and D) are the mean of the median values of the measured PE-intensity from both experiments. Count=10000

The new protocols did not infer any major changes on the amount of TLR4 expressed on the PM compared to CD14 (Fig. 8 and 9). We observed a small shift compared to the isotype control (Figure 10a and b), and an increase in the median values of TLR4 (Fig. 10 c and d). A considerably smaller population of TLR4 compared to CD14 was to be expected [106]. We concluded that the new protocols had no considerable effect upon the PM levels of TLR4 and decided to focus on CD14.

4.2.2 CD11b

CD11b, also known as integrin α M, is one of two components forming the heterodimer complement receptor 3 (CR3), the other being CD18 [123]. It is found predominantly expressed in cells involved in innate immunity such as monocytes, neutrophils, DCs and Mφs, and to a lesser extent B- and T-cells [123]. CD11b physically interacts with CD14 when cells are stimulated with LPS[124] in an event that affects CR3-mediated adhesion, it has been linked to influence LPS-mediated signaling [125], as well as playing an important part in phagocytosis [126]. Addressing any effect of the expression of CD11b was therefore interesting as the internalization and phagosome formation is an essential part of triggering the TRIF-dependent pathway [27].

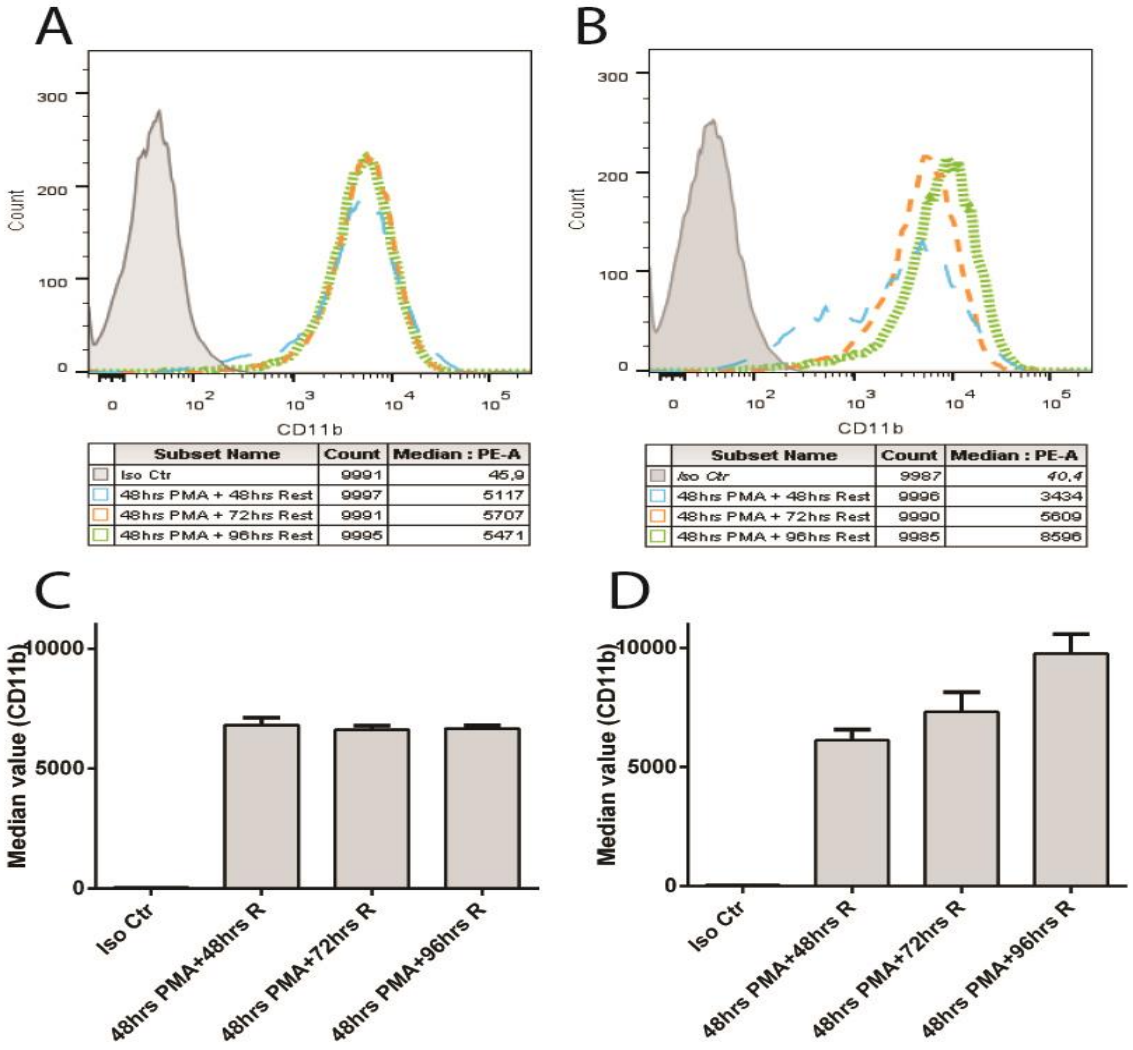

Figure 11: CD11b PM levels using the altered differentiation protocol.
THP-1 cells were differentiated using A) and C) 10 ng/ml PMA, B) and D) 100 ng/ml PMA. The cells were incubated in the PMA-medium for 48 hrs before the medium was replaced with PMA-free medium. The THP-1 cells were rested for 48 hrs, 72 hrs, and 96 hrs. The THP-1 cells were labeled with CD11b-PE conjugated antibodies and analyzed with flow cytometry. The data in A) and B) are representative of two parallel experiments. The data in C) and D) are the mean of the median values of the measured PE-intensity from both experiments. Count=10000

At 10 ng/ml PMA there was no significant difference between the different rest periods, as illustrated in both Figure 11a and 11c. The shift observed in Figure 11a indicate that the expression of CD11b on the plasma membrane is fairly stable after 48 hrs of rest and remained stable after 72 hrs and 96 hrs (Fig. 11a and c). In the cells treated with 100 ng/ml the expression of CD11b is notably weaker after only 48 hrs compared to 72 hrs and 96 hrs (Fig. 11b and d).

4.3 The effect of PMA concentrations and rest on LPS-induced IFN-β and TNF-α responses

Next we investigated the effect of the THP-1 differentiation protocols on the expression of IFN-β and TNF-α. Based on the prior results we determined that rest period was more essential than the actual PMA-concentration, so we excluded the protocol with 72 hrs on PMA without rest, and continued with 48 hrs and 72 hrs rest and both PMA concentrations in order to locate additional variations. In order to assess the status of MyD88 and TRIF-dependent signaling in THP-1 cells differentiated with the new protocols, we tested the expression of IFN-β and TNF-α. Cytokines induced by the MyD88-dependent and TRIF-dependent pathway.

4.3.1 IFN-β response in course of LPS stimulation

IFN-β is a cytokine that is tightly regulated by the nuclear translocation of IRF3 [62]. Since the TRIF-dependent pathway activates IRF3, we used IFN-β expression as a readout of TRIF signaling pathway.

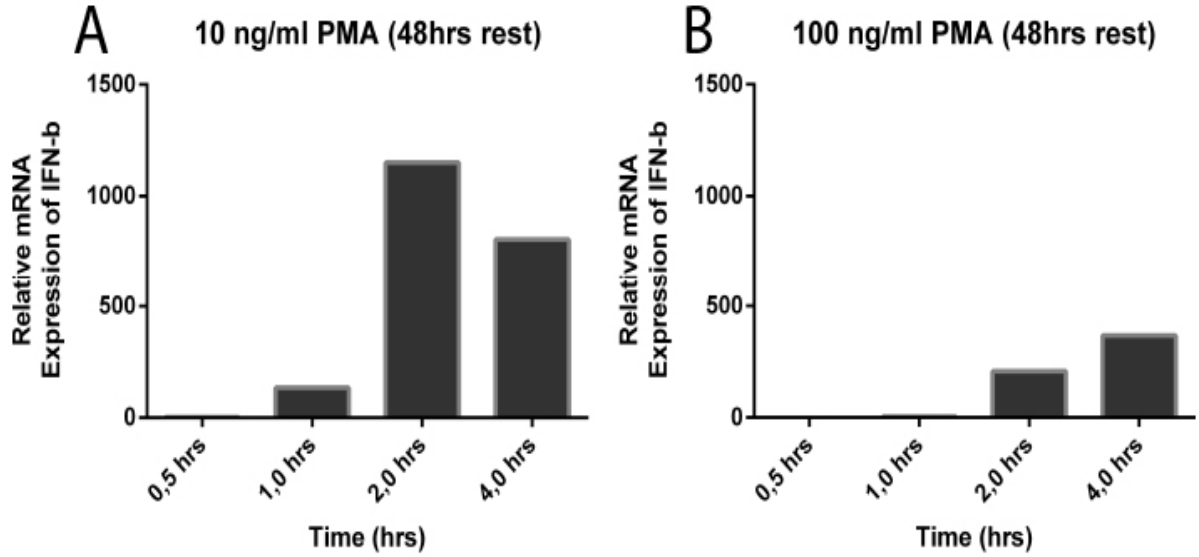

Figure 12: LPS stimulated IFN-β expression in THP-1 cells differentiated with 48 hrs rest.
THP-1 cells were differentiated with A) 10 ng/ml PMA and B) 100 ng/ml PMA for 48 hrs and rested for 48 hrs. The cells were treated with K12 LPS (100 ng/ml) at designated time points prior to cell lysis and RNA purification. The RNA was analyzed using Q-PCR and the Taqman probe system against IFN-β. The experiment was repeated twice and the results presented above are representative for these two experiments.

The THP-1 cells treated with 10 ng/ml PMA results in a significant response of IFN-β when stimulated with K12 LPS. After 0, 5 hrs there is no noteworthy changes in expression of IFN-β, however, the cells treated with 10 ng/ml PMA display a modest increase of expression

levels after 1 hr (Fig. 13a). After 2 hrs there is a substantial increase of IFN-β levels, while after 4 hrs the levels are lower (Fig. 12a).

The THP-1 cells treated with 100 ng/ml PMA (Fig 12b), display a lower expression of IFN-β mRNA than cells differentiated with 10 ng/ml PMA (Fig. 12a), when stimulated with K12 LPS. At 1 hr of LPS stimulation there is no indication of IFN-β expression. There is a very modest increase of the expression of IFN-β mRNA after 2 hrs and 4 hrs (Fig. 12b) compared to 10 ng/ml (Fig 12a)

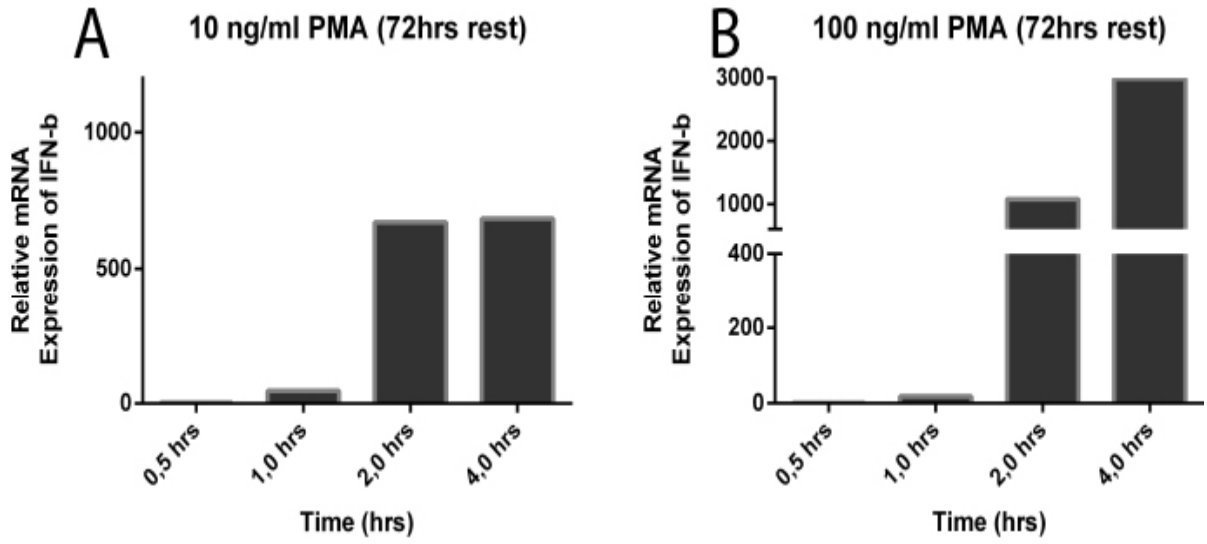

Figure 13: LPS stimulated IFN-β expression in THP-1 cells differentiated with 72 hrs rest.
THP-1 cells were differentiated with A) 10 ng/ml PMA and B) 100 ng/ml PMA for 48 hrs and rested for 72 hrs. The cells were treated with K12 LPS (100 ng/ml) at designated time points prior to cell lysis and RNA purification. The RNA was analyzed using Q-PCR and the Taqman probe system against IFN-β. The experiment was repeated twice and the results presented above are representative for these two experiments.

Increasing the rest period to 72 hrs in PMA-free medium after PMA differentiation resulted in some considerable changes in the expression of INF-β mRNA. THP-1 cells treated with 10 ng/ml PMA now displayed a somewhat more restrained production of INF-β (Fig. 13a) compared to the cells only rested for 48 hrs (Fig. 12a). At the 1 hr mark the amount of INF-β produced are still negligible, however, after 2 hrs the expression levels have significantly increased and remain stable and remain stable at 4 hrs (Fig 13a).

The most notable effect was however observed in cells treated with 100 ng/ml PMA (Fig. 13b). While the initial 1 hr response was basically nonexistent, after 2 hrs the INF-β expression levels have increased a thousand fold (Fig. 13b), comparable to expression levels seen in the cells treated with 10 ng/ml PMA at the same 2 hrs time point (Fig. 12a and 13a). After 4 hrs the expression levels has increased three-fold the amount observed after 2 hrs (Fig. 13b).

The same experiment was also conducted with other TLR4 ligands, such as *E. Coli*, and B4 LPS (data not shown). In the cells treated with *E. Coli* the cells gave a comparable response, although around twice the strength at the 2 hrs mark, but the overall expression behavior was comparable to that of K12 LPS (Data not shown). For B4 LPS the cells had an initially weaker response, giving a weaker signal at 2 hrs and 4 hrs (data not shown). However, these results were not further quantified and could only be used for preliminary estimates compared with the K12 LPS results.

4.3.2 TNF-α response in course of K12 LPS stimulation

TNF-α is a cytokine that is regulated by the MyD88-dependent pathway [127]. However, the TRIF-dependent pathway is also able to regulate the activity of NF-κB through its interactions with TRAF6 [67]. Nevertheless, TNF-α serves as an effective indicator for the activity of the MyD88-dependent pathway. For this reason we were interested in investigating the expression of TNF-α using the new protocols.

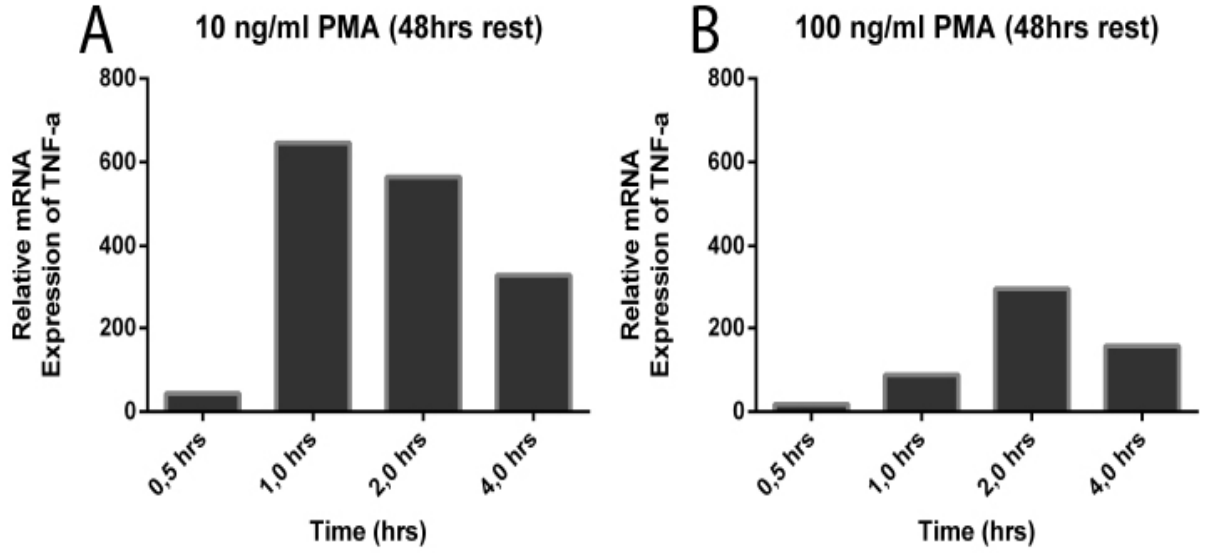

Figure 14: LPS stimulated TNF-α expression in THP-1 cells differentiated with 48 hrs rest.
THP-1 cells were differentiated with A) 10 ng/ml PMA and B) 100 ng/ml PMA for 48 hrs and rested for 48 hrs. The cells were treated with K12 LPS (100 ng/ml) at designated time points prior to cell lysis and RNA purification. The RNA was analyzed using Q-PCR and the Taqman probe system against TNF-α. The experiment was repeated twice and the results presented above are representative for these two experiments.

The TNF-α response after 48 hrs incubation of PMA and 48 hrs rest in PMA-free medium again shows an increased cytokine expression in THP-1 cells differentiated with 10 ng/ml PMA compared to the cells treated with 100 ng/ml PMA (Fig. 14). The cells treated with 10 ng/ml PMA show tendencies to expression after 0,5hrs, before reaching maximum expression after 1 hr (Fig 14a). The expression of TNF-α decline after 2 hrs, continuing to do so up to 4 hrs as well (Fig. 14a). THP-1 cells treated with 100 ng/ml PMA (Fig 14b) display a weaker, as well as delayed expression of TNF-α, compared to the cells treated with 10 ng/ml PMA (Fig. 14a). The production TNF-α increases marginally within the 1 hr time point, and reaches it maximum expression after 2 hrs (Fig. 14b), approximately reaching half the response to what observed after 1 hr in cells treated with 10 ng/ml PMA (Fig. 14a). This can theoretically be related to the difference in amount of CD14 expressed on the PM of THP-1 cells treated with the different protocols (Figure 8), considering CD14 plays an active part in the transfer of LPS

to the MD2-TLR4 complex ([128], as well as the internalization of the MD2-TLR4 complex required for the TRIF-dependent pathway [119].

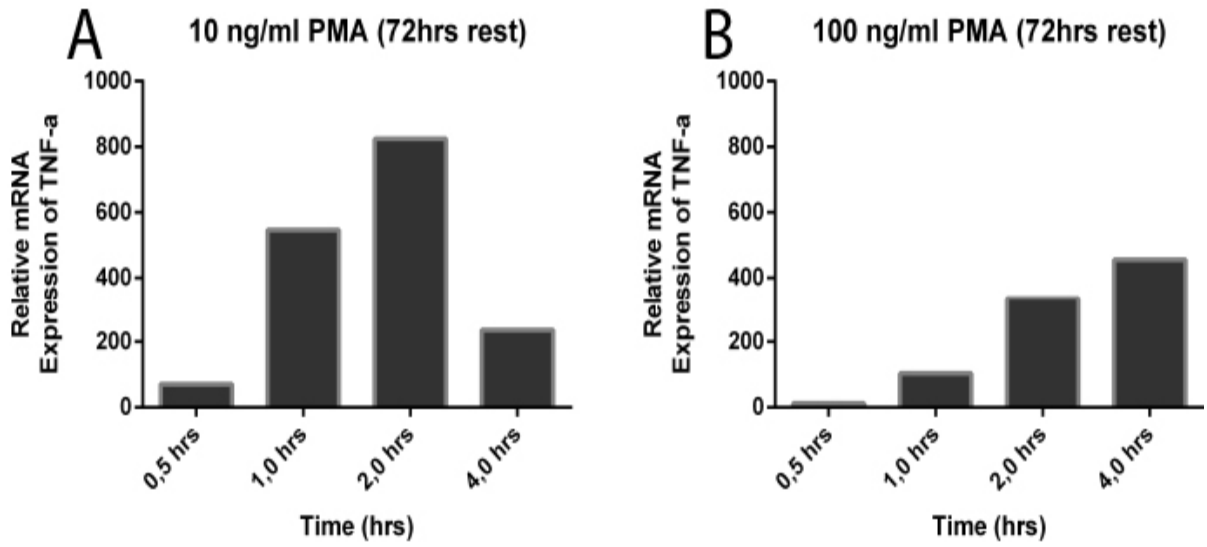

Figure 15: LPS stimulated TNF-α expression in THP-1 cells differentiated with 72 hrs rest.
THP-1 cells were differentiated with A) 10 ng/ml PMA and B) 100 ng/ml PMA for 48 hrs and rested for 72 hrs. The cells were treated with K12 LPS (100 ng/ml) at designated time points prior to cell lysis and RNA purification. The RNA was analyzed using Q-PCR and the Taqman probe system against TNF-α. The experiment was repeated twice and the results presented above are representative for these two experiments.

Increasing the rest period to 72 hrs on PMA-free medium (Fig. 15) changed the expression pattern compared to 48 hrs rest (Fig. 14). THP-1 cells treated with 10 ng/ml PMA (Fig. 15a) displayed an expression of TNF-α mRNA levels at 0,5hrs and 1,0 hrs comparable to the cells rested for 48 hrs (Fig. 14a). However, the expression continued to increase after 2 hrs of stimulation with K12 LPS (Fig. 15a) where it declined in cells given only 48 hrs rest (Fig. 14a). After 4 hrs the expression of TNF-α had greatly declined (Fig. 15a) to a level comparable to that of previously observed (Fig. 14a).

For THP-1 cells treated with 100 ng/ml PMA and rested 72 hrs (Fig. 15b) the TNF-α response was also lower than in cells treated with 10 ng/ml PMA (Fig. 15a). The onset of TNF-α expression is delayed and keeps increasing to ~450 fold at 4 hrs (Fig. 15b) in contrast to with 10 ng/ml PMA where TNF-α peaks at 2 hrs and thereafter decreases (Fig 15a).

4.4 Dynamics of CD14 on the PM in different protocols

We agreed upon favoring the new reduced concentration of 10 ng/ml of PMA, as well as including a rest period after 48 hrs of initial PMA differentiation. Based on the expression of the Mφ marker CD14 and the LPS-induced cytokine expression, we reasoned that this concentration is more beneficial to obtain a more Mφ-like system.

As the TLR4 levels detected on the PM were low, we chose CD14 as a target to measure the initial PM dynamics of the MD2-TLR4 signaling complex. We reasoned that since CD14 is essential for the endocytosis of TLR4, their dynamics are most likely closely linked.

We wanted to explore the optimal amount of rest further, and conducted two separate series of experiments for both 48 hrs and 72 hrs of rest in PMA-free medium following the initial 48 hrs of PMA differentiation with 10 ng/ml PMA. We stimulated the differentiated cells with the TLR4 ligand K12 LPS at chosen time points in order to investigate the dynamics of CD14 at the PM [129].

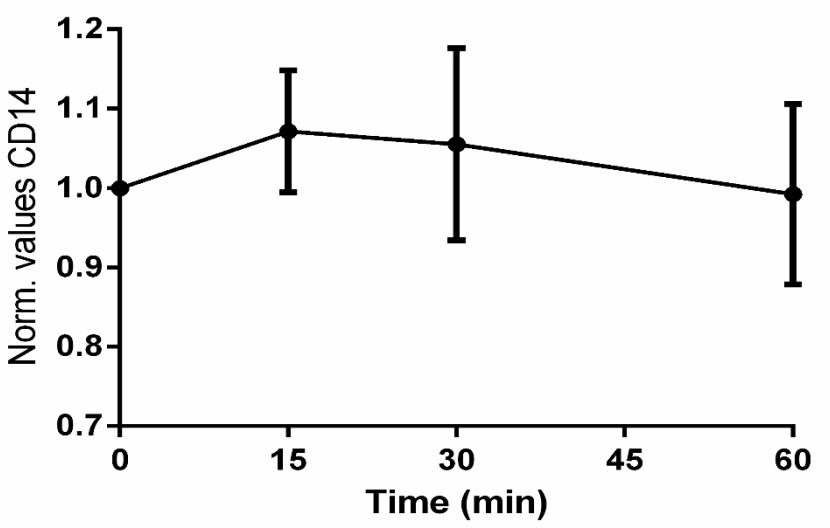

Figure 16: The PM dynamics of CD14 in LPS stimulated THP-1 cells (48 hrs rest PMA-free medium).
THP-1 cells were differentiated using 10 ng/ml PMA for 48 hrs, and rested for 48 hrs in PMA-free medium. The cells were stimulated using K12 LPS (100 ng/ml) at designated time points before labeled with a CD14 FITC-conjugated antibody and analyzed using flow cytometry. The Y-axis represents the normalized values of CD14 towards the unstimulated sample (0 min). The normalized values are derived from the percentage of CD14 positive cells. The experiment was repeated three times and presented as mean of normalized values ± standard deviation. Count = 10000

The flow cytometry data showed that the cells that had been treated for 48 hrs with PMA and 48 hrs of rest had a very limited dynamics of CD14 on the PM (Fig 16). We also wanted to study the dynamics in cells rested for 72 hrs. The levels of CD14 on the PM in these to protocols did not differ greatly as shown in Figure 8 and 9, but the IFN-β and TNF-α expression varied between protocols. Hence we wanted to investigate possible differences in the CD14 dynamics between protocols

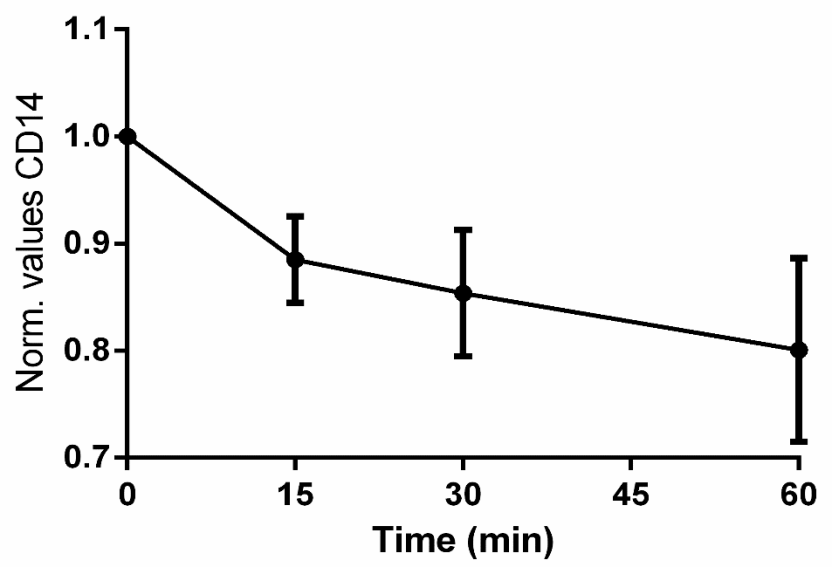

Figure 17: The PM dynamics of CD14 in LPS stimulated THP-1 cells (72 hrs rest PMA-free medium). *THP-1 cells were differentiated using 10 ng/ml PMA for 48 hrs, and rested for 72 hrs in PMA-free medium. The cells were stimulated using K12 LPS (100 ng/ml) at designated time points before labeled with a CD14 FITC-conjugated antibody and analyzed using flow cytometry. The Y-axis represents the normalized values of CD14 towards the unstimulated sample (0 min). The normalized values are derived from the percentage of CD14 positive cells. The experiment was repeated three times and presented as mean of normalized values ± standard deviation. . Count = 10000*

THP-1 cells that had been allowed to rest for 72 hrs displayed a much more active dynamics of CD14 PM expression (Fig 17). There was a steady decline of CD14 present on the PM over the course of 60 min, suggesting that the internalization rate of CD14 might be higher in cells rested for 72 hrs in PMA-free medium (Fig. 17).

These data, combined with the Q-PCR data, indicated that it might be advantageous to use 48 hrs PMA, followed by 72 hrs rest in PMA-free medium differentiating THP-1 cells, as the increased dynamics of CD14 might suggest an increased rate of trafficking of this receptor, and most likely concomitantly with TLR4.

4.5 The effect of Rab4a depletion on LPS-induced TLR4 inflammatory signaling

We wanted to explore potential effects of Rab4a on the surface expression of CD14. Rab4a has been extensively linked to the rapid recycling of endocytosed material directly back to the PM [83] and may play an important role in the recovery of important inflammatory signaling proteins, thus Rab4a might play a part in either delaying the TRIF-dependent response, or sustaining the MyD88-dependent response. The effect of Rab4a depletion in THP-1 cells was investigated using both 48 hrs and 72 hrs rest in PMA-free medium followed by stimulation with K12 LPS.

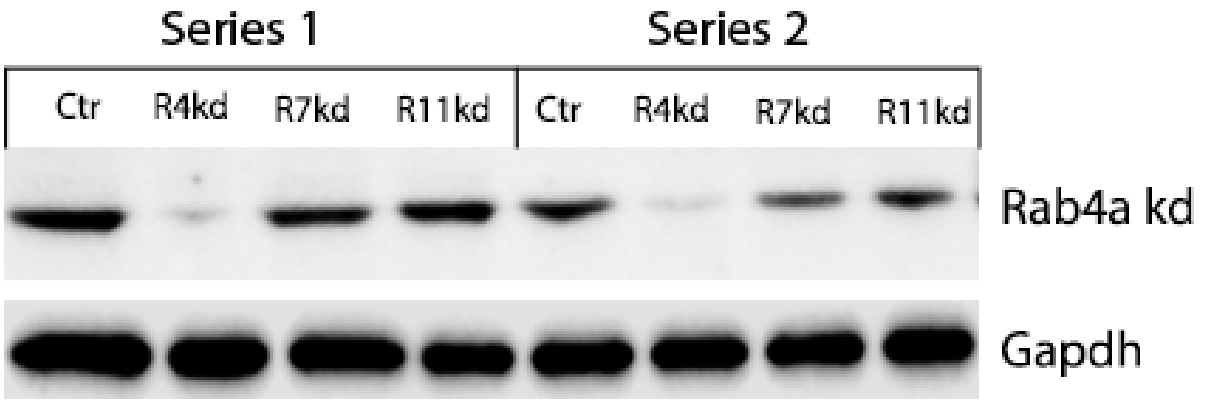

Figure 18: WB confirmation of Rab4a silencing (48 hrs PMA+ 48 hrs PM- free).
THP-1 cells were differentiated with 10 ng/ml PMA for 48 hrs, and rested for 48 hrs in PMA free medium. The cells were treated with siRNA towards Rab4a, and the lysate were used to confirm the depletion of Rab4a using WB. The experiment was repeated twice and both results are presented in the figure.

We confirmed that Rab4a had effectively been silenced using WB (Fig.18). We set up a flow cytometry experiment using 10 ng/ml PMA for 48 hrs and 48 hrs in PMA-free medium. We stimulated the cells with K12 LPS at certain time points, in order to investigate any effect on the surface levels of CD14.

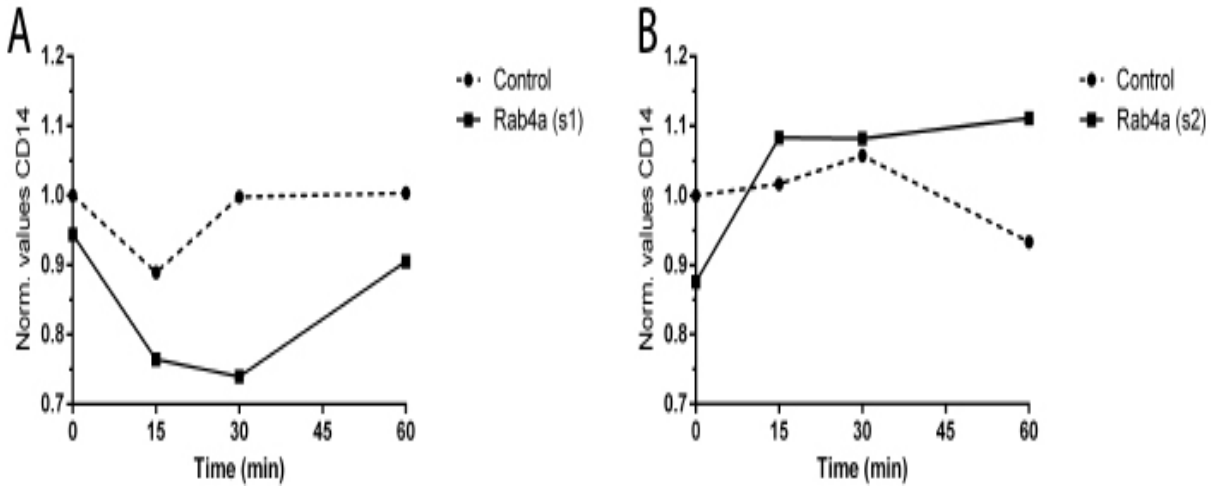

Figure 19: PM dynamics of CD14 in Rab4a depleted THP-1 cells (48 hrs PMA+ 48 hrs PMA-free).
THP-1 cells differentiated with 10 ng/ml PMA for 48 hrs, rested 48 hrs in PMA-free medium. The cells were treated with Rab4a siRNA. The Cells were stimulated with K12 LPS (100 ng/ml) at designated time points. Post-stimulation the cells were labeled with a CD14 FITC-conjugated antibody and analyzed using flow cytometry. A) and B) display the data from two individual series. Count = 10000

It was apparent that Rab4a siRNA silencing had some sort of effect on the system, however, from two independent experiments with cells treated 48 hrs on PMA and 48 hrs of rest, showed opposing effects on the CD14 dynamics on the PM (Fig. 19). While the CD14 surface levels rapidly declined in the first experiment (Fig. 19a), the amount of CD14 actually increased rapidly before stabilizing in the second experiment (Fig. 19b).

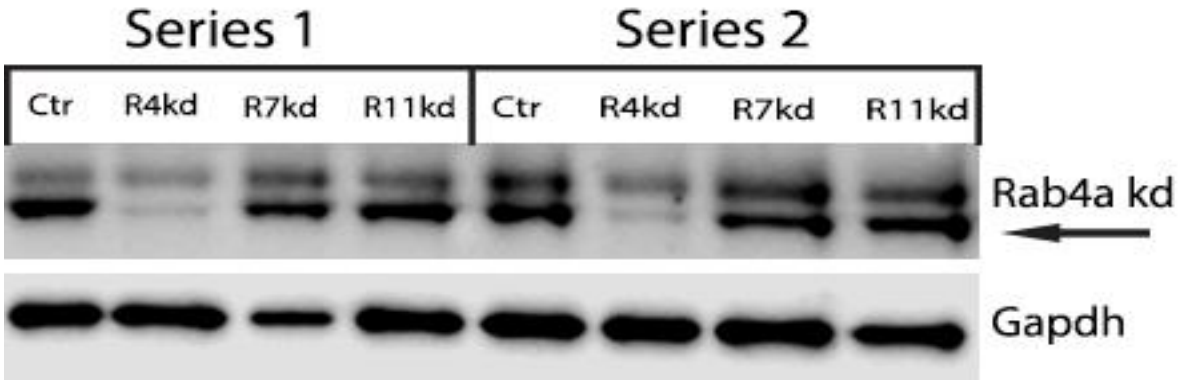

Figure 20: WB confirmation of Rab4a silencing (48 hrs PMA + 72 hrs PMA-free).
THP-1 cells were differentiated with 10 ng/ml PMA for 48 hrs, and rested for 72 hrs in PMA free medium. The cells were treated with siRNA towards Rab4a, and the lysate used to confirm the depletion of Rab4a using WB. The experiment was repeated twice and both results are presented in the figure.

We repeated the experiment using 72 hrs in PMA free medium. We confirmed the knockdown of Rab4a using WB (Fig. 20). Interestingly we noticed a band, above the signal representing Rab4a (indicated lower band)

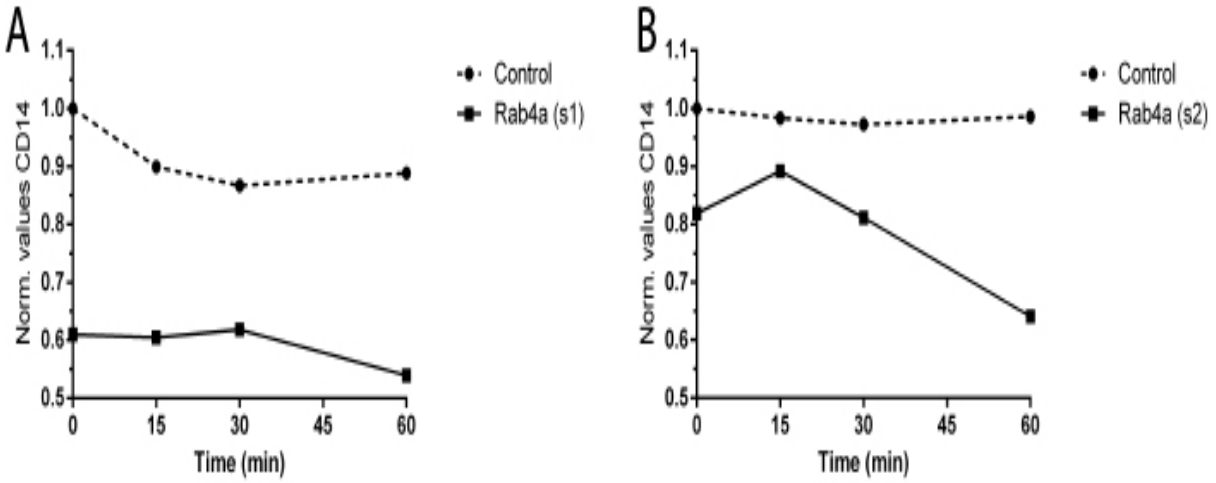

Figure 21: PM dynamics of CD14 in Rab4a depleted THP-1 cells (48 hrs PMA+ 72 hrs PMA free).
THP-1 cells differentiated with 10 ng/ml PMA for 48 hrs, rested 72 hrs in PMA-free medium, and treated with Rab4a siRNA. The cells were stimulated with K12 LPS (100 ng/ml) at designated time points. Post-stimulation the cells were labeled with a CD14 FITC-conjugated antibody and analyzed using flow cytometry. The experiment was repeated four times and A) and B) display representative data from two individual series. Count = 10000

After resting the cells for 72 hrs the similar variation in the results could be observed (Fig. 21). In the first experiment the LPS stimulation seemed to have little effect on the amount of CD14 dynamics on the PM (Fig. 21a), whereas in the second experiment the CD14 levels increases slightly at first (Fig. 21b), similar to the second experiment with 48 hrs rest (Fig 19b), before dropping steadily from 30 min and out.

Again, the variation in CD14 PM levels between the two experiments was too great to reach any form of proper conclusion. Nonetheless, the observation that CD14 levels in Rab4a siRNA treated cells given 72 hrs of rest (Fig. 21) are substantially lower than what is observed in Figure 19, strengthen our hypothesis that Rab4a indeed regulate events involved in inflammation.

4.1 The effect of Rab11a depletion on LPS-induced TLR4 inflammatory signaling

Rab11a is an essential regulator of the slow recycling of proteins from the endosomal pathway back to the PM, through the ERC. Rab11a has been linked to the trafficking of TLR4 to phagosomes, so examining if it has any effect on the internalization and potential recycling of CD14 from and to the PM is of great interest.

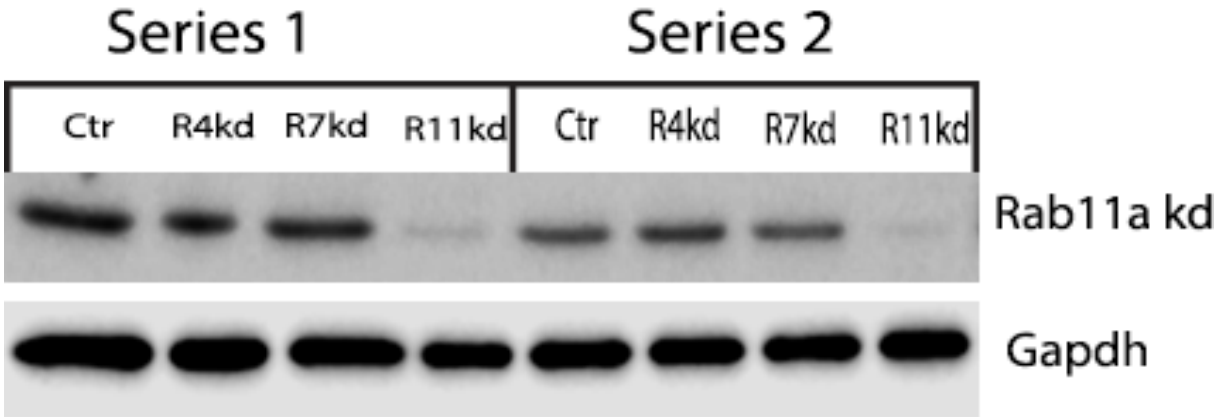

Figure 22: WB confirmation of Rab11a silencing (48 hrs PMA + 48 hrs PMA-free).
THP-1 cells were differentiated with 10 ng/ml PMA for 48 hrs, and rested for 48 hrs in PMA free medium. The cells were treated with siRNA towards Rab11a according to protocol, and the lysate used to confirm the depletion of Rab11a using WB. The experiment was repeated twice and both results are presented in the figure.

We confirmed that Rab11a had effectively been silenced using WB (Fig.22). We set up a flow cytometry experiment using 10 ng/ml PMA for 48 hrs and 48 hrs in PMA-free medium. We stimulated the THP-1 cells with K12 LPS at certain time points, in order to investigate any effect on the surface levels of CD14.

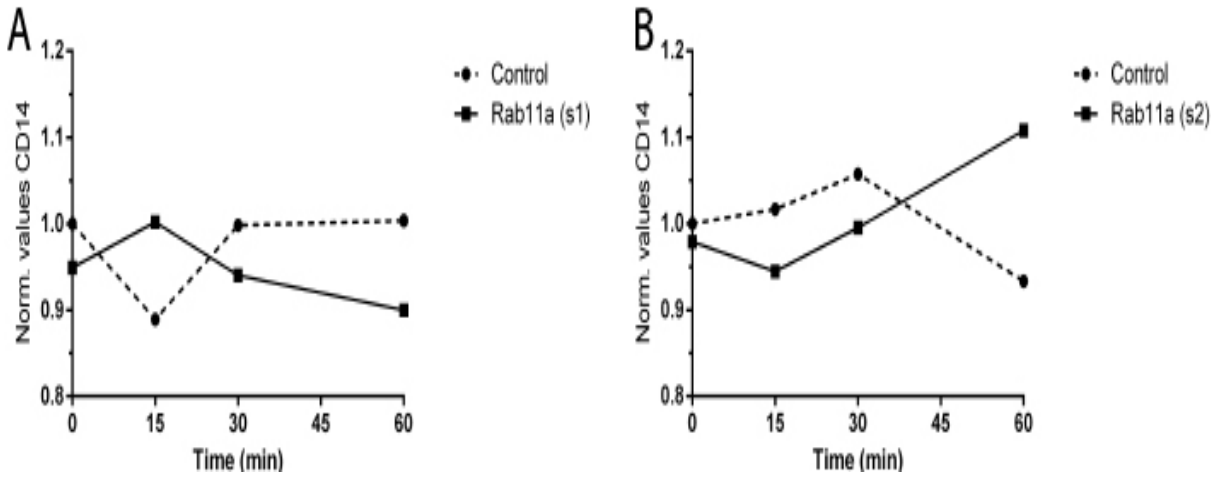

Figure 23: PM dynamics of CD14 in Rab11a depleted THP-1 cells (48 hrs PMA+ 48 hrs PMA-free).
THP-1 cells differentiated with 10 ng/ml PMA for 48 hrs, rested 48 hrs in PMA-free medium, and treated with Rab11a siRNA. The Cells were stimulated with K12 LPS (100 ng/ml) at designated time points. Post-stimulation the cells were labeled with a CD14 FITC-conjugated antibody and analyzed using flow cytometry. A) and B) display the data from two individual series. Count = 10000

After 48 hrs rest there do not seem to be any noteworthy effect of the siRNA Rab11a knockdown. The initial amount of CD14 on the PM is not significantly shifted compared to the THP-1 cells treated with control siRNA in either of the experiments. The dynamics of CD14 the first 30 min of LPS stimulation in the Rab11a knockdown cells remain fairly stable and at no time seems to deviate greatly from what observed in the control siRNA samples (Fig. 23). After 60 min the dynamics of CD14 in siRNA treated cells appear to deviate some from the control samples, resulting on opposing behavior (Fig. 23).

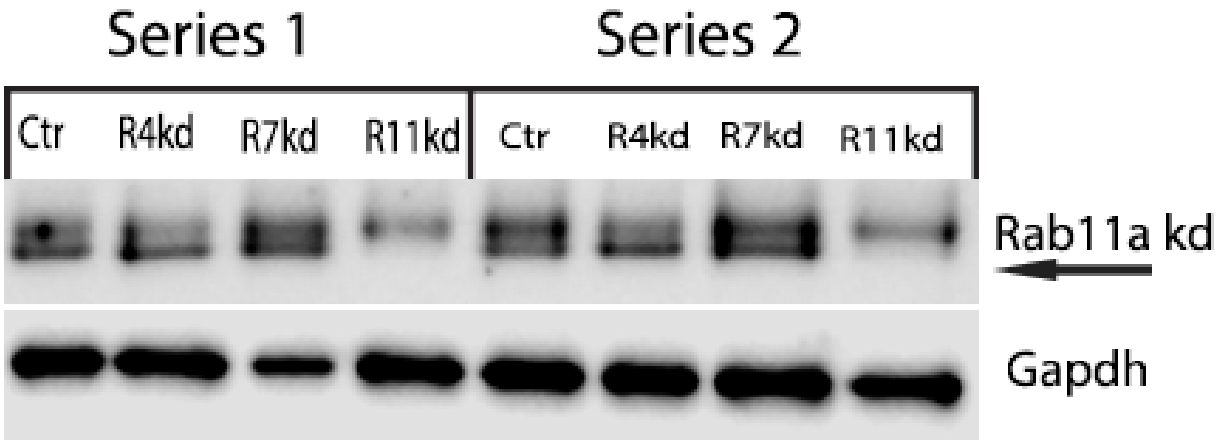

Figure 24: WB confirmation of Rab11a silencing (48 hrs PMA + 72 hrs PMA-free).
THP-1 cells were differentiated with 10 ng/ml PMA for 48 hrs, and rested for 72 hrs in PMA free medium. The cells were treated with siRNA towards Rab11a according to protocol, and the lysate used to confirm the depletion of Rab11a using WB (Rab11a lower band indicated with arrow). The experiment was repeated twice and both results are represented in the figure.

When we confirmed the silencing of Rab11a in cells rested for 72 hrs we now could see two distinct bands compared to the single band observed band in Figure 24. The lower band represents Rab11a and also confirms the depletion of Rab11a. We have previous data (*Harald Husebye*. *Unpublished data*) confirming that the upper band is indeed Rab11b and this indicate that there likely has occurred a change in cellular protein composition, increasing focus on trafficking. These results may be interesting considering trafficking in inflammatory pathways.

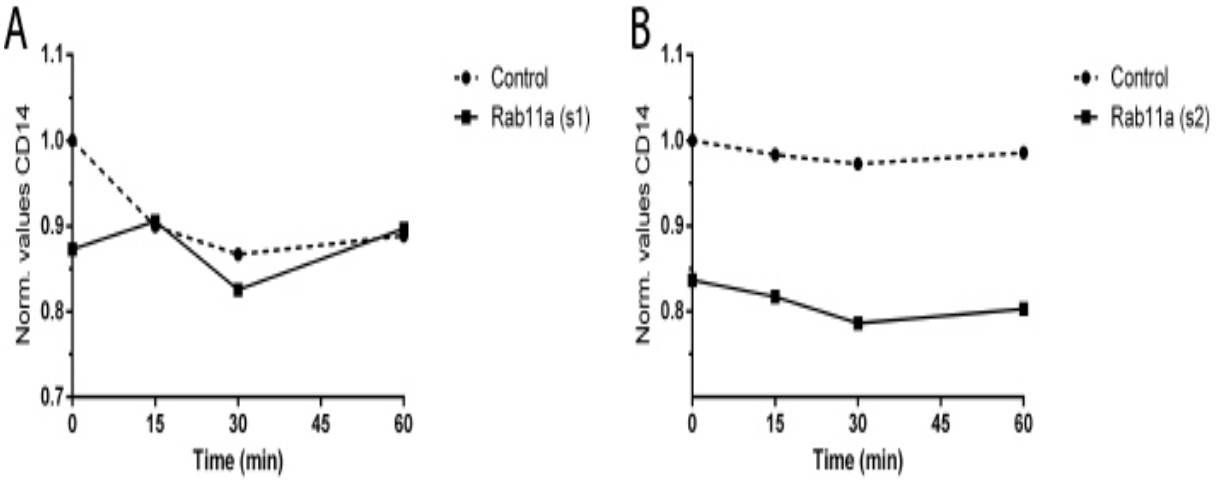

Figure 25: PM dynamics of CD14 in Rab11a depleted THP-1 cells (48 hrs PMA+ 72 hrs PMA-free).
THP-1 cells differentiated with 10 ng/ml PMA for 48 hrs, and rested 72 hrs in PMA-free medium, and treated with Rab7a siRNA. The Cells were stimulated with K12 LPS (100 ng/ml) at designated time points. Post-stimulation the cells were labeled with a CD14 FITC-conjugated antibody and analyzed using flow cytometry. The experiment was repeated four times and A) and B) display the data from two individual series. Count = 10000

There are not much difference in cells given 72 hrs of rest compared to those of 48 hrs rest (Fig. 23 and 25). Although the starting levels of CD14 on the PM seems to have slightly decreased, the internalization behavior when stimulated with K12 LPS don't digress greatly from what is observed in their corresponding control siRNA samples (Fig 25).

4.1.1 The effect of Rab11a depletion on LPS-induced cytokine expression

Rab11a's role in slow recycling towards the PM [97], as well as trafficking of TLR4 to phagosomes [27], makes it an apparent target to study. Using both Q-PCR and WB we wanted to investigate Rab11a depletions effect in the THP-1 system.

We put our focus on the protocol using 10 ng/ml PMA for differentiation, and 72 hrs of rest in PMA-free medium after the initial 48 hrs of PMA incubation. We based that decision on the expression levels of CD14 appeared to be stable using this protocol (Fig. 9b), a good IFN-β and TNF-α mRNA expression (Fig. 13a and 15a), and what appeared to be an increase in the dynamics of CD14 on the PM (fig. 17). We stimulated the cells with K12 LPS at indicated time points, and analyzed the cells using Q-PCR and WB as described in *Materials and Methods*.

Using Q-PCR we analyzed the expression levels of both IFN-β and TNF-α, using the same set up as illustrated in *Results 4.3*. First we measured the IFN-β in cells treated in THP-1 cells treated with Rab11a siRNA to explore any effect Rab11a would have on the TRIF-dependent pathway.

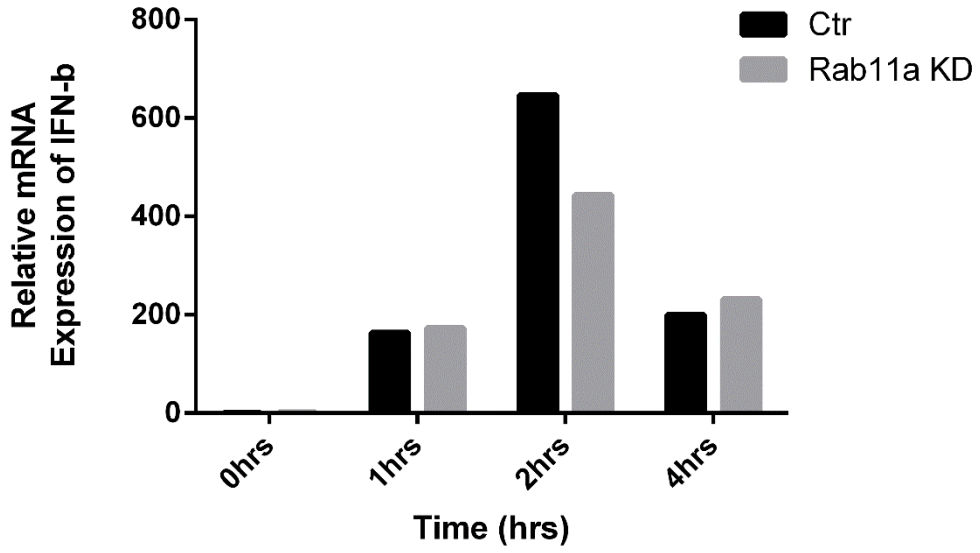

Figure 26: Expression of IFN-β in Rab11a depleted cells.
THP-1 cells were differentiated with 10 ng/ml PMA for 48 hrs and rested for 72 hrs. The cells were treated with siRNA towards Rab11a according to protocol. The cells were stimulated with K12 LPS (100 ng/ml) at designated time points before the cells were lysed and the RNA purified. The RNA was analyzed using Q-PCR and the Taqman probe system against IFN-β. The experiment was repeated four times and the results above are representative data of these.

Rab11a did not display any pronounced influence upon the IFN-β mRNA expression. After 1 hr the expression of IFN-β mRNA is basically identical (Fig. 26). The IFN-β response reaches its maximum after 2 hrs in both samples, and the Rab11a siRNA samples now display

a somewhat weaker IFN-β response compared to the control samples (Fig. 26). After 4 hrs the IFN-β response has started to decline, and the difference between the control samples and Rab11a siRNA treated samples has more or less equalized (Fig. 26). It could be speculated that Rab11a plays a supportive role in the sustainability in IFN-β signaling, as the initial and final IFN-β response are fairly equal. If Rab11a is involved in replenishing receptors or adaptors to the signaling compartment, it could explain the modest decrease in IFN-β expression levels at the peak of signaling.

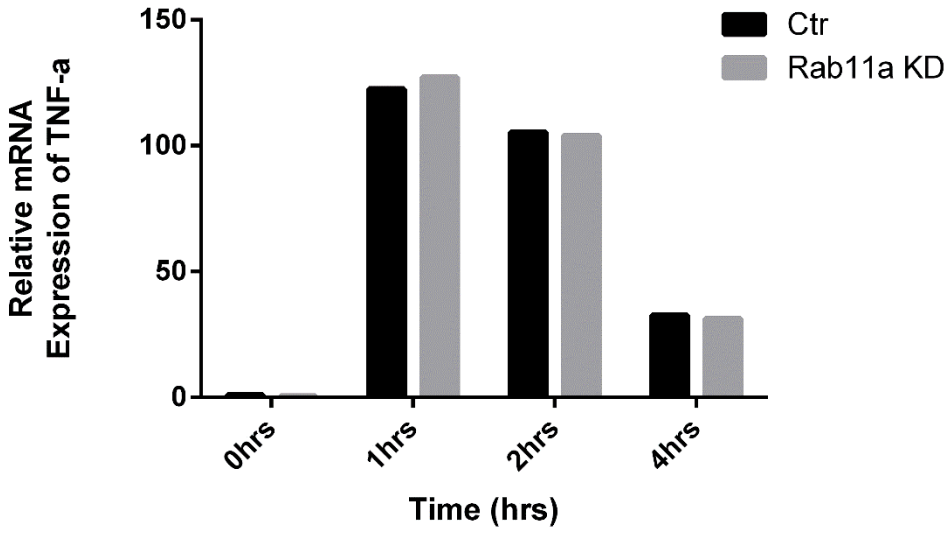

Figure 27: Expression of TNF-α in Rab11a depleted cells.
THP-1 cells were differentiated with 10 ng/ml PMA for 48 hrs and rested for 72 hrs. The cells were treated with siRNA towards Rab11a according to protocol. The cells were stimulated with K12 LPS (100 ng/ml) at designated time points before the cells were lysed and the RNA purified. The RNA was analyzed using Q-PCR and the Taqman probe system against TNF-α. The experiment was repeated four times and the results above are representative data of these. .

When analyzing the TNF-α results there seem to be no apparent effect of Rab11a KD (Fig. 27). The samples reach their response maximum for TNF-α after 1 hr, and both the control samples and the Rab11a siRNA treated samples display essentially the same amount of TNF-α expressed (Fig. 27). After 2 hrs and 4 hrs the expression levels of TNF-α gradually decline, however, they remain equal between the control samples and the KD samples (Fig. 27). It seems apparent that Rab11a has no significant role to play, direct or indirectly, in the TNF-α MyD88-dependent signaling pathway.

4.1.2 The effect of Rab11a depletion on proteins involved in regulation of LPS-induced TLR4 signaling

We wanted to investigate if Rab11a KD had any effect on the regulation of phosphorylated proteins that are |involved in TLR4 inflammatory signaling. The samples were seeded and stimulated with K12 LPS in parallel with the Q-PCR samples in order to keep the variation between the two experiments to a minimum. After stimulation the samples were treated

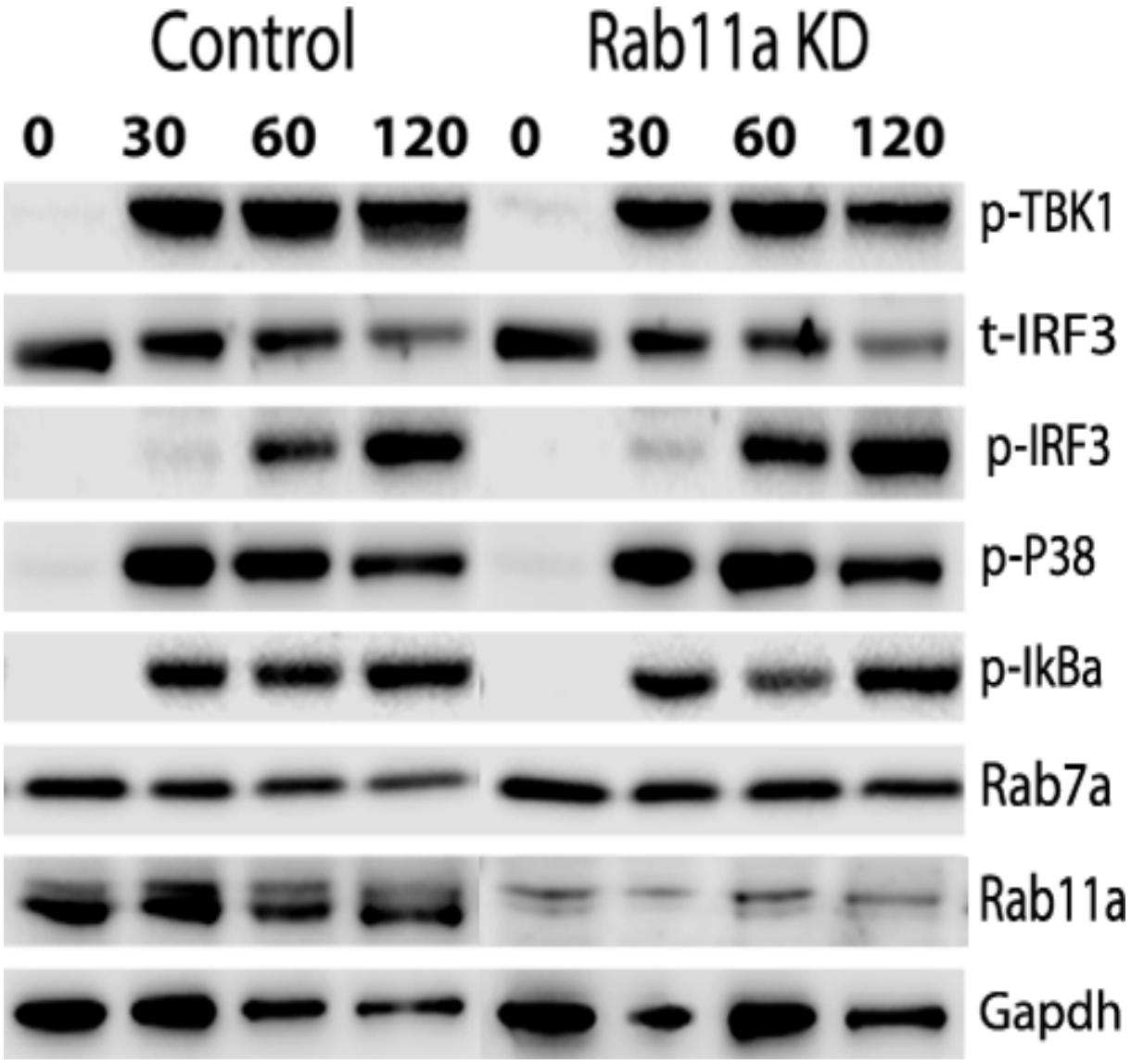

Figure 28: WB analysis of key regulators of the TLR4 signaling pathways in Rab7 depleted cells.
THP-1 cells were differentiated with 10 ng/ml PMA for 48 hrs and rested for 72 hrs. The cells were treated with siRNA towards Rab11a according to protocol. The cells were stimulated with K12 LPS (100 ng/ml) at designated time points, before the cells were lysed. The cell lysate was used to study the protein levels by WB. The experiment was repeated twice and the results above are representative data of these.

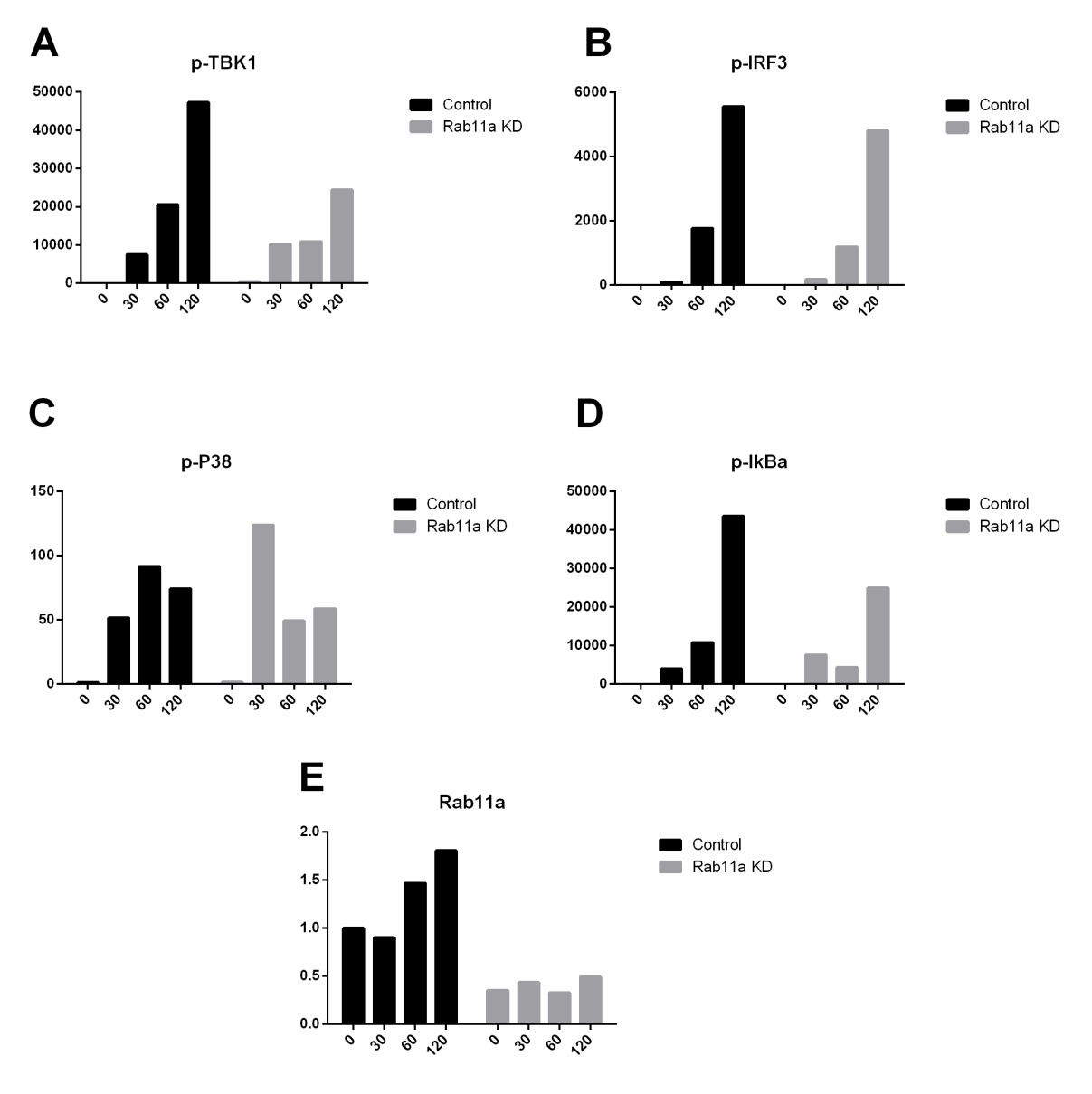

Figure 29: WB analysis of proteins regulating TLR4 signaling pathways in Rab11a depleted cells.
The blots were analyzed using Li-cor Odyssey and information about signal strength obtained using the Image Studio software. The graphs show the Gapdh-normalized results of A) p-TBK1, B) p-IRF3, C) p-P38, D) p-IkBa and E) Rab11a. The unstimulated control sample (Time point 0) was set to 1 and the rest of the values normalized towards this value. The Y-axis represents the increase of phosphorylated protein according to this normalization. The X-axis represents time in minutes.

Considering we did not observe any great variation in the expression of IFN-β (Fig. 26) and TNF- α (Fig. 27) we did not expect to see any great variation in the phosphorylation of the proteins involved in the signaling pathways (Fig. 28 and 29).

The phosphorylation of TBK1 indicates that there is a decreased activation of TBK1 in the Rab11a siRNA treated cells compared to the control samples (Fig. 29a). After 30 min the amount of p-TBK1 is basically equal between the controls and the siRNA samples, while it after 60 min is doubled in the control compared to the siRNA samples (Fig. 29a). If this is the case it shows no substantial effect on either the Q-PCR results (Fig. 27) nor any extensive

transference of this difference upon the phosphorylation of IRF3 (Fig. 29b). After 120 min there is a noteworthy difference between the control samples and the Rab11a siRNA treated cells. The control samples express an amount of p-TBK1 about two times higher than what is observed in the siRNA treated samples (Fig. 29a), however, this expressively higher amount of p-TBK1 does not seem to affect the amount of p-IRF3 correspondingly (Fig. 29b), nor the outcome of IFN-β (Fig. 26). If these results are indeed significant, then reason behind this could be that since TBK1 works together with TANK1 and IKKι to activate IRF3, there might be enough redundancy in the system, allowing for a proper activation of IRF3. One could also attain the possibility of Rab11a being involved in the activation or trafficking of this complex, or a step prior to this.

Correlating to the results of IFN-β in Figure 26, we did not see any great variation in the phosphorylation of IRF3 (Fig. 29b). There is essentially no amount of p-IRF3 within the first 30 min, and there is a slight increase after 60 min (fig. 29b) in both the control sample and the Rab11a siRNA treated cells. This result connects well to the results in Figure 4.24 where we start to see the first expression of IFN-β, the end product of IRF3 activation. After 120 min we still see no significant variations between the control samples and the Rab11a siRNA treated samples, as they both reach their recorded maximum values of p-IRF3, again agreeing with the results observed in Figure 4.24. Both the Q-PCR results (Fig. 26) and these WB results (Fig. 28 and Fig. 29b) suggest that Rab11a has little or no effect upon the TRIF-dependent pathway's outcome in the THP-1 model system.

The activation of P38 indicated that this part of the MyD88-dependent pathway was not significantly affected (Fig. 29c). While the Rab11a siRNA treated cells display a notably higher activation of P38 after 30 min compared to the control samples (Fig 29c), the overall activation, considering all time points, is not remarkably uneven.

The knockdown of Rab11a was also confirmed (Fig. 29e). The results indicated that there had been a depletion, though not as extensive as we had predicted. It might be that this slightly ineffective depletion of Rab11a affected the outcome of the experiments.

4.1 The effect of Rab7a depletion on LPS-induced TLR4 inflammatory signaling

Rab7a is a novel marker of the limiting membrane of the LEs, and plays an important part in the maturation of EEs to LEs [80]. As TLR4 receptors are internalized into EEs from the PM, where they consequently activate the TRIF-dependent pathway, they are also detained in the endosomes as they mature, resulting in the degradation of TLR4 in the endolysosome [94].

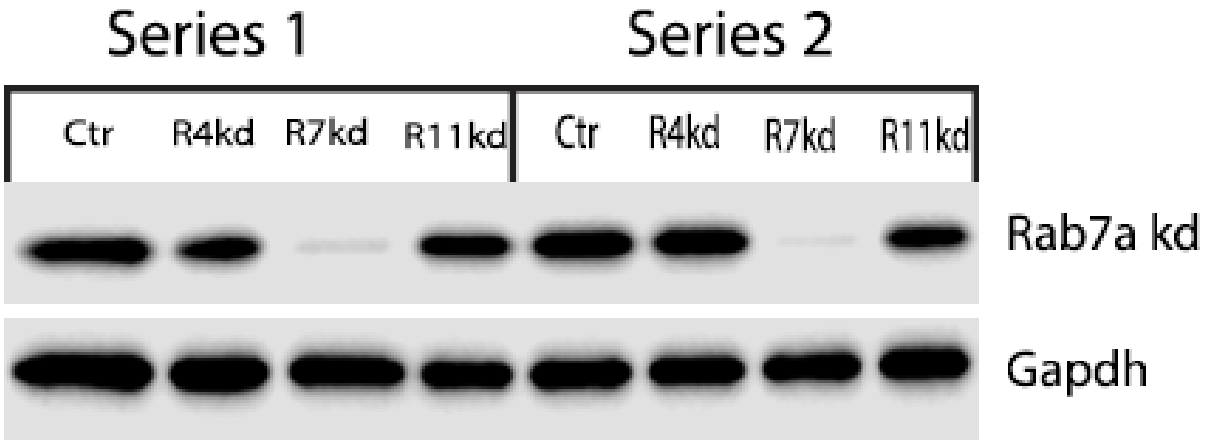

Figure 30: WB confirmation of Rab7a silencing (48 hrs PMA + 48 hrs PMA-free).
THP-1 cells were differentiated with 10 ng/ml PMA for 48 hrs, rested for 48 hrs in PMA free medium. The cells were treated with siRNA towards Rab7a according to protocol, and the lysate used to confirm the depletion of Rab7a using WB. The experiment was repeated twice and both results are presented in the figure.

THP-1 cells differentiated in medium with 10ng/ml PMA for 48 hrs in PMA free medium were treated with siRNA towards Rab7a. We confirmed that Rab7a had effectively been silenced using WB (Fig.30). We stimulated with K12 LPS at certain time points, and the CD14 surface levels of these cells were then investigated using Flow cytometry.

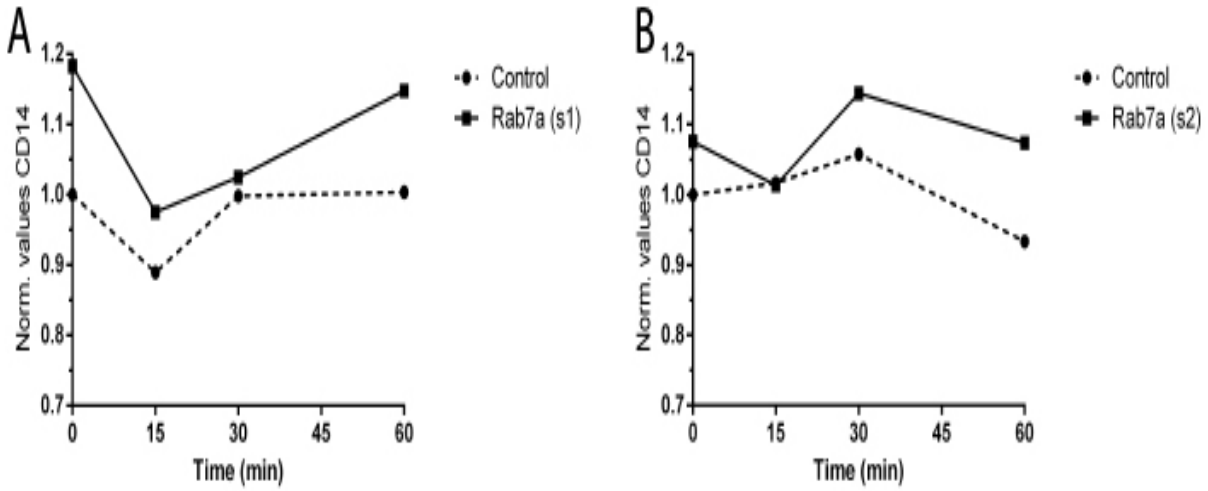

Figure 31: PM dynamics of CD14 in Rab7a depleted THP-1 cells (48 hrs PMA+ 48 hrs PMA-free).
THP-1 cells differentiated with 10 ng/ml PMA for 48 hrs, rested 48 hrs in PMA-free medium, and treated with Rab7a siRNA. The Cells were stimulated with K12 LPS (100 ng/ml) at designated time points. Post-stimulation the cells were labeled with a CD14 FITC-conjugated antibody and analyzed using flow cytometry. A) and B) display the data from two individual series. Count = 10000

As observed in Figure 31 the amount of CD14 on the PM was somewhat elevated compared to the control siRNA in both experiments. When stimulated with K12 LPS, CD14 seemed to drop the initial 15 min, before slightly increasing and stabilizing towards 60 min in siRNA treated cells. Nonetheless, CD14 levels remain elevated at all time points compared to the control in both experiments (Fig. 31).

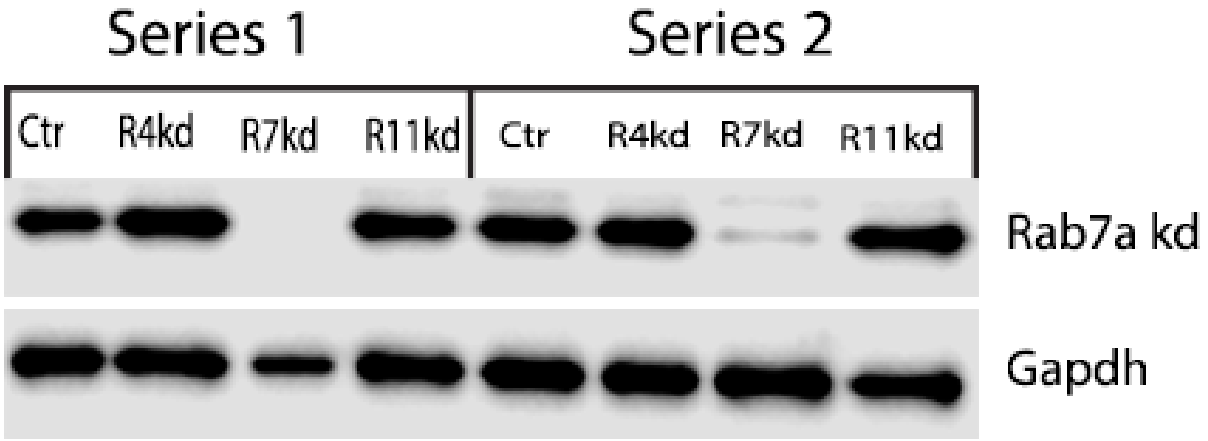

Figure 32: WB confirmation of Rab7a silencing (48 hrs PMA + 72 hrs PMA-free).
THP-1 cells were differentiated with 10 ng/ml PMA for 48 hrs, rested for 72 hrs in PMA free medium. The cells were treated with siRNA towards Rab7a according to protocol, and the lysate used to confirm the depletion of Rab7a using WB. The experiment was repeated twice and both results are presented in the figure.

We repeated the experiment with cells rested for 72 hrs. We confirmed that Rab7a had been depleted (Fig. 32) and repeated the Flow cytometry analysis in these cells.

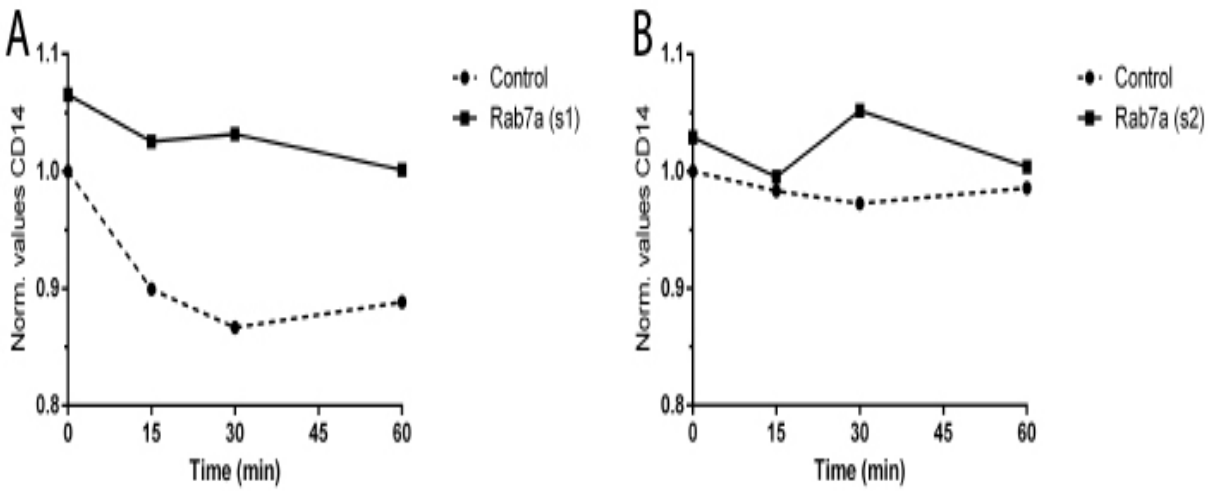

Figure 33: PM dynamics of CD14 in Rab7a depleted THP-1 cells (48 hrs PMA+ 72 hrs PMA-free).
THP-1 cells differentiated with 10 ng/ml PMA for 48 hrs, rested 72 hrs in PMA-free medium and treated with Rab7a siRNA. The Cells were stimulated with K12 LPS (100 ng/ml) at designated time points. Post-stimulation the cells were labeled with a CD14 FITC-conjugated antibody and analyzed using flow cytometry. A) and B) display the data from two individual series. Count = 10000

After 72 hrs of rest the amount of PM located CD14 remains slightly elevated in Rab7a siRNA treated cells during the entire course of the LPS stimulation. However, the amount of CD14 remains, on average, quite stable over the first 60 min (Fig. 33).

Overall it seems that Rab7a don't have any extensive intrusions upon the internalization of CD14 other than its elevated levels on the PM. This could be due to Rab7a's role in sustaining a normal endosomal pathway and an increased recycling of CD14 from EE. Even so, there might be certain interactions in both the MyD88-dependent pathway and TRIF-dependent pathway that actively influence the behavior of endosomal maturation, as well as endolysosomal formation.

4.1.1 The effect of Rab7a depletion on cytokine expression

We wanted to study the effect of Rab7a in the MyD88-dependent and the TRIF-dependent signaling pathways. We investigate the expression levels of IFN-β and TNF-α with Q-PCR to determine the effect of Rab7a depletions effect on signaling.

Using Q-PCR we analyzed the expression levels of both IFN-β and TNF-α, using the same set up as illustrated in *Results 4.3*. First we measured the IFN-β in cells treated with Rab7a siRNA.

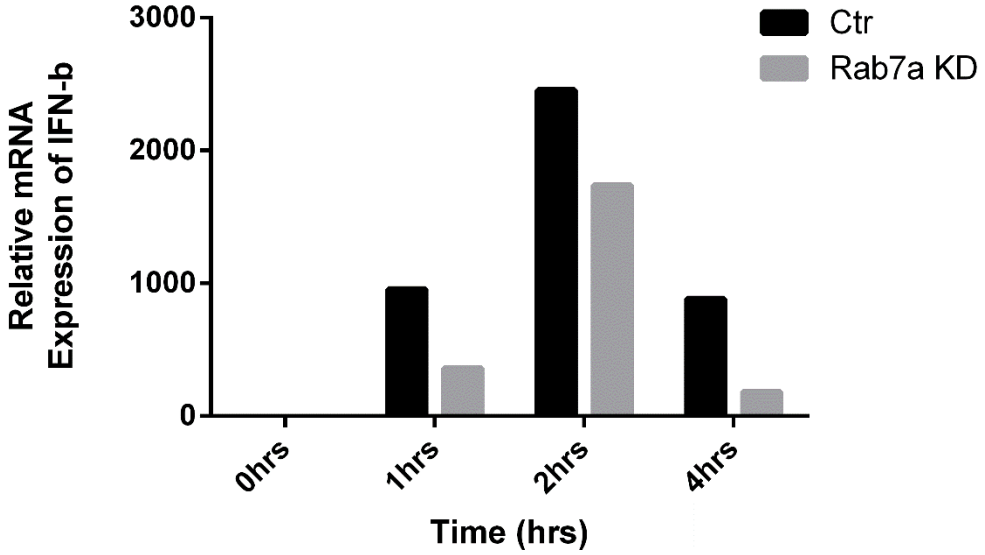

Figure 34: Expression of IFN-b in Rab7a depleted cells.
THP-1 cells were differentiated with 10 ng/ml PMA for 48 hrs and rested for 72 hrs. The cells were treated with siRNA towards Rab7a according to protocol. The cells were stimulated with K12 LPS (100 ng/ml) at designated time points, before the cells were lysed and the RNA purified. The RNA was analyzed using Q-PCR and the Taqman probe system against IFN-β. The experiment was repeated four times and the results above are representative data of these.

It became quite apparent that Rab7a plays a role in the regulation of IFN-β mRNA expression. At all time points, the cells treated with siRNA towards Rab7a displayed a considerably lower amount of IFN-β mRNA than their control siRNA (Fig. 34). After 1 hr the cells display a moderate response, however, the IFN-β expression is one third in Rab7a siRNA treated cells compared to what is observed in the control samples (Fig. 34). After 2 hrs both samples reach their expression maximum, still we see that the IFN-β is lower in the Rab7a knockdown cells (Fig. 34). After 4 hrs the total expression of IFN-β considerably drops, but the effect of the Rab7a knockdown remains (Fig. 34).

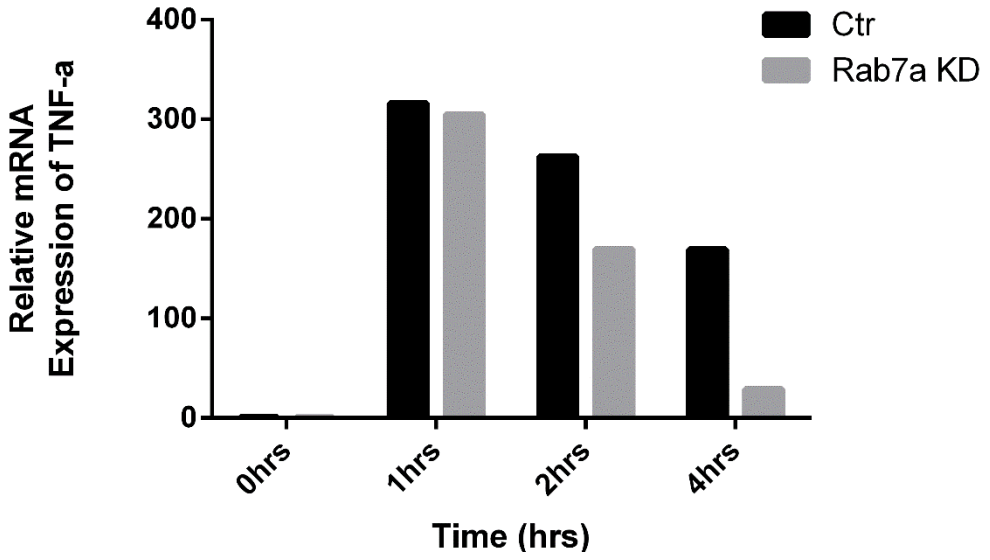

Figure 35: Expression of TNF-a in Rab7a depleted cells.
THP-1 cells were differentiated with 10 ng/ml PMA for 48 hrs and rested for 72 hrs. The cells were treated with siRNA towards Rab7a according to protocol. The cells were stimulated with 100 ng/ml K12 LPS (100 ng/ml) at designated time points, before the cells were lysed and the RNA purified. The RNA was analyzed using Q-PCR and the Taqman probe system against TNF-α. The experiment was repeated four times and the results above are representative data of these.

Rab7a also proved to have an effect on the expression of TNF-α mRNA. After 1 hr of LPS stimulation, the TNF-α expression levels peaked in both siRNA treated samples and the control samples. There is not a significant difference between the control samples and the Rab7a siRNA treated cells in terms of the expression of TNF-α mRNA at this point (Fig. 35). The cells treated with Rab7a siRNA express somewhat reduced levels of TNF-α after 2 hrs, and this effect is seen to reoccur at the 4 hrs time point (Fig. 35).

4.1.2 The effect of Rab7a depletion on proteins involved in regulation of LPS-induced TLR4 signaling

We wanted results that would give us an indication of the effect the Rab7a KD had on the signaling cascade leading up to the cytokine induction we observed in the Q-PCR results (Fig. 34 and 35). We were interested in locating a potential stage in the signaling cascade that could be a candidate for any direct regulation of Rab7a.

The samples were seeded and stimulated with K12 LPS in parallel with the Q-PCR samples in order to keep the variation between the two experiments to a minimum. After stimulation the samples were treated

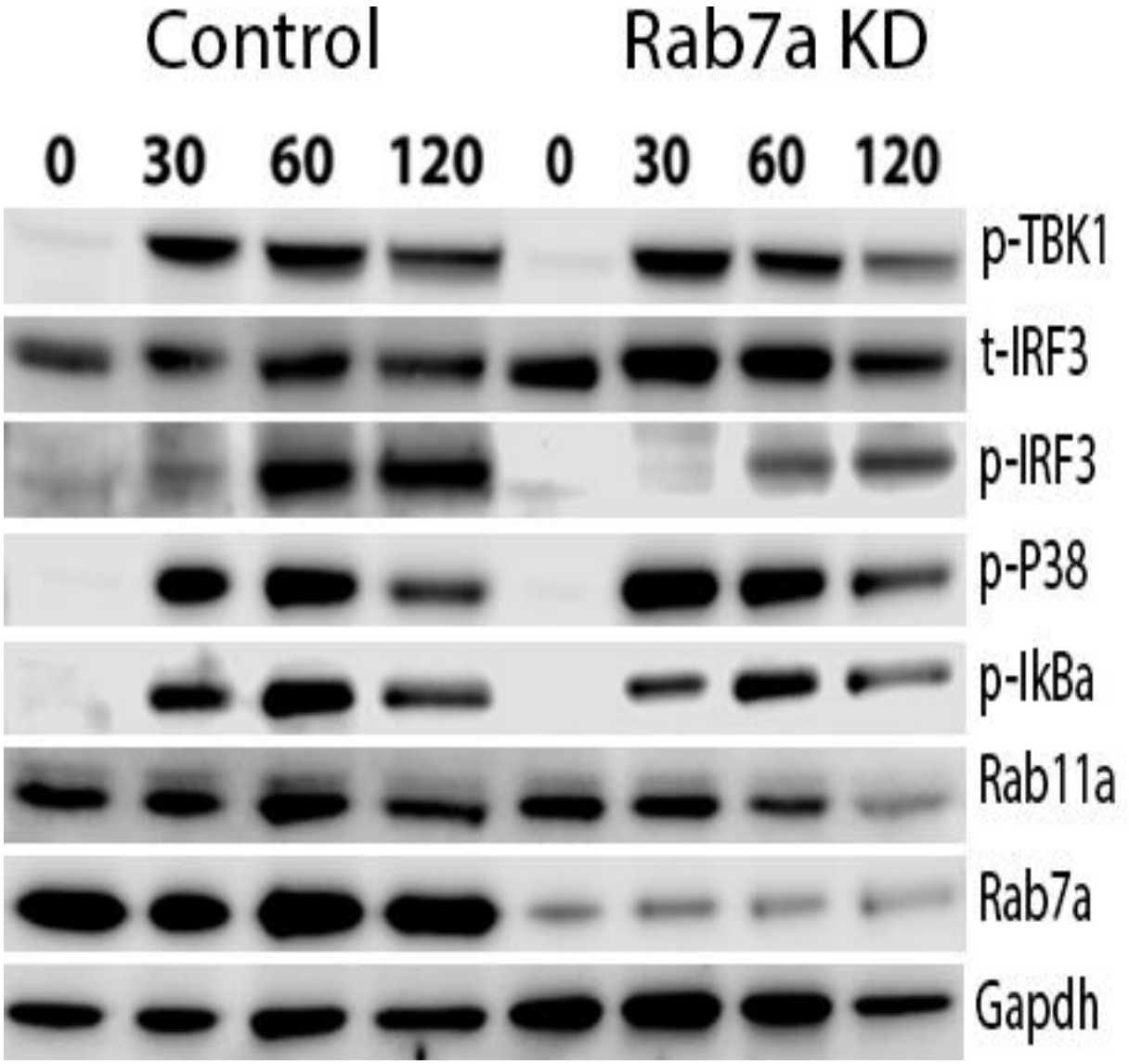

Figure 36: WB analysis of key regulators of the TLR4 signaling pathways in Rab7 depleted cells.
THP-1 cells were differentiated with 10 ng/ml PMA for 48 hrs and rested for 72 hrs. The cells were treated with siRNA towards Rab7a according to protocol. The cells were stimulated with K12 LPS (100 ng/ml) at designated time points, before the cells were lysed. The cell lysate was used to study the protein levels using WB. The experiment was repeated twice and the results above are representative data of these.

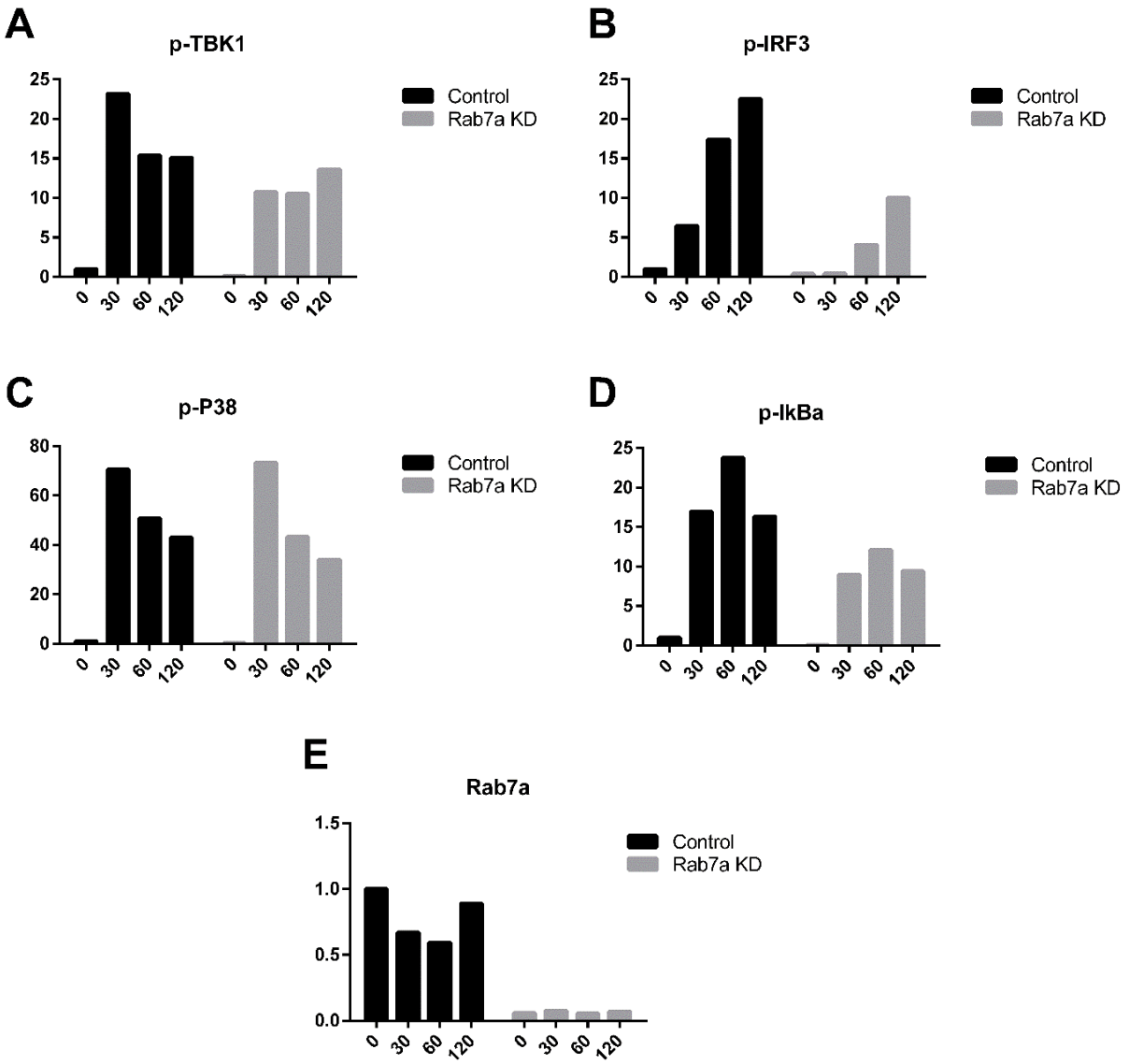

Figure 37: WB analysis of proteins regulating TLR4 signaling pathways in Rab7 depleted cells.
The value of signal strength from blots was obtained using Li-cor Odyssey and Image Studio software. The graphs show the Gapdh-normalized results of A) p-TBK1, B) p-IRF3, C) p-P38, D) p-IkBa and E) Rab7a. The unstimulated control sample (Time point 0) was set to 1 and the rest of the values normalized towards this value. The data above represents the results from 2 individual experiments. The Y-axis represents the increase of phosphorylated protein according to this normalization. The X-axis represents time in minutes.

The effects of the Rab7a siRNA treatment, which were demonstrated in the Q-PCR results (Fig. 34 and 35), were confirmed in the WB results as well (Fig. 36 and 37). The results indicate a significantly impaired phosphorylation of both TBK1 and IRF3, both regulators of the TRIF-dependent pathway (Fig. 37a and b). TBK-1 phosphorylation, in the Rab7a siRNA treated cells, is essentially half of what is observed in the control samples after 30 min (Fig. 37a). After 60 min and 120 min, the amount of p-TBK1 diminishes in the control samples, while the levels of p-TBK1 in the Rab7a siRNA treated cells remain stable (Fig. 37a)

The effect on the phosphorylation of IRF3 is even greater. In the control samples we could observe a modest increase in p-IRF3 after 30 min, which continued to increase at both 60 min and 120 min (Fig. 37b). In the cells treated with Rab7a siRNA there is no increase of p-IRF3 after 30 min, in contrast to what we could see in the control samples (Fig. 37b). After 60 min we begin to see a modest increase in p-IRF3, which continues to increase after 120 min, however, substantially lower to what was observed in the control samples (Fig. 37b). As to why there is such a drastic decrease in p-IRF3 in Rab7a siRNA treated samples (Fig. 37b), when there is only an approximate 50 % reduction of p-TBK1 (Fig. 37a) one could speculate that the trafficking of co-activators of IRF3, such as TANK and Ikkι is impeded, effectively delaying the activation of IRF3. Alternatively it suggests that even a moderate down regulation of TBK1 is hindering any downstream amplification, resulting in a substantially lower IRF3 activation.

The phosphorylation of P38 is not affected in any significant manner. The amount of p-P38 is essentially the same at all of the time points in both the control samples and the cells treated with Rab7a siRNA (Fig 37c). This indicates that Rab7a infer no significant impact upon the MyD88-dependent pathway, which occur at the PM

IκBα, which is responsible for the activation of NF-κB, displayed some variations between the control samples and the Rab7a siRNA treated. The control samples indicate a strong phosphorylation after 30 min, which peaks after 60 min, and somewhat decrease after 120 min (Fig. 37d). The same pattern is seen in Rab7a siRNA treated cells, but with half the intensity (Fig. 37d).

We also confirmed the KD of Rab7a, and the results show that the Rab7a siRNA treatment was efficient (Fig. 37e).

5 Discussion

THP-1 DIFFERENTIATION PROTOCOL OPTIMIZATION

THP-1 cells have been established as a human model system to explore the properties of monocytes and Mφs [107, 108, 122]. In this study we sought to develop a reliable method of THP-1 differentiation into Mφ-like phenotypes, optimizing it towards studies of TLR4 inflammatory signaling and trafficking.

One of the most common ways to differentiate THP-1 cells in order for them do adopt Mφ-like properties is by treating the cells with 100 ng/ml PMA (~120 nM) [108, 122, 130-132] for 72 hrs. However, concentrations ranging from 10 ng/ml [133] to 400 ng/ml [134] have been published. At the start of the project we adopted the protocol using 100 ng/ml PMA over a course of 72 hrs [130]. Using this protocol we found that the level of expression of CD14 and TLR4 on the PM was very limited (Fig.6 and Fig 7c) and we therefore decided to make a new protocol for THP-1 cell differentiation into Mφs. We developed a protocol based on two formerly published protocols [121, 122] where we lowered the PMA concentration and included PMA-free rest period.

PROTOCOL OPTIMIZATION AND THE EFFECT ON PM PROTEIN LEVELS

We observed that both reduced PMA concentration and the PMA-free rest period had positive effects on the surface levels of CD14 compared to the initial protocol. The reduction of PMA-concentration alone resulted in no substantial difference (Fig. 7), but with an inclusion of a rest period in PMA-free medium we saw a robust increase in the CD14 positive populations (Fig. 8 and 9). The rest period had a positive effect both cells differentiated with 100 ng/ml and 10 ng/ml PMA. We also observed that the THP-1 cells treated with the reduced PMA concentration resulted in a more defined CD14 positive population compared to the 100 ng/ml PMA (Fig. 8 and 9). Based on these results we concluded that 10 ng/ml PMA and a resting period in PMA-free medium for 48 or 72 hrs were important to boost CD14 expression levels on the PM.

Using the original differentiation protocol (100 ng/ml PMA for 72 hrs and a 3hrs incubation step in serum-free medium) we could not detect TLR4 on the PM using flow cytometry (data not shown). These indications had also been confirmed using confocal microscopy, where no substantial amount of TLR4 was observed on the PM in differentiated THP-1 cells (*Kristian K. Starheim. Unpublished data*). Using the new modified protocols we were able to observe a TLR4 positive population (Fig. 10), however, due to the minimal shift and low detection levels we chose to focus our studies on CD14. It has been formerly reported that humane monocytes express relatively low amount of TLR4 on the PM, so these results were not all that surprising.

CD11b is another PM expressed protein that is involved in inflammatory events, and is also up regulated in Mφs. We noticed a difference in the expression of CD11b when comparing 10 ng/ml PMA and 100 ng/ml PMA after 48 hrs of rest, where an apparently heterogeneous population expressed different levels of CD11b. This difference evened out into a homogenous expression of CD11b after 72 hrs (Fig. 11). It appeared that 100 ng/ml PMA delayed the stable expression of CD11b on the PM after 48 hrs of rest. We determined that, even though TLR4 PM levels were lower than we expected, the CD11b and CD14 levels indicate a more complete differentiation towards Mφ-like morphology in cells differentiated with the new optimized PMA concentration and the inclusion of a rest period.

PROTOCOL OPTIMIZATION AND THE EFFECT ON TLR4 SIGNALING

To explore any further effects the modified differentiation protocols had on the cells, as well as determining the most advantageous protocol to our needs, we decided to quantify some end products of the LPS-activated signaling. Using Q-PCR we monitored MyD88-dependent and TRIF-dependent signaling pathways, as defined by the expression of TNF-α and IFN-β mRNA levels, respectively. In cells rested for 48 hrs in PMA-free medium we observed a substantial increase induction of IFN-β mRNA levels following LPS stimulation when differentiated with 10 ng/ml PMA (Fig 12a), compared to cells differentiated with 100 ng/ml PMA (Fig 12b). Therefore we suggest that a higher concentration impedes a full TLR4 response upon LPS stimulation. One could speculate if the lower CD14 levels on the PM cells treated with 100 ng/ml (Fig. 8c) is one of the factors involved in the observed weaker or delayed IFN-β response, as these cells also displayed a weakened TNF-α response (Fig. 15b) compared to cells differentiated with 10 ng/ml PMA (Fig. 14a and 15a). A lower amount of CD14 could

impair the TNF-α response from the PM [31], as well as decrease the TRIF activation due to the reduction of the CD14-dependent endocytosis if the activated MD2-TLR4 complex [11, 35].

The cells differentiated using 10 ng/ml PMA and allowed to rest for 72 hrs showed a well-developed LPS response inducing high levels of both IFN-β and TNF-α mRNA (Fig. 13a and 15a). In contrast the cells differentiated with 100 ng/ml PMA showed an even higher induction of IFN-β mRNA levels during the course of LPS stimulation (Fig 13b), however, the induction of TNF-α mRNA was markedly reduced (Fig. 15b). It has been reported that an excessively high PMA concentration can induce unwarranted cytokine expression [121], and this may explain why we observed an increase of IFN-β expression in cells differentiated with 100 ng/ml PMA, but it does not account for the reduced TNF-α levels we observed. Taking these results in consideration there were a substantial amount of CD14 positive cells (Fig 9) argues that the CD14 amount on the PM alone does not explain the extensive response of IFN-β or TNF-α. Other factors are likely to be involved which are also affected by the differences in differentiation protocol. Taking all these results into consideration we concluded that the 10 ng/ml PMA differentiation protocol was a better protocol than using 100 ng/ml PMA when studying the TLR4 signaling pathways.

LPS-INDUCED CD14 DYNAMICS

When comparing LPS-induced dynamics of CD14 on the PM in the different protocols there were a substantial difference between the cells that had been rested for 48 hrs and 72 hrs (Fig. 16 and 17). While, 48 hrs rest only gave a small variation in the CD14 levels during LPS stimulation the 72 hrs rested cells displayed a general reduction in the PM CD14 levels over the course of 60 min LPS stimulation. This observation in the 72 hrs rested cells may be explained by an increased rate of endocytosis of the CD14-MD2-TLR4 complex. LPS induced endocytosis of the LPS bound CD14-MD2-TLR4 complex has previously been described and shown to limit MyD88-dependent signaling by targeting the complex for lysosomal degradation [11]. Endocytosis of TLR4 upon LPS stimulation has further been shown to depend on CD14 [119] and to be instrumental to TRIF-dependent signaling occurring from endosomes [36].

Effect of Rab4a depletions on TLR4 trafficking and signaling

Rab4a is most known for its role in the rapid recycling of endocytosed content directly back to the PM [83]. When we repeated the studies of the dynamics of CD14 on the PM following LPS stimulation on Rab4a depleted cells we observed highly variable results. The THP-1 cells rested for both 48 hrs and 72 hrs following the initial 48 hrs in 10 ng/ml PMA showed a generally lower amount of CD14 on the PM at early time points after the LPS stimulation (Fig 19 and 21). However, the cells rested for 72 hrs had considerably lower CD14 levels compared to the cells rested for 48 hrs. This suggests that Rab4a play a part in the maintenance of CD14 levels on the PM in differentiated THP-1 cells. During the course of LPS stimulation we observed the CD14 dynamics on the PM in Rab4a KD cells to vary from experiment to experiment although the same condition were being applied (Fig 19 and 21). We have yet to determine any conclusion to why this is the case, however, as the level of CD14 were lower in the Rab4a depleted cells than in the control siRNA treated cells in all our experiments, Rab4a could probably have a role in maintaining the CD14 levels by rapid recycling from EEs as reported for a number of other receptors [83, 135] .

Effect of Rab11a depletions on TLR4 trafficking and signaling

Rab11a is a small Rab GTPase that controls the slow recycling of internalized content back to the PM, through the ERC [97]. It has also been linked in recruitment of TLR4 to phagosomes [27]. We observed that the amount of CD14 on the PM in Rab11a depleted cells were lower than compared to the control siRNA, but not to the same extent as Rab4a depleted cells, particularly after a 72 hrs rest. This could be due to Rab4a having a greater role than Rab11a in maintaining the surface levels of CD14. We also observed that the dynamics of CD14 did not vary noteworthy compared to the control siRNA samples in LPS stimulated cells.

The observation that Rab11a depletion had no striking effect upon the expression of neither IFN-β (Fig. 34) nor TNF-α (Fig. 35) seemed to indicate that Rab11a has no noteworthy effect upon neither the MyD88-dependent signaling pathway, nor the TRIF-dependent signaling pathway in the THP-1 model system. This observation was strengthened by the observation that the activation of IRF3 remained equal when Rab11a siRNA treated cells were compared to control samples (Fig. 37b). We did observe a decrease in the phosphorylation of IκBα, however, this did not result in any notable changes in the expression of TNF-α. Likely the activation of NF-κB is more complex too be illustrated by this event alone.

Considering that Rab11 has been linked to the trafficking of TLR to *E. coli* phagosomes [27] and a reported effect in the HEK-293 model system in a separate study (*Clement Ajayi, Astrid Skjesol, Harald Husbye. Unpublished Data*), it was unexpected that the Rab11a depletion had just a weak effect on the expression of IFN-β mRNA levels. It could be that stimulation with K12 LPS is not enough to illustrate Rab11a's role fully, and that stimulation with *E. coli* and phagosome formation is required. Another possibility for the lack of effect in Rab11a depleted cells could be that the Rab11 siRNA treatment was not as efficient as expected (Fig. 37e). It could be that the reduced, but not diminished, levels of Rab11a was enough to maintain the function of the inflammatory signaling response.

An interesting observation is that in the Rab11a depleted cells the other Rab11 isoform Rab11b seems to be up regulated after 72 hrs of rest (Fig 32), while undetected after 42 hrs rest (Fig. 30). The lower band in Figure 32 represents Rab11a, and we resolved that the upper band represents the isoform Rab11b based on former observations (*Harald Husebye. Unpublished data*). Rab11b appear unaffected by the Rab11a depletion (Fig. 32). This observation along with the weak effect on cytokine expression in Rab11a depleted cells may indicate that Rab11b has a redundant effect towards Rab11a. This could explain why we did not see any strong effect of the Rab11 depletion on IFN-β nor TNF-α in the THP-1 system, similar to those effects observed in the HEK-293 cell line in a separated study (Data not shown). It could also explain why the amount of CD14 on the PM in Rab11a depleted cells were not as heavily impacted such as in Rab4a depleted cells.

Effect of Rab7a depletions on TLR4 trafficking and signaling

In Rab7a depleted cells we observed that the initial levels of CD14 on the PM were substantially elevated compared to the control siRNA samples, in both 48 hrs and 72 hrs of rest, and differentiation with 10 ng/ml PMA. Considering Rab7a's role in maintaining the integrity of the endolysomal pathway [136], and as a key regulator of endosomal maturation [80] the elevated level of CD14 on the PM might be explained by decreased trafficking of CD14 into the endolysomal pathway and impaired lysosomal degradation of CD14. The CD14 levels on the PM in Rab7a siRNA treated cells remain elevated following LPS-stimulation and the dynamics of CD14 largely mimic those of the control samples in all the experiments.

When we analyzed the effect of Rab7a depletion on IFN-β and TNF-α we observed that the induction of IFN-β mRNA was substantially lowered during the entire course of LPS

stimulation (Fig 26). This suggests Rab7a depletion affects the activation of the TRIF-pathway considerably. This data was supported by the observation that the activation of IRF3 was substantially down regulated in Rab7a depleted cells (Fig. 29b). Additional support to this effect was obtained in similar experiments in a separate study in HEK-293 study (*Clement Ajayi, Astrid Skjesol, Harald Husbye. Unpublished Data*). Rab7a depletion affects endosomal maturation and the delivery of cargo to the lysosomes [136, 137], but does not affect the internalization of cargo from the PM [138]. Taking this into consideration, the MD2-TLR4 complex is most likely internalized as normal, but other factors result in the decreased IFN-β mRNA levels. It could be that the TRIF-dependent pathway is most effectively activated from RAb7a positive LEs. TNF-α mRNA levels were unaffected after 1 hr of LPS-stimulation, however, at both 2 hrs and 4 hrs the levels of TNF-α were markedly lower than compared to the controls (Fig. 27). This delayed reduction of TNF-α could be due to a lower activation of TRAF6 and RIP1 through TRIF. TRAF6 and RIP1 are reported to regulate the late activation of NF-κB [61, 67]

Cell death

Finally we have to address the observed cell death. While we did not have time to properly assess the extent or rate of apoptosis, we did however, manage to obtain some preliminary data that could help explain the instability of the results observed in some of the experiments with cells differentiated with 10 ng/ml PMA (Appendix Fig. 38 and 39). In the primary loading control of the WB lysates, we generally observed very low protein levels after 2 hrs of K12 LPS stimulation (Data not shown). The same tendencies could be observed in the purified RNA concentration after 4 hrs of LPS stimulation (Data not shown). Even though we adjusted the experiments according to these low concentrations in both the WB and Q-PCR experiments, it is not unlikely that the cellular response is substantially disturbed at these time points to yield exact data.

Cells differentiated with 10 ng/ml PMA appeared to be susceptible to apoptosis compared to cells treated with 100 ng/ml PMA. Cultures of differentiated THP-1 cells seemed to be visibly affected by this after 1 hr of LPS-stimulation. The reason for this could be that the higher expression of TNF-α, and possibly IFN-β, in these cells induces a higher response of Caspace8/3 through receptors such as TNFR [69]. The rate of this cell death seemed to be up regulated in cells treated with siRNA as well (Data not shown), further complicating the

collection of data. However, it is not surprising that the depletion of certain proteins may cause lower cell viability. It might be possible to assess this problem with further optimization of the differentiation of THP-1 cells, in order to maintain most the benefits that the new protocols yielded.

6 Final remarks and future aims

In this study we show that THP-1 cells is a good model system for studying TLR trafficking and signaling, given that they are differentiated in a proper way. We have demonstrated that the differentiation of THP-1 cells can be enhanced in order to increase the TLR4 induced inflammatory signaling response and to obtain Mφ-like structures. The reduced concentration of 10 ng/ml PMA resulted in an improved cytokine expression, as well as an up regulation of the CD14 amount on the PM. The introduction of either a 48 hrs or 72 hrs rest period in PMA-free medium, after the initial 48 hrs of differentiation with PMA, also proved essential for the CD14 amount on the PM and cytokine expression.

Due to the observations of the substantial changes induced by the different protocols, we believe that differentiation of THP-1 cells can be further optimized. We consider this to be necessary considering that THP-1 cells differentiated with 10 ng/ml PMA seem to easily undergo apoptosis. A study assessing the viability of the THP-1 cells during the course of LPS-stimulation should be conducted. The possibility that we might have to increase the PMA concentration slightly in order to generate THP-1 cells that remain stable within 2-3hrs of LPS stimulation is likely. There is also a possibility that increasing the rest period might alleviate some of these effects. It could be that newly differentiated THP-1 cells are weaker, and that increasing the rest period might yield a population of THP-1 cells more resistant towards these apoptotic influences.

If increasing the cell viability is possible, then repeating most of the experiments are in order. Creating a more complete picture of the dynamics of PM proteins using flow and/or alternatively confocal microscopy would be beneficial to compare the effects of Rab GTPases on these initial events of TLR4 trafficking.

We also observed that the Rab4a oligo gave highly variable data when the CD14 levels at the PM were monitored during LPS stimulation using flow cytometry. This may due to how the flow analysis was carried out (eg. many samples analyzed over a short time period) or may be a result of side effect induced by that particular siRNA. The latter is probably true as less variation and more consistent results were observed when the siRNA targeting Rab11a and Rab7a were used. Further, when analyzing the MyD88- and TRIF-dependent signaling in cells treated with Rab11a and Rab7a siRNA using Q-PCR or WB, less variation was observed and we feel confident about the strength of the data

A future aim will be to target Rab4a, Rab11a and Rab7a using several other siRNA oligos to test if the results presented holds true. One should also test the effect of these oligos in primary cells such as human macrophages and look for a similar effect of Rab knock down on TLR4 signaling observed in this study. This is especially interesting considering Rab7a, as it provided the most consistent results. Optimizing the THP-1 protocol and verifying these data using several oligos would be a top priority. Future experiments could be trying to specifically targeting Rab7a effectors in an attempt to reveal a specific function in TLR4 signaling. Targeting components of the endosomal maturation complex, such as Mon-1, could be a way to determine if endosomal maturation is required for the activation of the TRIF-dependent pathway, without targeting other functions of Rab7a. Addressing any changes in the internalization rate, as well as investigating whether there is an increase or decrease in the rate of LE biogenesis, and the formation of intraluminal vesicles in an unstimulated resting state would also be interesting.

Addressing the potential role of these Rab GTPases in TLR4 signaling and trafficking, as well as the function of other TLRs is an interesting issue. Considering the main focus in TLR research has mainly been focused on signaling interactions and the regulation of this, trafficking has been largely untouched. Increasing our efforts into the understanding of these processes will undoubtedly result in a greater understanding of the innate immunity and the mechanism behind inflammation.

7 References

1. Akira, S. and H. Hemmi, *Recognition of pathogen-associated molecular patterns by TLR family.* Immunol Lett, 2003. **85**(2): p. 85-95.
2. Medzhitov, R., P. Preston-Hurlburt, and C.A. Janeway, Jr., *A human homologue of the Drosophila Toll protein signals activation of adaptive immunity.* Nature, 1997. **388**(6640): p. 394-7.
3. Kawai, T. and S. Akira, *The role of pattern-recognition receptors in innate immunity: update on Toll-like receptors.* Nat Immunol, 2010. **11**(5): p. 373-84.
4. Yoneyama, M. and T. Fujita, *Function of RIG-I-like receptors in antiviral innate immunity.* J Biol Chem, 2007. **282**(21): p. 15315-8.
5. Fritz, J.H., et al., *Nod-like proteins in immunity, inflammation and disease.* Nat Immunol, 2006. **7**(12): p. 1250-7.
6. Geijtenbeek, T.B.H. and S.I. Gringhuis, *Signalling through C-type lectin receptors: shaping immune responses.* Nature Reviews Immunology, 2009. **9**(7): p. 465-479.
7. Re, F. and J.L. Strominger, *Monomeric recombinant MD-2 binds Toll-like receptor 4 tightly and confers lipopolysaccharide responsiveness.* Journal of Biological Chemistry, 2002. **277**(26): p. 23427-23432.
8. Jin, M.S., et al., *Crystal structure of the TLR1-TLR2 heterodimer induced by binding of a tri-acylated lipopeptide.* Cell, 2007. **130**(6): p. 1071-82.
9. Hayashi, F., et al., *The innate immune response to bacterial flagellin is mediated by Toll-like receptor 5.* Nature, 2001. **410**(6832): p. 1099-1103.
10. Hemmi, H., et al., *A Toll-like receptor recognizes bacterial DNA.* Nature, 2000. **408**(6813): p. 740-5.
11. Husebye, H., et al., *Endocytic pathways regulate Toll-like receptor 4 signaling and link innate and adaptive immunity.* EMBO J, 2006. **25**(4): p. 683-92.
12. Kumar, H., T. Kawai, and S. Akira, *Pathogen recognition by the innate immune system.* Int Rev Immunol, 2011. **30**(1): p. 16-34.
13. Shi, C. and E.G. Pamer, *Monocyte recruitment during infection and inflammation.* Nature Reviews Immunology, 2011. **11**(11): p. 762-774.
14. Murray, P.J. and T.A. Wynn, *Protective and pathogenic functions of macrophage subsets.* Nat Rev Immunol, 2011. **11**(11): p. 723-37.
15. Wang, J., et al., *Toll-like receptors expressed by dermal fibroblasts contribute to hypertrophic scarring.* J Cell Physiol, 2011. **226**(5): p. 1265-73.

16. Abreu, M.T., *Toll-like receptor signalling in the intestinal epithelium: how bacterial recognition shapes intestinal function (vol 10, pg 131, 2010).* Nature Reviews Immunology, 2010. **10**(3).

17. Bell, J.K., et al., *Leucine-rich repeats and pathogen recognition in Toll-like receptors.* Trends Immunol, 2003. **24**(10): p. 528-33.

18. Barton, G.M. and J.C. Kagan, *A cell biological view of Toll-like receptor function: regulation through compartmentalization.* Nat Rev Immunol, 2009. **9**(8): p. 535-42.

19. Choe, J., M.S. Kelker, and I.A. Wilson, *Crystal structure of human Toll-like receptor 3 (TLR3) ectodomain.* Science, 2005. **309**(5734): p. 581-585.

20. Farhat, K., et al., *Heterodimerization of TLR2 with TLR1 or TLR6 expands the ligand spectrum but does not lead to differential signaling.* Journal of Leukocyte Biology, 2008. **83**(3): p. 692-701.

21. Kawai, T., et al., *Unresponsiveness of MyD88-deficient mice to endotoxin.* Immunity, 1999. **11**(1): p. 115-22.

22. Lu, Y.C., W.C. Yeh, and P.S. Ohashi, *LPS/TLR4 signal transduction pathway.* Cytokine, 2008. **42**(2): p. 145-51.

23. O'Neill, L.A.J. and A.G. Bowie, *The family of five: TIR-domain-containing adaptors in Toll-like receptor signalling.* Nature Reviews Immunology, 2007. **7**(5): p. 353-364.

24. Tsujimoto, H., et al., *Role of Toll-like receptors in the development of sepsis.* Shock, 2008. **29**(3): p. 315-21.

25. Armstrong, L., et al., *Differential expression of Toll-like receptor (TLR)-2 and TLR-4 on monocytes in human sepsis.* Clin Exp Immunol, 2004. **136**(2): p. 312-9.

26. Ospelt, C. and S. Gay, *TLRs and chronic inflammation.* Int J Biochem Cell Biol, 2010. **42**(4): p. 495-505.

27. Husebye, H., et al., *The Rab11a GTPase controls Toll-like receptor 4-induced activation of interferon regulatory factor-3 on phagosomes.* Immunity, 2010. **33**(4): p. 583-96.

28. Poltorak, A., et al., *Defective LPS signaling in C3H/HeJ and C57BL/10ScCr mice: mutations in Tlr4 gene.* Science, 1998. **282**(5396): p. 2085-8.

29. Kawai, T., et al., *Lipopolysaccharide stimulates the MyD88-independent pathway and results in activation of IFN-regulatory factor 3 and the expression of a subset of lipopolysaccharide-inducible genes.* Journal of Immunology, 2001. **167**(10): p. 5887-5894.

30. Fitzgerald, K.A., D.C. Rowe, and D.T. Golenbock, *Endotoxin recognition and signal transduction by the TLR4/MD-2 complex.* Microbes and Infection, 2004. **6**(15): p. 1361-1367.

31. Latz, E., et al., *The LPS receptor generates inflammatory signals from the cell surface.* J Endotoxin Res, 2003. **9**(6): p. 375-80.

32. Lamping, N., et al., *Effects of site-directed mutagenesis of basic residues (Arg 94, Lys 95, Lys 99) of lipopolysaccharide (LPS)-binding protein on binding and transfer of LPS and subsequent immune cell activation.* J Immunol, 1996. **157**(10): p. 4648-56.

33. Schumann, R.R., et al., *The lipopolysaccharide-binding protein is a secretory class 1 acute-phase protein whose gene is transcriptionally activated by APRF/STAT/3 and other cytokine-inducible nuclear proteins.* Mol Cell Biol, 1996. **16**(7): p. 3490-503.

34. Wright, S.D., et al., *Cd14, a Receptor for Complexes of Lipopolysaccharide (Lps) and Lps Binding-Protein.* Science, 1990. **249**(4975): p. 1431-1433.

35. Zanoni, I., et al., *CD14 controls the LPS-induced endocytosis of Toll-like receptor 4.* Cell, 2011. **147**(4): p. 868-80.

36. Kagan, J.C., et al., *TRAM couples endocytosis of Toll-like receptor 4 to the induction of interferon-beta.* Nature Immunology, 2008. **9**(4): p. 361-368.

37. Zweigner, J., et al., *High concentrations of lipopolysaccharide-binding protein in serum of patients with severe sepsis or septic shock inhibit the lipopolysaccharide response in human monocytes.* Blood, 2001. **98**(13): p. 3800-8.

38. Triantafilou, K., M. Triantafilou, and R.L. Dedrick, *A CD14-independent LPS receptor cluster.* Nat Immunol, 2001. **2**(4): p. 338-45.

39. Perera, P.Y., et al., *CD14-dependent and CD14-independent signaling pathways in murine macrophages from normal and CD14 knockout mice stimulated with lipopolysaccharide or taxol.* Journal of Immunology, 1997. **158**(9): p. 4422-4429.

40. Jiang, Z.F., et al., *CD14 is required for MyD88-independent LPS signaling.* Nature Immunology, 2005. **6**(6): p. 565-570.

41. Viriyakosol, S., et al., *MD-2 binds to bacterial lipopolysaccharide.* J Biol Chem, 2001. **276**(41): p. 38044-51.

42. Latz, E., et al., *Lipopolysaccharide rapidly traffics to and from the Golgi apparatus with the toll-like receptor 4-MD-2-CD14 complex in a process that is distinct from the initiation of signal transduction.* J Biol Chem, 2002. **277**(49): p. 47834-43.

43. Nagai, Y., et al., *Essential role of MD-2 in LPS responsiveness and TLR4 distribution.* Nat Immunol, 2002. **3**(7): p. 667-72.

44. Shimazu, R., et al., *MD-2, a molecule that confers lipopolysaccharide responsiveness on Toll-like receptor 4.* J Exp Med, 1999. **189**(11): p. 1777-82.

45. Medzhitov, R., et al., *MyD88 is an adaptor protein in the hToll/IL-1 receptor family signaling pathways.* Molecular Cell, 1998. **2**(2): p. 253-258.

46. Horng, T., et al., *The adaptor molecule TIRAP provides signalling specificity for Toll-like receptors.* Nature, 2002. **420**(6913): p. 329-33.

47. Yamamoto, M., et al., *Essential role for TIRAP in activation of the signalling cascade shared by TLR2 and TLR4.* Nature, 2002. **420**(6913): p. 324-9.

48. Kagan, J.C. and R. Medzhitov, *Phosphoinositide-mediated adaptor recruitment controls Toll-like receptor signaling.* Cell, 2006. **125**(5): p. 943-55.

49. Suzuki, N., S. Suzuki, and W.C. Yeh, *IRAK-4 as the central TIR signaling mediator in innate immunity.* Trends in Immunology, 2002. **23**(10): p. 503-506.

50. Lye, E., et al., *The role of interleukin 1 receptor-associated kinase-4 (IRAK-4) kinase activity in IRAK-4-mediated signaling.* Journal of Biological Chemistry, 2004. **279**(39): p. 40653-40658.

51. Gohda, J., T. Matsumura, and J. Inoue, *Cutting edge: TNFR-associated factor (TRAF) 6 is essential for MyD88-dependent pathway but not toll/IL-1 receptor domain-containing adaptor-inducing IFN-beta (TRIF)-dependent pathway in TLR signaling.* Journal of Immunology, 2004. **173**(5): p. 2913-2917.

52. Deng, L., et al., *Activation of the I kappa B kinase complex by TRAF6 requires a dimeric ubiquitin-conjugating enzyme complex and a unique polyubiquitin chain.* Cell, 2000. **103**(2): p. 351-361.

53. Sato, S., et al., *Essential function for the kinase TAK1 in innate and adaptive immune responses.* Nat Immunol, 2005. **6**(11): p. 1087-95.

54. Karin, M. and Y. Ben-Neriah, *Phosphorylation meets ubiquitination: The control of NF-kappa B activity.* Annual Review of Immunology, 2000. **18**: p. 621-+.

55. Pathak, S.K., et al., *TLR4-dependent NF-kappa B activation and mitogen- and stress-activated protein kinase 1-triggered phosphorylation events are central to Helicobacter pylori peptidyl prolyl cis-, trans-isomerase (HP0175)-mediated induction of IL-6 release from macrophages.* Journal of Immunology, 2006. **177**(11): p. 7950-7958.

56. Deak, M., et al., *Mitogen- and stress-activated protein kinase-1 (MSK1) is directly activated by MAPK and SAPK2/p38, and may mediate activation of CREB.* Embo Journal, 1998. **17**(15): p. 4426-4441.

57. Kawai, T. and S. Akira, *TLR signaling.* Cell Death Differ, 2006. **13**(5): p. 816-25.

58. Shaulian, E. and M. Karin, *AP-1 as a regulator of cell life and death.* Nature Cell Biology, 2002. **4**(5): p. E131-E136.

59. Siednienko, J., et al., *Absence of MyD88 results in enhanced TLR3-dependent phosphorylation of IRF3 and increased IFN-beta and RANTES production.* J Immunol, 2011. **186**(4): p. 2514-22.

60. Muroi, M. and K. Tanamoto, *TRAF6 distinctively mediates MyD88- and IRAK-1-induced activation of NF-kappaB.* J Leukoc Biol, 2008. **83**(3): p. 702-7.

61. Cusson-Hermance, N., et al., *Rip1 mediates the Trif-dependent toll-like receptor 3- and 4-induced NF-{kappa}B activation but does not contribute to interferon regulatory factor 3 activation.* J Biol Chem, 2005. **280**(44): p. 36560-6.

62. Honda, K. and T. Taniguchi, *IRFs: master regulators of signalling by Toll-like receptors and cytosolic pattern-recognition receptors.* Nature Reviews Immunology, 2006. **6**(9): p. 644-658.

63. Fitzgerald, K.A., et al., *LPS-TLR4 signaling to IRF-3/7 and NF-kappaB involves the toll adapters TRAM and TRIF.* J Exp Med, 2003. **198**(7): p. 1043-55.

64. Tanimura, N., et al., *Roles for LPS-dependent interaction and relocation of TLR4 and TRAM in TRIF-signaling.* Biochemical and Biophysical Research Communications, 2008. **368**(1): p. 94-99.

65. Yamamoto, M., et al., *Role of adaptor TRIF in the MyD88-independent toll-like receptor signaling pathway.* Science, 2003. **301**(5633): p. 640-3.

66. Kagan, J.C., et al., *TRAM couples endocytosis of Toll-like receptor 4 to the induction of interferon-beta.* Nat Immunol, 2008. **9**(4): p. 361-8.

67. Sato, S., et al., *Toll/IL-1 receptor domain-containing adaptor inducing IFN-beta (TRIF) associates with TNF receptor-associated factor 6 and TANK-Binding kinase 1, and activates two distinct transcription factors, NF-kappa B and IFN-regulatory factor-3, in the toll-like receptor signaling.* Journal of Immunology, 2003. **171**(8): p. 4304-4310.

68. Meylan, E., et al., *RIP1 is an essential mediator of Toll-like receptor 3-induced NF-kappa B activation.* Nature Immunology, 2004. **5**(5): p. 503-507.

69. Ofengeim, D. and J.Y. Yuan, *Regulation of RIP1 kinase signalling at the crossroads of inflammation and cell death.* Nature Reviews Molecular Cell Biology, 2013. **14**(11): p. 727-736.

70. Oganesyan, G., et al., *Critical role of TRAF3 in the Toll-like receptor-dependent and -independent antiviral response.* Nature, 2006. **439**(7073): p. 208-211.

71. Hacker, H., et al., *Specificity in Toll-like receptor signalling through distinct effector functions of TRAF3 and TRAF6.* Nature, 2006. **439**(7073): p. 204-207.

72. Tseng, P.H., et al., *Different modes of ubiquitination of the adaptor TRAF3 selectively activate the expression of type I interferons and proinflammatory cytokines.* Nature Immunology, 2010. **11**(1): p. 70-1819.

73. Fitzgerald, K.A., et al., *IKK epsilon and TBK1 are essential components of the IRF3 signaling pathway.* Nature Immunology, 2003. **4**(5): p. 491-496.

74. Hemmi, H., et al., *The roles of two IkappaB kinase-related kinases in lipopolysaccharide and double stranded RNA signaling and viral infection.* J Exp Med, 2004. **199**(12): p. 1641-50.

75. Lin, R.T., et al., *Essential role of interferon regulatory factor 3 in direct activation of RANTES chemokine transcription.* Molecular and Cellular Biology, 1999. **19**(2): p. 959-966.

76. Stenmark, H., *Rab GTPases as coordinators of vesicle traffic.* Nature Reviews Molecular Cell Biology, 2009. **10**(8): p. 513-525.

77. Shapiro, A.D. and S.R. Pfeffer, *Quantitative analysis of the interactions between prenyl Rab9, GDP dissociation inhibitor-alpha, and guanine nucleotides.* J Biol Chem, 1995. **270**(19): p. 11085-90.

78. Sivars, U., D. Aivazian, and S.R. Pfeffer, *Yip3 catalyses the dissociation of endosomal Rab-GDI complexes.* Nature, 2003. **425**(6960): p. 856-9.

79. Dirac-Svejstrup, A.B., T. Sumizawa, and S.R. Pfeffer, *Identification of a GDI displacement factor that releases endosomal Rab GTPases from Rab-GDI.* EMBO J, 1997. **16**(3): p. 465-72.

80. Huotari, J. and A. Helenius, *Endosome maturation.* EMBO J, 2011. **30**(17): p. 3481-500.

81. Garg, S., et al., *Lysosomal Trafficking, Antigen Presentation, and Microbial Killing Are Controlled by the Arf-like GTPase Arl8b.* Immunity, 2011. **35**(2): p. 182-193.

82. Raposo, G.A., et al., *Lysosome-related organelles: a view from immunity and pigmentation.* Cell Structure and Function, 2002. **27**(6): p. 443-456.

83. van der Sluijs, P., et al., *The small GTP-binding protein rab4 controls an early sorting event on the endocytic pathway.* Cell, 1992. **70**(5): p. 729-40.

84. Liu, S.S., et al., *Knockdown of Rab5a expression decreases cancer cell motility and invasion through integrin-mediated signaling pathway.* Journal of Biomedical Science, 2011. **18**.

85. Prada-Delgado, A., et al., *Interferon-gamma listericidal action is mediated by novel Rab5a functions at the phagosomal environment.* Journal of Biological Chemistry, 2001. **276**(22): p. 19059-19065.

86. Pei, G., M. Bronietzki, and M.G. Gutierrez, *Immune regulation of Rab proteins expression and intracellular transport.* J Leukoc Biol, 2012. **92**(1): p. 41-50.

87. Krawczyk, M., et al., *Expression of RAB4B, a protein governing endocytic recycling, is co-regulated with MHC class II genes.* Nucleic Acids Research, 2007. **35**(2): p. 595-605.

88. Nagy, G., et al., *Regulation of CD4 expression via recycling by HRES-1/RAB4 controls susceptibility to HIV infection.* Journal of Biological Chemistry, 2006. **281**(45): p. 34574-34591.

89. Poteryaev, D., et al., *Identification of the switch in early-to-late endosome transition.* Cell, 2010. **141**(3): p. 497-508.

90. Johansson, M., et al., *Activation of endosomal dynein motors by stepwise assembly of Rab7-RILP-p150Glued, ORP1L, and the receptor betalll spectrin.* J Cell Biol, 2007. **176**(4): p. 459-71.

91. Pankiv, S. and T. Johansen, *FYCO1: linking autophagosomes to microtubule plus end-directing molecular motors.* Autophagy, 2010. **6**(4): p. 550-2.

92. Rojas, R., et al., *Regulation of retromer recruitment to endosomes by sequential action of Rab5 and Rab7.* J Cell Biol, 2008. **183**(3): p. 513-26.

93. Levine, B., *Eating oneself and uninvited guests: autophagy-related pathways in cellular defense.* Cell, 2005. **120**(2): p. 159-62.

94. Wang, Y.Z., et al., *Lysosome-associated small Rab GTPase Rab7b negatively regulates TLR4 signaling in macrophages by promoting lysosomal degradation of TLR4.* Blood, 2007. **110**(3): p. 962-971.

95. Yang, M.J., et al., *Rab7b, a novel lysosome-associated small GTPase, is involved in monocytic differentiation of human acute promyelocytic leukemia cells.* Biochemical and Biophysical Research Communications, 2004. **318**(3): p. 792-799.

96. Progida, C., et al., *Rab7b controls trafficking from endosomes to the TGN.* Journal of Cell Science, 2010. **123**(9): p. 1480-1491.

97. Ullrich, O., et al., *Rab11 regulates recycling through the pericentriolar recycling endosome.* J Cell Biol, 1996. **135**(4): p. 913-24.

98. Goldenring, J.R., et al., *Identification of a small GTP-binding protein, Rab25, expressed in the gastrointestinal mucosa, kidney, and lung.* J Biol Chem, 1993. **268**(25): p. 18419-22.

99. Lapierre, L.A., et al., *Rab11b resides in a vesicular compartment distinct from Rab11a in parietal cells and other epithelial cells.* Exp Cell Res, 2003. **290**(2): p. 322-31.

100. Jordens, I., et al., *Rab proteins, connecting transport and vesicle fusion.* Traffic, 2005. **6**(12): p. 1070-7.

101. Wei, J., et al., *Disorder and structure in the Rab11 binding domain of Rab11 family interacting protein 2.* Biochemistry, 2009. **48**(3): p. 549-57.

102. Cox, D., et al., *A Rab11-containing rapidly recycling compartment in macrophages that promotes phagocytosis.* Proc Natl Acad Sci U S A, 2000. **97**(2): p. 680-5.

103. Murray, R.Z., et al., *A role for the phagosome in cytokine secretion.* Science, 2005. **310**(5753): p. 1492-5.

104. Hornef, M.W., et al., *Toll-like receptor 4 resides in the Golgi apparatus and colocalizes with internalized lipopolysaccharide in intestinal epithelial cells.* J Exp Med, 2002. **195**(5): p. 559-70.

105. Misaki, R., et al., *Spatial segregation of degradation- and recycling-trafficking pathways in COS-1 cells.* Biochem Biophys Res Commun, 2007. **360**(3): p. 580-5.

106. Calvano, J.E., et al., *Modulation of the lipopolysaccharide receptor complex (CD14, TLR4, MD-2) and toll-like receptor 2 in systemic inflammatory response syndrome-positive patients with and without infection: Relationship to tolerance.* Shock, 2003. **20**(5): p. 415-419.

107. Tsuchiya, S., et al., *Establishment and Characterization of a Human Acute Monocytic Leukemia-Cell Line (Thp-1).* International Journal of Cancer, 1980. **26**(2): p. 171-176.

108. Schwende, H., et al., *Differences in the state of differentiation of THP-1 cells induced by phorbol ester and 1,25-dihydroxyvitamin D-3.* Journal of Leukocyte Biology, 1996. **59**(4): p. 555-561.

109. Zanoni, I., et al., *Similarities and differences of innate immune responses elicited by smooth and rough LPS.* Immunol Lett, 2012. **142**(1-2): p. 41-7.

110. Invivogen. *LPS from E. coli K12*. 2014; Available from: http://www.invivogen.com/lps-ek.

111. Hannon, G.J. and J.J. Rossi, *Unlocking the potential of the human genome with RNA interference.* Nature, 2004. **431**(7006): p. 371-8.

112. Brown, M. and C. Wittwer, *Flow cytometry: principles and clinical applications in hematology.* Clin Chem, 2000. **46**(8 Pt 2): p. 1221-9.

113. Thermo. *Accutase™*

Cell Detachment Solution. Accutase™

Cell Detachment Solution 2014; Available from: http://www.thermo.com.cn/Resources/200802/productPDF_26369.pdf.

114. Arya, M., et al., *Basic principles of real-time quantitative PCR.* Expert Review of Molecular Diagnostics, 2005. **5**(2): p. 209-219.

115. Abcam. *WB beginners guide*. 2014; Available from: http://www.abcam.com/ps/pdf/protocols/WB-beginner.pdf.

116. immunoleader, B. *Western Blot principle*. Western Blot principle 2014; Online referance]. Available from: http://www.bosterbio.com/category-s/5927.htm.

117. Invitrogen. *The iBlot® Dry Blotting System vs. Conventional Semi-Dry and Wet Transfer Systems*. 2014; Available from: http://www.lifetechnologies.com/no/en/home/life-science/protein-expression-and-analysis/western-blotting/western-blot-transfer/iblot-dry-blotting-system/iblot-dry-blotting-comparison-to-semi-dry-and-wet.html.

118. Li-Cor. *ODYSSEY Fc*

Dual-Mode Imaging System. 2014; Available from: http://biosupport.licor.com/docs/Fc_Digital_Brochure2.pdf.

119. Zanoni, I., et al., *CD14 controls the LPS-induced endocytosis of Toll-like receptor 4.* Cell, 2011. **147**(4): p. 868-880.

120. Lehtonen, A., et al., *Gene expression profiling during differentiation of human monocytes to macrophages or dendritic cells.* Journal of Leukocyte Biology, 2007. **82**(3): p. 710-720.

121. Park, E.K., et al., *Optimized THP-1 differentiation is required for the detection of responses to weak stimuli.* Inflamm Res, 2007. **56**(1): p. 45-50.

122. Daigneault, M., et al., *The identification of markers of macrophage differentiation in PMA-stimulated THP-1 cells and monocyte-derived macrophages.* PLoS One, 2010. **5**(1): p. e8668.

123. Ross, G.D., *Role of the lectin domain of Mac-1/CR3 (CD11b/CD18) in regulating intercellular adhesion.* Immunologic Research, 2002. **25**(3): p. 219-227.

124. Zarewych, D.M., et al., *LPS induces CD14 association with complement receptor type 3, which is reversed by neutrophil adhesion.* J Immunol, 1996. **156**(2): p. 430-3.

125. Flaherty, S.F., et al., *CD11/CD18 leukocyte integrins: new signaling receptors for bacterial endotoxin.* J Surg Res, 1997. **73**(1): p. 85-9.

126. Dai, S.P., et al., *Fine Tuning Inflammation at the Front Door: Macrophage Complement Receptor 3-mediates Phagocytosis and Immune Suppression for Francisella tularensis.* Plos Pathogens, 2013. **9**(1).

127. Dong, J., et al., *Constitutively active NF-kappa B triggers systemic TNF alpha-dependent inflammation and localized TNF alpha-independent inflammatory disease.* Genes & Development, 2010. **24**(16): p. 1709-1717.

128. Correia, J.D., et al., *Lipopolysaccharide is in close proximity to each of the proteins in its membrane receptor complex - Transfer from CD14 to TLR4 and MD-2.* Journal of Biological Chemistry, 2001. **276**(24): p. 21129-21135.

129. Hoebe, K., et al., *Identification of Lps2 as a key transducer of MyD88-independent TIR signalling.* Nature, 2003. **424**(6950): p. 743-8.

130. Aerbajinai, W., et al., *Glia maturation factor-gamma negatively modulates TLR4 signaling by facilitating TLR4 endocytic trafficking in macrophages.* J Immunol, 2013. **190**(12): p. 6093-103.

131. Tamegai, H., et al., *Aureobasidium pullulans culture supernatant significantly stimulates R-848-activated phagocytosis of PMA-induced THP-1 macrophages.* Immunopharmacology and Immunotoxicology, 2013. **35**(4): p. 455-461.

132. Suzuki, M. and M. Mihara, *Adiponectin induces CCL20 expression synergistically with IL-6 and TNF-alpha in THP-1 macrophages.* Cytokine, 2012. **58**(3): p. 344-50.

133. Juliet, P.A., et al., *Concomitant production of nitric oxide and superoxide in human macrophages.* Biochem Biophys Res Commun, 2003. **310**(2): p. 367-70.

134. Hirakata, M., et al., *Comparison of the effects of pioglitazone and rosiglitazone on macrophage foam cell formation (vol 323, pg 782, 2004).* Biochemical and Biophysical Research Communications, 2005. **327**(3): p. 967-968.

135. McCaffrey, M.W., et al., *Rab4 affects both recycling and degradative endosomal trafficking.* Febs Letters, 2001. **495**(1-2): p. 21-30.

136. Vanlandingham, P.A. and B.P. Ceresa, *Rab7 Regulates Late Endocytic Trafficking Downstream of Multivesicular Body Biogenesis and Cargo Sequestration.* Journal of Biological Chemistry, 2009. **284**(18): p. 12110-12124.

137. Rink, J., et al., *Rab conversion as a mechanism of progression from early to late endosomes.* Cell, 2005. **122**(5): p. 735-49.

138. Zhang, M., et al., *Rab7: roles in membrane trafficking and disease.* Biosci Rep, 2009. **29**(3): p. 193-209.

8 Appendix

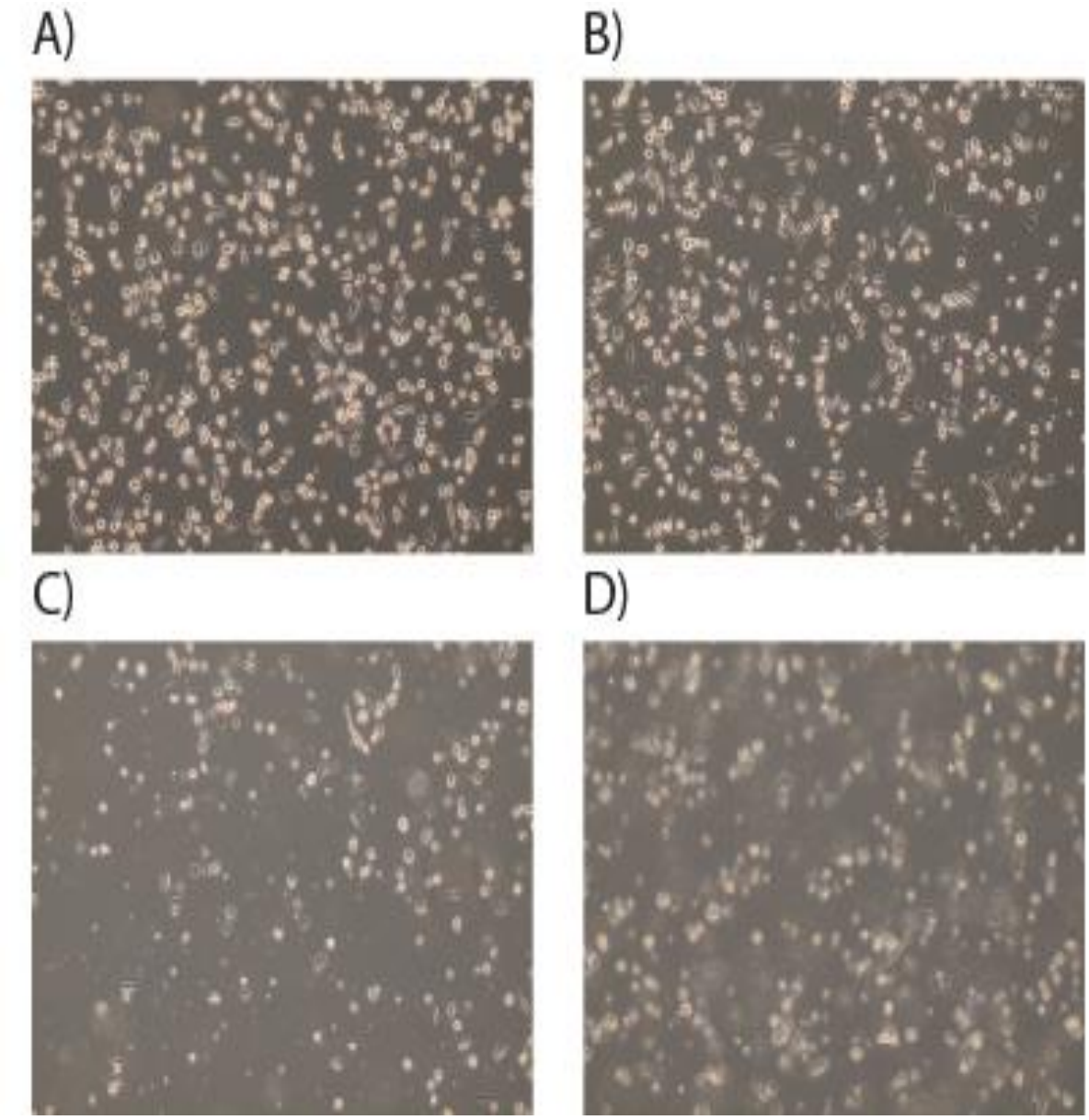

Figure 38: LPS stimulated THP-1 cells become apoptotic (10x magnification).
THP-1 cells differentiated with 10 ng/ml PMA for 48 hrs and rested for 48 hrs. The cells pictured has been treated with control siRNA and stimulated with 100 ng/ml LPS for A) 0hrs, B) 1 hr, C) 2 hrs, and D) 4 hrs. The picture indicate an increasing apoptotic tendency over time in LPS-stimulated THP-1 cells. Cells were seeded by Marria Y. and the pictures were taken by the student using a light microscope with an attached camera.

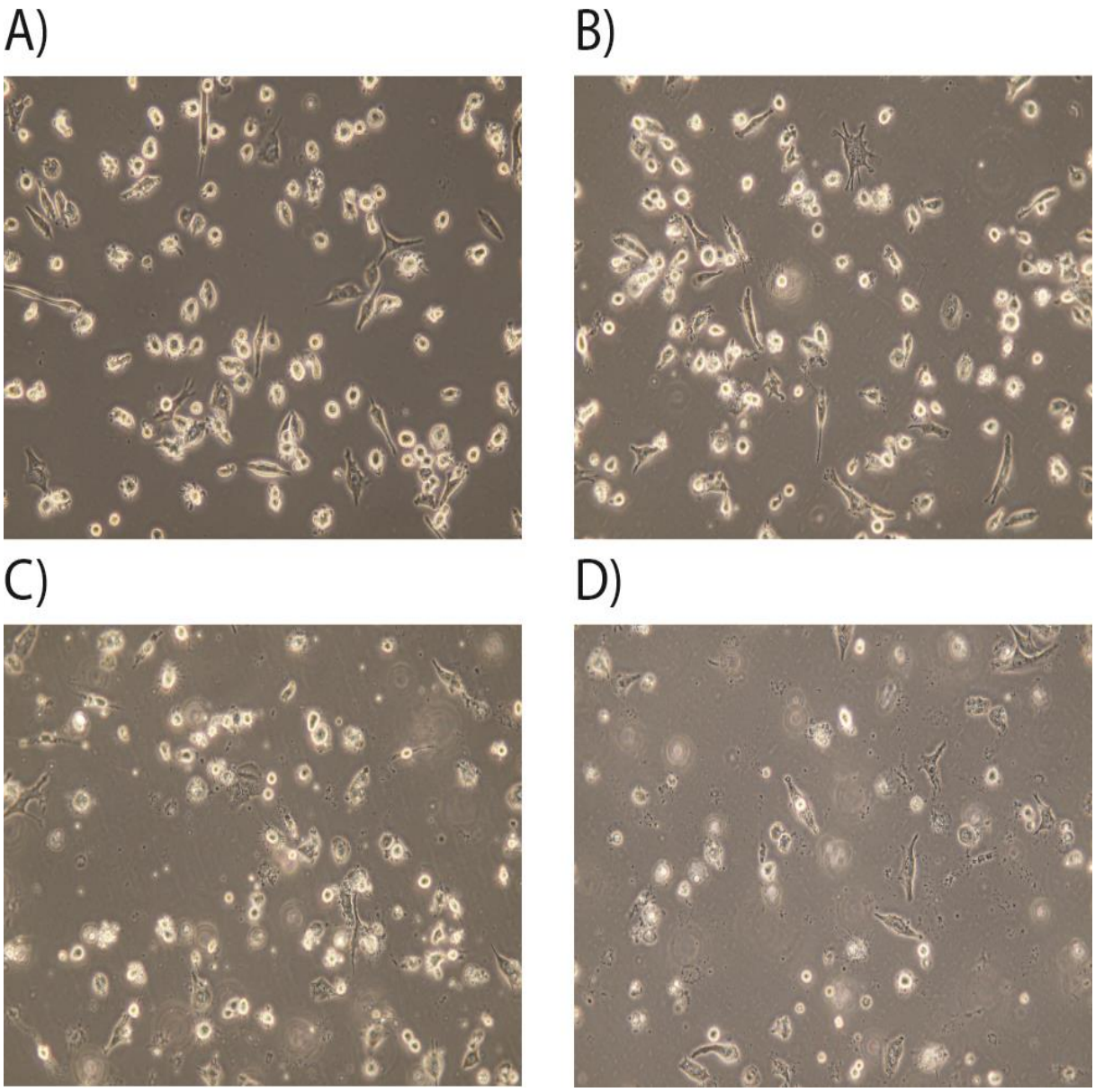

Figure 39: LPS stimulated THP-1 cells become apoptotic (40x magnification).
THP-1 cells differentiated with 10 ng/ml PMA for 48 hrs and rested for 48 hrs. The cells pictured has been treated with control siRNA and stimulated with 100 ng/ml LPS for A) 0hrs, B) 1 hr, C) 2 hrs, and D) 4 hrs. The picture indicate an increasing apoptotic tendency over time in LPS-stimulated THP-1 cells. Cells were seeded by Marria Y. and the pictures were taken by the student using a light microscope with an attached camera.

Table 5: Antibodies used in WB

Distributor	Antibody
Abcam	GAPDH Ab8245
Cell signaling Technologies	TBK1/NAK (D1B4)
	Phospho-TBK1/NAK (Ser172) (D52C2)
	IRF-3 (D83B9)
	Phospho-IRF-3 (Ser396) (4D4G)
	Phospho-IκBα (Ser32) (14D4)
	p38δ MAPK (10A8)
	Phospho-p38 MAPK (Thr180/Tyr182)
	Rab7 (D95F2)
	Rab11 (D4F5)
Santa Cruz	Rab 4A Antibody (D-20)